

แทรนส์เอสเทอร์ฟิเคชันของน้ำมันปาล์มโดยใช้ตัวเร่งปฏิกิริยาอีอาร์บี-1 ที่เติมเบส

เพื่อผลิตไบโอดีเซล



นางสาวนัญชญา ศรีคงอยู่

ศูนย์วิทยทรัพยากร
จุฬาลงกรณ์มหาวิทยาลัย

วิทยานิพนธ์นี้เป็นส่วนหนึ่งของการศึกษาตามหลักสูตรปริญญาวิทยาศาสตรมหาบัณฑิต

สาขาวิชาปิโตรเคมี และวิทยาศาสตร์พอลิเมอร์

คณะวิทยาศาสตร์ จุฬาลงกรณ์มหาวิทยาลัย

ปีการศึกษา 2550

ลิขสิทธิ์ของจุฬาลงกรณ์มหาวิทยาลัย

TRANSESTERIFICATION OF PALM OIL USING
BASE LOADED ERB-1 CATALYSTS FOR BIODIESEL PRODUCTION



Miss Nanchana Srikongyoo

ศูนย์วิทยทรัพยากร
จุฬาลงกรณ์มหาวิทยาลัย

A Thesis Submitted in Partial Fulfillment of the Requirements
for the Degree of Master of Science Program in Petrochemistry and Polymer Science

Faculty of Science

Chulalongkorn University

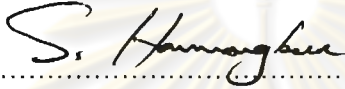
Academic Year 2007

Copyright of Chulalongkorn University

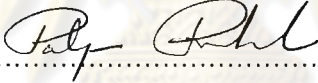
500456


Thesis Title TRANSESTERIFICATION OF PALM OIL USING BASE
 LOADED ERB-1 CATALYSTS FOR BIODIESEL PRODUCTION
By Miss Nanchana Srikongyoo
Field of Study Petrochemistry and Polymer Science
Thesis Advisor Duangamol Nuntasri, Ph.D.

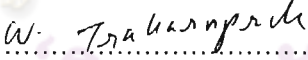
Accepted by the Faculty of Science, Chulalongkorn University in Partial Fulfillment
of the Requirements for the Master's Degree

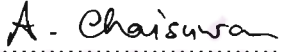

.....Dean of the Faculty of Science
(Professor Supot Hannongbua, Ph.D.)

THESIS COMMITTEE


.....Chairman
(Professor Pattarapan Prasassarakich, Ph.D.)


.....Thesis Advisor
(Duangamol Nuntasri, Ph.D.)


.....Member
(Associate Professor Wimonrat Trakarnpruk, Ph.D.)


.....Member
(Aticha Chaisuwan, Ph.D.)

ัญชนา ศรีคงอยู่ : แทรนส์เอสเทอร์ฟิเคชันของน้ำมันปาล์มโดยใช้ตัวเร่งปฏิกิริยา
 อีอาร์บี-1 ที่เติมเบสเพื่อผลิตไบโอดีเซล. (TRANSESTERIFICATION OF PALM
 OIL USING BASE LOADED ERB-1 CATALYSTS FOR BIODIESEL
 PRODUCTION) อ.ที่ปรึกษา: ดร.ดวงกมล นันทศรี, 120 หน้า.

สามารถสังเคราะห์อีอาร์บี-1 แบบวิธีไฮโดรเทอร์มัลด้วยการตกผลึกแบบหมุนได้ และใช้
 พิเพอริดีน หรือ พีดี เป็นสารต้นแบบโครงสร้าง องค์ประกอบของเจลคือ $1.50 \text{ SiO}_2 : \text{B}_2\text{O}_3 : 0.60 \text{ NaOH} : 1.80 \text{ PD} : 28.50 \text{ H}_2\text{O}$ นำเจลไปตกผลึกที่อุณหภูมิ 175 องศาเซลเซียส เป็นเวลา 7 วัน
 และกำจัดสารต้นแบบอินทรีย์จากตัวอย่างชนิดที่สังเคราะห์ได้โดยการเผาในเตาเผาที่อุณหภูมิ 550
 องศาเซลเซียส ได้เตรียม คีลามีเนท-อีอาร์บี-1 โดยการทำให้ฟริเคอร์เซอร์บวมตัวและแยกชั้น
 คีลามีเนท-อีอาร์บี-1 เป็นแผ่นซีทบาง ๆ ที่มีพื้นที่ผิวด้านนอกสูงมาก โซเดียมอีอาร์บี-1 และ โซเดียม
 คีลามีเนท-อีอาร์บี-1 ได้จากการกวนด้วยสารละลายโซเดียมไฮดรอกไซด์ ที่มีความเข้มข้น 0.10
 โมลาร์ ที่อุณหภูมิห้อง เป็นเวลา 3 ชั่วโมง และ ได้นำภาวะนี้ไปประยุกต์ใช้กับการเพิ่มโลหะ
 อัลคาไลอื่นๆ คือ K, Rb และ Cs ตัวเร่งปฏิกิริยาทุกตัวได้ตรวจสอบลักษณะของตัวเร่งปฏิกิริยาที่
 สังเคราะห์ได้ด้วยเทคนิคการเลี้ยวเบนของรังสีเอ็กซ์ ไอซีพี-เออีเอส การดูดซับไนโตรเจน และ
 กล้องจุลทรรศน์แบบส่องกราดและทดสอบความว่องไวในปฏิกิริยาแทรนส์เอสเทอร์ฟิเคชันของ
 น้ำมันปาล์มกับเมทานอล เพื่อผลิตเมทิลเอสเทอร์ของกรดไขมันหรือไบโอดีเซล ได้ศึกษาผลของ
 ภาวะต่างๆ เช่น ปริมาณของตัวเร่งปฏิกิริยา อัตราส่วนโดยโมลของเมทานอลต่อน้ำมัน เวลาและ
 อุณหภูมิในการเกิดปฏิกิริยา ผลผลิตกันที่ได้นำไปวิเคราะห์ด้วยเทคนิคแก๊สโครมาโทกราฟี ในกรณี
 ของ คีลามีเนท-อีอาร์บี-1 แสดงให้เห็นว่า ค่าการเปลี่ยนของไตรกลีเซอไรด์สูงกว่าตัวเร่งปฏิกิริยาที่
 ไม่ได้แยกชั้นเล็กน้อย (2.28%) ขณะที่ค่าการเปลี่ยนเมื่อใช้ตัวเร่งปฏิกิริยาโซเดียมคีลามีเนท-อีอาร์บี-1
 มีค่าน้อยกว่าตัวเร่งปฏิกิริยาโซเดียมอีอาร์บี-1 (4.49%) ดังนั้น เมื่อใช้โซเดียมอีอาร์บี-1 เป็นตัวเร่ง
 ปฏิกิริยาจะให้ความว่องไวสูงสุดสำหรับปฏิกิริยาแทรนส์เอสเทอร์ฟิเคชัน และได้ค่าการเปลี่ยนและ
 ปริมาณผลิตภัณฑ์เมทิลเอสเทอร์สูงสุดที่ 73.04% และ 42.45% ตามลำดับ นอกจากนี้ ได้ศึกษาความ
 ว่องไวในการเร่งปฏิกิริยาของตัวเร่งปฏิกิริยาที่ผ่านการใช้งานแล้วและที่ปรับสภาพเหมือนใหม่อีก
 ด้วย ตัวเร่งปฏิกิริยาที่ปรับสภาพเหมือนใหม่ มีความว่องไวสูงกว่าตัวเร่งปฏิกิริยาที่ผ่านการใช้งาน
 แล้วเล็กน้อย แต่น้อยกว่าตัวเร่งปฏิกิริยาที่ยังไม่ได้ใช้งาน

สาขาวิชา ปิโตรเคมีและวิทยาศาสตร์พอลิเมอร์ลายมือชื่อนิสิต ัญชนา ศรีคงอยู่
 ปีการศึกษา 2550ลายมือชื่ออาจารย์ที่ปรึกษา ดร.ดวงกมล นันทศรี

4872333723: MAJOR PETROCHEMISTRY AND POLYMER SCIENCE

KEY WORD: ERB-1/ DELAMINATED ERB-1/ TRANSESTERIFICATION/ BIODIESEL

NANCHANA SRIKONGYOO: TRANSESTERIFICATION OF PALM OIL USING
BASE LOADED ERB-1 CATALYSTS FOR BIODIESEL PRODUCTION. THESIS
ADVISOR: DUANGAMOL NUNTASRI, Ph.D., 120 pp.

ERB-1 was hydrothermally synthesized by rotating crystallization and using piperidine (PD) as a structure directing agent with the gel composition 1.50 SiO₂ : B₂O₃ : 0.60 NaOH : 1.80 PD : 28.50 H₂O. The gel was crystallized at 175°C for 7 days and removed template from as-synthesized sample by calcination in a muffle furnace at 550°C. The del-ERB-1 was prepared by swelling and exfoliating the ERB-1 precursor. The del-ERB-1 consists of thin sheet with an extremely high external surface area. NaERB-1 and Na-del-ERB-1 catalysts could be obtained by stirring with 0.10 M NaOH solution at RT for 3 h and this condition was applied to load with other alkali ions (K, Rb and Cs). All catalysts were characterized using X-ray diffraction, inductively coupled plasma atomic emission, nitrogen adsorption and scanning electron microscopy and tested catalytic activity in transesterification reaction of palm oil with methanol to produce fatty acid methyl esters (biodiesel). The various reaction conditions such as catalyst amount, methanol to oil mole ratio including reaction time and temperature were studied. The product was analyzed by GC technique. In case of del-ERB-1 catalyst, it shows the triglyceride conversion slightly higher than non-delaminated one (2.28%), while conversion over Na-del-ERB-1 is lower than NaERB-1 (4.49%). Thus, the highest transesterification activity is achieved when NaERB-1(0.10, RT) was used as catalyst, the conversion and methyl esters yield can be reached to 74.03% and 42.45%, respectively. Moreover, catalytic activities of used and Na-reloaded catalysts were also investigated. The activity of Na-reloaded ERB-1 catalyst is slightly higher than used ERB-1 but lower than the fresh one.

Field of Study: Petrochemistry and Polymer Science Student's Signature: Nanchana Srikongyoo

Academic year: 2007 Advisor's Signature: Duangamol Nuntasri

ACKNOWLEDGEMENTS

I would like to express my gratitude to my advisor, Dr. Duangamol Nuntasri, for her inspiring guidance and encouragement throughout this research. I am also thankful to my best co-worker Miss Narumol Kerdsa for her ideas and solving some problems in my research. My appreciation is also extended to all the lectures of Program of Petrochemistry and Polymer Science, Faculty of Science, Chulalongkorn University for valuable knowledge and experience.

Moreover, I would like to gratefully thank OLEEN, Co., Ltd for supporting the palm oil details. In addition, I also thank to the financial support from Rachadapisek Sompoch Endowment Chulalongkorn University and research grant from the Graduate School.

Finally, I deeply wish to thank my family for their entirely care, understanding and financial support, the members of Materials Chemistry and Catalysis Research Unit and my friends for their encouragement and friendship.



ศูนย์วิจัยทรัพยากร
จุฬาลงกรณ์มหาวิทยาลัย

CONTENTS

	Page
ABSTRACT (THAI)	iv
ABSTRACT (ENGLISH)	v
ACKNOWLEDGEMENTS	vi
CONTENETS	vii
LIST OF TABLES	xii
LIST OF FIGURES	xv
LIST OF SCHEMES	xviii
LIST OF ABBREVIATIONS	xix
CHAPTER	
I INTRODUCTION	1
1.1 Background	1
1.2 Literature reviews on the ERB-1 catalyst	4
1.3 Literature reviews on the basic modification and application of catalysts	7
1.4 Literature reviews on transesterification reaction of triglycerides	7
1.5 Objectives	11
1.6 Scope of work	11
II THEORY	12
2.1 The phenomenon catalysis	12
2.2 Definition of catalysis	13
2.3 Mode of action of catalysts	13
2.3.1 Activity	13
2.3.2 Selectivity	15
2.3.3 Stability	15
2.4 Classification of catalytic systems	16
2.5 Comparison of homogeneous and heterogeneous catalysis	18
2.6 Porous materials	19
2.7 Shape-Selective catalysis: Zeolites	20
2.7.1 Composition and structure of zeolites	20
2.7.2 Production of zeolites	21

CHAPTER	Page
2.8 Catalytic properties of the zeolites	22
2.8.1 Shape selectivity	22
2.8.1.1 Reactant selectivity	24
2.8.1.2 Product Selectivity	24
2.8.1.3 Restricted transition state selectivity	24
2.8.2 Acidity of zeolites	24
2.9 Structure of ERB-1 catalyst	25
2.10 Preparation of del-ERB-1	27
2.11 Ion-exchange	28
2.12 Catalyst deactivation and regeneration	28
2.13 Characterization of materials	29
2.13.1 X-ray powder diffraction (XRD)	29
2.13.2 Nitrogen adsorption-desorption technique	30
2.13.3 Inductively coupled plasma atomic emission spectrometry (ICP-AES)	34
2.14 Diesel oil	34
2.14.1 Petroleum diesel	35
2.14.2 Chemical composition	35
2.14.3 Alternative diesel fuels	35
2.15 Natural palm oil	35
2.16 Palm oil composition	36
2.16.1 Triglyceride	36
2.16.2 Mono- and diglycerides and free fatty acid (FFA)	37
2.16.3 Moisture and dirt	37
2.16.4 Minor component	38
2.17 The production of biodiesel	38
2.17.1 Direct use and blending	38
2.17.2 Microemulsions	38
2.17.3 Thermal cracking (Pyrolysis)	39
2.17.4 Transesterification (Alcoholysis)	40
2.17.4.1 Esterification	41
2.17.4.2 Saponification	41
2.17.4.3 Hydrolysis	42
2.17.5 Other forms of catalysis	43
2.17.5.1 Biocatalysts	43

CHAPTER	Page
2.17.5.2 Supercritical methanol.....	43
2.17.5.3 Catalyst free.....	44
2.18 Transesterification kinetic and mechanism.....	44
2.19 Transesterification parameters.....	46
2.19.1 Moisture and free fatty acid.....	46
2.19.2 Reaction time.....	46
2.19.3 Reaction temperature.....	46
2.19.4 Molar ratio of alcohol to oil.....	46
2.20 Silylation.....	46
III EXPERIMENTS.....	48
3.1 Instrument and Apparatus.....	48
3.1.1 Pressure reactor.....	48
3.1.2 Furnace.....	48
3.1.3 X-Ray powder diffractometer.....	49
3.1.4 Inductively coupled plasma-atomic emission spectrometer.....	49
3.1.5 Atomic absorption spectrometer.....	49
3.1.6 Surface area analyzer.....	49
3.1.7 Scanning electron microscope.....	50
3.1.8 Gas Chromatography.....	50
3.2 Chemical reagents.....	50
3.3 Synthesis procedure of ERB-1.....	51
3.4 Organic template removal.....	53
3.5 Preparation of delaminated ERB-1 (del-ERB-1).....	53
3.6 Loading of XERB-1 (X = Na, K, Rb or Cs).....	55
3.7 ICP-AES Analysis.....	55
3.7.1 CsCl stock solution, 1000 ppm.....	55
3.7.2 Sample Preparation.....	55
3.8 Transesterification reaction procedure.....	56
3.8.1 Effect of reaction time.....	57
3.8.2 Effect of methanol/palm oil molar ratio.....	57
3.8.3 Effect of catalyst amount.....	57
3.8.4 Effect of reaction temperature.....	58

CHAPTER	Page
3.9 Determination of free and total glycerol and mono-, di- and triglyceride contents.....	58
3.9.1 Internal stand No.1 stock solution, 1 mg/ml.....	58
3.9.2 Internal stand No.2 stock solution, 8 mg/ml.....	58
3.9.3 Glycerol stock solution, 0.5 mg/ml.....	58
3.9.4 Calibration solutions.....	58
3.9.5 Preparation and analysis of the calibration solutions.....	59
3.10 Determination of methyl ester contents.....	59
3.10.1 Internal stand No.3 stock solution, 10 mg/ml.....	59
3.10.2 Methyl ester calibration solutions.....	59
3.10.3 Preparation and analysis of the calibration solutions.....	60
3.11 The stability and regeneration of catalyst.....	60
3.12 Analysis of leached Na content.....	60
IV RESULTS AND DISCUSSIONS.....	61
4.1 ERB-1 catalyst.....	61
4.1.1 X-ray powder diffraction (XRD).....	61
4.1.2 Sorption properties.....	62
4.1.3 Elemental analysis.....	62
4.2 Alkali ion loaded on ERB-1.....	62
4.2.1 Na loaded ERB-1.....	62
4.2.1.1 X-ray powder diffraction (XRD).....	62
4.2.1.2 Sorption properties.....	65
4.2.1.3 Elemental analysis.....	66
4.2.2 The different alkali ions loaded ERB-1.....	66
4.2.2.1 X-ray powder diffraction (XRD).....	66
4.2.2.2 Sorption properties.....	67
4.2.2.3 Elemental analysis.....	68
4.2.2.4 Scanning electron microscopy (SEM).....	68
4.3 Reaction mixture qualitative analysis.....	70
4.4 Reaction mixture quantitative analysis.....	71
4.5 Catalytic activities of ERB-1 in transesterification reaction.....	71
4.6 Catalytic activities of alkali metal loaded ERB-1 in transesterification reaction.....	73

CHAPTER	Page
4.6.1 Na loaded ERB-1.....	73
4.6.2 The different alkali ions loaded ERB-1.....	76
4.7 Catalytic activities of NaERB-1(0.10, RT) in transesterification reaction.....	78
4.7.1 Effect of reaction time.....	78
4.7.2 Effect of methanol to oil molar ratio.....	79
4.7.3 Effect of catalyst amount.....	81
4.7.4 Effect of reaction temperature.....	82
4.8 Delaminated ERB-1 (Del-ERB-1).....	84
4.8.1 X-ray powder diffraction (XRD).....	84
4.9 Na loaded delaminated ERB-1 (Na-del-ERB-1).....	87
4.9.1 X-ray powder diffraction (XRD).....	87
4.9.2 Elemental analysis.....	88
4.9.3 Scanning electron microscopy (SEM).....	88
4.10 Catalytic activities of del-ERB-1 and Na-del-ERB-1(0.10, RT) catalysts.....	90
4.11 Used and Na-reloaded catalysts.....	92
4.11.1 X-ray powder diffraction (XRD).....	92
4.11.2 Sorption properties.....	93
4.11.3 Scanning electron microscopy (SEM).....	93
4.12 Catalytic activities of used and Na-reloaded catalysts.....	94
4.13 Comparison of catalytic activity in transesterification reaction of palm oil over NaERB-1(0.10, RT) with other catalysts.....	96
4.14 Transesterification mechanism for ERB-1.....	97
V CONCLUSION	98
REFERENCES	100
APPENDICES	104
VITAE	120

LIST OF TABLES

Table	Page
1.1 Typical fatty acid composition of common oil source	3
2.1 Phase combinations for heterogeneous catalysis	17
2.2 Comparison of homogeneous and heterogeneous catalysts	19
2.3 IUPAC classification of porous materials	20
2.4 Features of adsorption isotherms	34
2.5 Typical fatty acid composition of palm oil	37
2.6 Compositional data of pyrolysis of oils	39
2.7 Comparison between production of biodiesel	44
3.1 Conditions of del-ERB-1 preparation	54
3.2 Conditions of NaERB-1 preparation	55
3.3 Fatty acid composition (wt.%) of commercial oleen palm oil	56
3.4 Preparation of calibration solutions	59
3.5 Preparation of calibration solutions	60
4.1 Textural properties of various NaOH solution concentrations loaded on ERB-1 by stirring at RT	65
4.2 Textural properties of various NaOH solution concentrations loaded on ERB-1 by refluxing at 60°C	65
4.3 The Na/SiO ₂ ratio of various NaOH solution concentrations loaded on ERB-1 by stirring at RT	66
4.4 The Na/SiO ₂ ratio of various NaOH solution concentrations loaded on ERB-1 by refluxing at 60°C	66
4.5 Textural properties of different alkali ions loaded on ERB-1	68
4.6 Alkali contents in alkali ion loaded on ERB-1 catalysts	68
4.7 Conversion and product yield in transesterification reaction of palm oil over non- catalyst and ERB-1 catalyst at 120 and 150°C (Condition: 10 wt% catalyst, MeOH to oil molar ratio of 9:1 for 24 h)	72

Table	Page
4.8 Conversion and product yield in transesterification reaction of palm oil over various NaOH solution concentrations loaded on ERB-1 by stirring at RT (Condition: 10 wt% catalyst, MeOH to oil molar ratio of 9:1 at 120°C for 24 h).....	74
4.9 Conversion and product yield in transesterification reaction of palm oil over various NaOH solution concentrations loaded on ERB-1 by refluxing at 60°C (Condition: 10 wt% catalyst, MeOH to oil molar ratio of 9:1 at 120°C for 24 h).....	75
4.10 Conversion and product yield in transesterification reaction of palm oil over different alkali ions loaded on ERB-1 (Condition: 10 wt% catalyst, MeOH to oil molar ratio of 9:1 at 120°C for 24 h).....	77
4.11 Conversion and product yield in transesterification reaction of palm oil over NaERB-1(0.10, RT) for different reaction times (Condition: 10 wt% catalyst, MeOH to oil molar ratio of 9:1 at 120°C).....	78
4.12 Conversion and product yield in transesterification reaction of palm oil over NaERB-1(0.10, RT) at various ratios of methanol to oil (Condition: 10 wt% catalyst at 120°C for 24 h).....	80
4.13 Conversion and product yield in transesterification reaction of palm oil over NaERB-1(0.10, RT) at various catalyst amount (Condition: MeOH to oil molar ratio of 9:1 at 120°C for 24 h).....	81
4.14 Conversion and product yield in transesterification reaction of palm oil over NaERB-1(0.10, RT) at various reaction temperatures (Condition: 10 wt% catalyst, MeOH to oil molar ratio of 9:1 for 24 h).....	83
4.15 Textural properties of del-ERB-1 samples with various conditions.....	86
4.16 Textural properties of del- ERB-1 and Na-del-ERB-1.....	88
4.17 The Na/SiO ₂ ratio of del-ERB-1 and Na-del-ERB-1(0.10, RT).....	88
4.18 Conversion and product yield in transesterification reaction of palm oil over ERB-1, del-ERB-1, NaERB-1(0.10, RT) and Na-del-ERB-1(0.10, RT) (Condition: 10 wt% catalyst, MeOH to oil molar ratio of 9:1 at 120°C for 24 h).....	91
4.19 Textural properties of used and Na-reloaded ERB-1.....	93
4.20 The Na/SiO ₂ of used and Na-reloaded ERB-1.....	93

Table

Page

4.21 Conversion and product yield in transesterification reaction of palm oil over used and Na-reloaded catalysts (Condition: 10 wt% catalyst, MeOH to oil molar ratio of 9:1 at 120°C for 24 h).....	95
---	----



ศูนย์วิทยทรัพยากร
จุฬาลงกรณ์มหาวิทยาลัย

LIST OF FIGURES

Figure	Page
1.1 World energy consumption.....	1
1.2 Diglyceride.....	3
1.3 Preparation of MCM-22 from as-synthesized MCM-22.....	5
1.4 The structure of calcined MCM-22.....	6
2.1 Catalytic cycle.....	12
2.2 Potential energy profile for an exothermic reaction, showing the lower activation energy of the catalyzed reaction.....	14
2.3 Framework of zeolite.....	20
2.4 Shape selectivity of zeolites with examples of reactions.....	23
2.5 Zeolite in the H form.....	25
2.6 Framework of ERB-1 catalyst.....	25
2.7 MWW structure of ERB-1 catalyst.....	26
2.8 Preparation of del-ERB-1 from as-synthesized ERB-1.....	27
2.9 Proposed structural model for del-ERB-1.....	28
2.10 Diffraction of X-rays by a crystal.....	29
2.11 The IUPAC classification of adsorption isotherm.....	33
2.12 Formation of triglyceride.....	36
2.13 Transesterification of triglycerides with alcohol.....	40
2.14 Esterification.....	41
2.15 Saponification from free fatty acid and ester.....	42
2.16 Hydrolysis of triglycerides.....	43
2.17 Mechanism of the acid-catalyzed transesterification.....	45
2.18 Mechanism of the base-catalyzed transesterification.....	45
2.19 Silylation of alcohol with MSTFA.....	47
3.1 Apparatus for ERB-1 synthesis.....	53
3.2 Apparatus for transesterification reaction.....	57
4.1 XRD patterns of as-synthesized (a) and calcined (b) of ERB-1.....	61

Figure	Page
4.2 The XRD patterns of various NaOH solution concentrations loaded on ERB-1 by stirring at RT: calcined ERB-1 (a), NaERB-1(0.05, RT) (b), NaERB-1(0.10, RT) (c), NaERB-1(0.30, RT) (d) and NaERB-1(0.50, RT) (e).....	63
4.3 The XRD patterns of various NaOH solution concentrations loaded on ERB-1 by refluxing at 60°C: calcined ERB-1 (a), NaERB-1(0.05, 60) (b), NaERB-1(0.10, 60) (c), NaERB-1(0.30, 60) (d) and NaERB-1(0.50, 60) (e).....	64
4.4 The XRD patterns of different alkali ions loaded on ERB-1: NaERB-1(0.10, RT) (a), KERB-1(0.10, RT) (b), RbERB-1(0.10, RT) (c) and CsERB-1(0.10, RT) (d).....	67
4.5 SEM images of different alkali ions loaded on ERB-1: calcined ERB-1 (a), NaERB-1(0.10, RT) (b), KERB-1(0.10, RT) (c), RbERB-1(0.10, RT) (d) and CsERB-1(0.10, RT) (e).....	69
4.6 Product yield from transesterification reaction of palm oil over non-catalyst and ERB-1 at 120°C and 150°C (Condition: 10 wt% catalyst, MeOH to oil of 9:1 for 24 h).....	73
4.7 Product yield from transesterification reaction of palm oil over various NaOH solution concentrations loaded on ERB-1 by stirring at RT (Condition: 10 wt% catalyst, MeOH to oil molar ratio of 9:1 at 120°C for 24 h).....	75
4.8 Product yield from transesterification reaction of palm oil over various NaOH solution concentrations loaded on ERB-1 by refluxing at 60°C (Condition: 10 wt% catalyst, MeOH to oil molar ratio of 9:1 at 120°C for 24 h).....	76
4.9 Product yield from transesterification reaction of palm oil over different alkali ions loaded on ERB-1 (Condition: 10 wt% catalyst, MeOH to oil molar ratio of 9:1 at 120°C for 24 h).....	77
4.10 Product yield from transesterification reaction of palm oil over NaERB-1(0.10, RT) for different reaction times (Condition: 10 wt% catalyst, MeOH to oil molar ratio of 9:1 at 120°C).....	79
4.11 Product yield from transesterification reaction of palm oil over NaERB-1(0.10, RT) at various ratios of methanol to oil (Condition: 10 wt% catalyst at 120°C for 24 h).....	80

Figure	Page
4.12 Product yield from transesterification reaction of palm oil over NaERB-1(0.10, RT) at various catalyst amounts (Condition: MeOH to oil molar ratio of 9:1 at 120°C for 24 h).....	82
4.13 Product yield from transesterification reaction of palm oil over NaERB-1(0.10, RT) at various reaction temperatures (Condition: 10 wt% catalyst, MeOH to oil molar ratio of 9:1 for 24 h).....	83
4.14 The XRD patterns of calcined ERB-1 (a), as-synthesized ERB-1 (b), swollen ERB-1 (c) and del-ERB-1 (d).....	85
4.15 The XRD patterns of del-ERB-1 samples with various conditions: D1 (a), D2 (b), D3 (c) and D4 (d).....	86
4.16 The XRD patterns of del-ERB-1 (a) and Na-del-ERB-1(0.10, RT) (b).....	87
4.17 SEM images of del-ERB-1: calcined ERB-1 (a), NaERB-1(0.10, RT) (b), del-ERB-1 (c) and Na-del-ERB-1(0.10, RT) (d).....	89
4.18 Product yield from transesterification reaction of palm oil over del-ERB-1 and Na-del-ERB-1(0.10, RT) (Condition: 10 wt% catalyst, MeOH to oil molar ratio of 9:1 at 120°C for 24 h).....	91
4.19 The XRD patterns of fresh NaERB-1(0.10, RT) (a), used ERB-1 (b) and Na-reloaded ERB-1 (c).....	92
4.20 SEM images of NaERB-1(0.10, RT) (a), used ERB-1 (b) and Na-reloaded ERB-1 (c).....	94
4.21 Product yield from transesterification reaction of palm oil over used and Na-reloaded catalysts (Condition: 10 wt% catalyst, MeOH to oil molar ratio of 9:1 at 120°C for 24 h).....	96
4.22 Proposed transesterification mechanism for ERB-1 catalyst.....	97

LIST OF SCHEMES

Scheme	Page
2.1 Parallel and sequential reactions.....	15
2.2 Classification of catalysts.....	16
3.1 The temperature program for transesterification reaction.....	48
3.2 The temperature program for calcination.....	49
3.3 The GC heating program for methyl esters, free glycerol, mono-, di- and triglyceride contents analysis.....	50
3.4 Preparation diagram for ERB-1.....	52
3.5 Preparation diagram for del-ERB-1.....	54



ศูนย์วิทยทรัพยากร
จุฬาลงกรณ์มหาวิทยาลัย

LIST OF ABBREVIATIONS

Btu	British thermal unit
AAS	Atomic absorption spectrometer
BET	Brunauer Emmett and Teller
ERB-1	Eni Ricerche Boralite-1
GC	Gas chromatograph
SEM	Scanning electron microscopy
SEM-EDX	Scanning electron microscopy-energy dispersive X-ray
XRD	X-ray diffraction
ICP-AES	Inductively coupled plasma-atomic emission spectrometry
MO	Methyl oleate
MP	Methyl palmitate
ML	Methyl linoleate
MS	Methyl stearate
IS	Internal standard
RT	Room temperature
RRT	Relative retention time
°C	Degree Celsius
rpm	Rounds per minute
ppm	Part per million
wt%	Percent by weight

ศูนย์วิทยทรัพยากร
จุฬาลงกรณ์มหาวิทยาลัย

CHAPTER I

INTRODUCTION

1.1 Background

World energy consumption is projected to increase by 59 percent over a 21-year forecast horizon, from 1999 to 2020. Worldwide energy use grows from 382 quadrillion British thermal units (Btu) in 1999 to 607 quadrillion Btu in 2020.

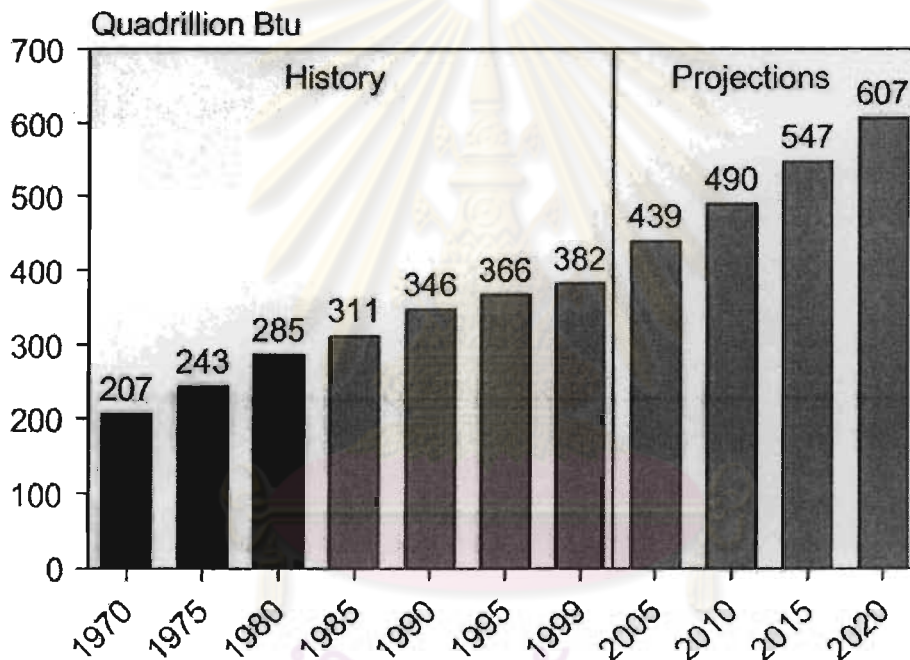


Figure 1.1 World energy consumption [1].

Majority of the world's energy needs are supplied through petrochemical sources, coal and natural gases, with the exception of hydroelectricity and nuclear energy, of all, these sources are finite and at current usage rates will be consumed shortly. Diesel fuels have an essential function in the industrial economy of a developing country and are used for transport of industrial and agricultural goods,

operation of diesel tractor and pump sets in agricultural sector. Economic growth is always accompanied by commensurate increase in the transport. The high energy demand in the industrialized world as well as in the domestic sector, the increase in diesel prices and environmental concerns causes the widespread use of fossil fuels. It is increasingly necessary to develop the renewable energy sources of limitless duration and smaller environmental impact than the traditional one. This has stimulated recent interest in alternative sources for petroleum-based fuels. An alternative fuel must be technically feasible, economically competitive, environmentally acceptable and readily available. One possible alternative to fossil fuel is the use of oils of plant origin like vegetable oils. This alternative diesel fuel can be termed as biodiesel. This fuel is biodegradable, non-toxic and has low emission profiles as compared to petroleum diesel. Usage of biodiesel will allow a balance to be sought between agriculture, economic development and the environment [1].

The use of vegetable oils as alternative fuels has been around for 100 years when the inventor of the diesel engine Rudolph Diesel first tested them, in his compression engine. To date there have been many problems found with using vegetable oils directly in diesel engines (especially in direct injection engines). These include;

1. Coking formation on the injectors to such an extent that fuel atomization does not occur properly or is even prevented as a result of plugged orifices
2. Carbon deposits
3. Oil ring sticking
4. Thickening and gelling of the lubricating oil as a result of contamination by vegetable oils
5. Lubricating problems

Other disadvantages to the use of vegetable oils and especially animal fats are the high viscosity (about 11-17 times higher than diesel fuel), lower volatilities that causes the formation of deposits in engines due to incomplete combustion and incorrect vaporization characteristics. These problems are associated with large triglyceride molecule and its higher molecular mass and avoided by modifying the engine less or more according to the conditions of use and the oil involved. At high temperatures there can be some problems with polymerization of unsaturated fatty

acids, this is where cross linking starts to occur between other molecules, causing very large agglomerations to be formed and consequently gumming occurs. This problem does not occur with fats as they have a very low concentration of unsaturated fatty acids as can be seen in Table 1.1.

Table 1.1 Typical fatty acid composition of common oil source

Lipid	Fatty acid composition, % by weight						
	Lauric 12:00*	Myristic 14:00	Palmitic 16:00	Stearic 18:00	Oleic 18:01	Linoleic 18:02	Linolenic 18:03
Soybean	0.1	0.1	10.2	3.7	22.8	53.7	8.6
Cottonseed	0.1	0.7	20.1	2.6	19.2	55.2	0.6
Palm	0.1	1.0	42.8	4.5	40.5	10.1	0.2
Lard	0.1	1.4	23.6	14.2	44.2	10.7	0.4
Tallow	0.1	2.8	23.3	19.4	42.4	2.9	0.9
Coconut	46.5	19.2	9.8	3.0	6.9	2.2	0.0

12:00 denotes a carbon length of 12 with one double bond.

Alcohol can be used as an additive to improve these properties, but pure vegetable oils are rarely used for a straight diesel fuel substitute. Fats, due to their high melting point and viscosity, can not be used directly in diesel engines or mixed with diesel fuels. The degree of saturation of the fatty acids attached to the glycerol backbone determines the boiling point of the triglyceride. Fat and oils are primarily composed of triglycerides, ester of glycerol (mono- and diglyceride) and fatty acids. The term monoglyceride or diglyceride refers to the number of fatty acids that are attached to the glycerol backbone i.e. a diglyceride would have one hydroxyl group and two fatty acid groups attached to the glycerol backbone as in Figure 1.2.

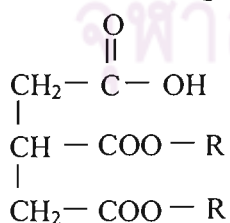


Figure 1.2 Diglyceride

Moreover, the plant oils usually contain phospholipids, sterols, water and other impurities. Because of these, the oil cannot be used fuel directly. To overcome these problems the oil requires slight chemical modification mainly transesterification, pyrolysis and emulsification. Among these, the transesterification is the key and foremost important step to produce the cleaner and environmentally safe fuel from vegetable oils [2].

Mono-alkyl esters are usually produced by transesterification of triglyceride with mono-alkyl alcohols, such as methanol. Also known as methanolysis, this reaction is commonly carried out in the presence of homogeneous base or acid catalysts. The acid-catalyzed process often uses sulfonic acid and hydrochloric acid as catalysts; however the reaction time is very long (48-96 h) even at reflux of methanol and a high molar ratio of methanol to oil is need (30-150:1 mol.%). Potassium hydroxide, sodium hydroxide and their carbonates as well as potassium and sodium alkoxides such as NaOCH_3 , are usually used as base catalysts for this reaction. As the catalytic activity of a base is higher than that of an acid and acid catalysts are more corrosive, the base catalyzed process is preferred to acid catalyzed one and is thus most often used commercially. However, in the conventional homogeneous manner, removal of the base catalysts is technically difficult and a large amount of wastewater is produced to separate and clean the catalyst and the product. Therefore, conventional homogeneous catalysts are expected to be replaced in the near future by environmentally friendly heterogeneous catalysts mainly because of environmental constraints and simplifications in the existing processes [3].

In this work, the solid catalyst of base loaded on ERB-1 and on delaminated ERB-1 is first adopted for the production of biodiesel. The catalytic efficiency in methanolysis of palm oil is studied regarding the yield of palm oil to methyl esters.

1.2 Literature reviews on the ERB-1 catalyst

In 1994, Millini *et al.* [4] synthesized the borosilicate molecular sieve, hereafter referred to as ERB-1 (EniRicercheBoralite-1), to study the structure of ERB-1 precursor. The crystallization of ERB-1 took place under hydrothermal condition in the presence of piperidine (PD) as organic template at 175°C for seven days and had the several gel compositions. The results shown that $\text{SiO}_2/\text{B}_2\text{O}_3$ molar ratio appeared to be a critical parameter; in fact, ERB-1 was preferably obtained with this molar ratio ranging between 1.5 and 3. At higher boron concentration, new phases

probably non-porous borosilicates appeared, at low concentration ($\text{SiO}_2/\text{B}_2\text{O}_3 > 10$) amorphous materials were obtained together with quartz or other compact silicates. ERB-1 was formed in the absence of sodium ions from gels containing only PD. However, if sodium was added to the starting gel, it was retained only in minor amounts in the recovered solid. This indicated a negligible, if any, role played by the alkali metal ion in directing the formation of ERB-1. ERB-1 might be obtained in the presence of both boron and aluminium. Increasing the amount of aluminium in the synthesis gels resulted in increased aluminium concentration and decreased boron concentration in the crystalline solid. This feature gave the opportunity to tailor the acidity of the materials in view of their use as heterogeneous catalysts.

The framework topology of ERB-1, similar to MCM-22, has been characterized by two types of independent ten-membered ring (10MR) pore systems; one is constituted by two-dimensional sinusoidal channels, the other by micropores possessing twelve-membered ring (12MR) supercages. The two-dimensional sinusoidal 10MR channels, which exist in the MWW sheets, have been designated “interlayer micropores”. The 10MR micropores with 12MR supercages, which form between stacked MWW sheets through the calcination of ERB-1 precursor (which causes the removal of hexamethyleneimine template in the ERB-1 precursor and hydration condensation between facing silanols on the sheets), have been designated “intralayer micropores” [5].

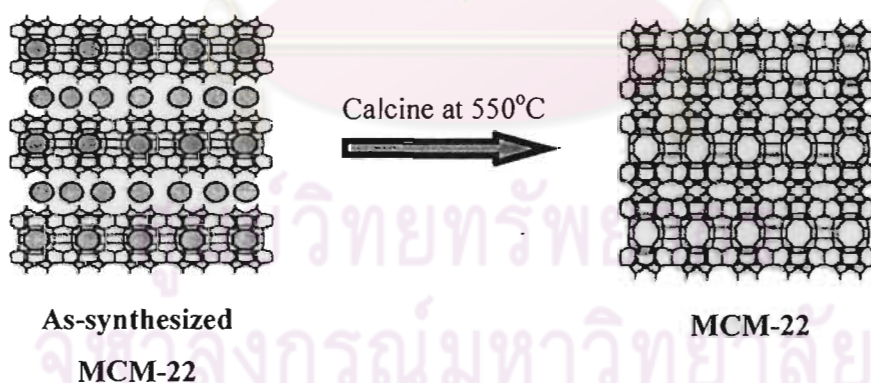


Figure 1.3 Preparation of MCM-22 from as-synthesized MCM-22.

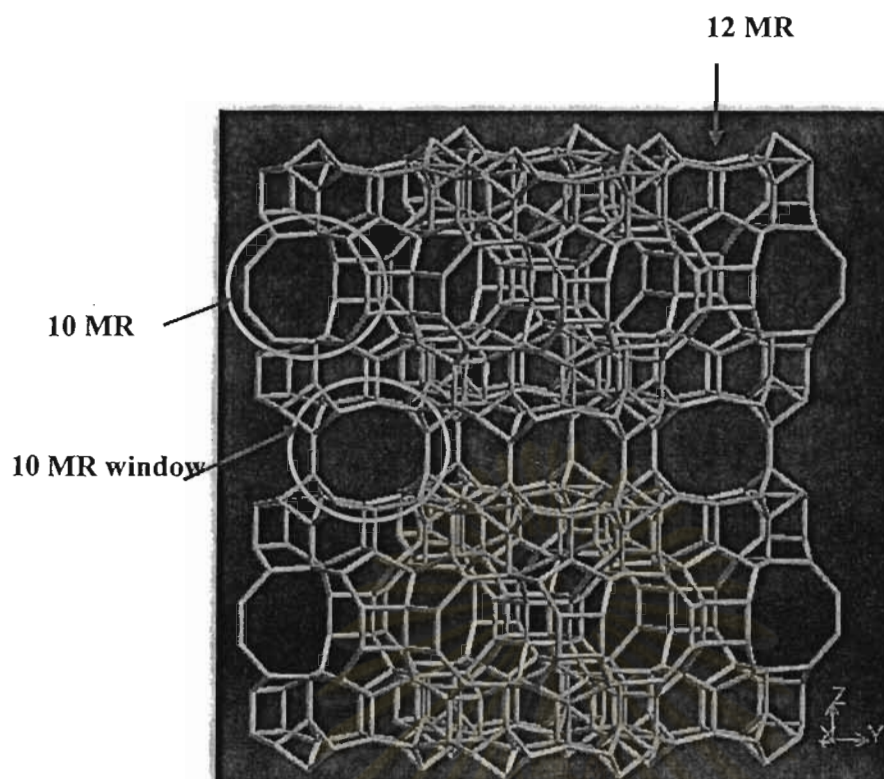


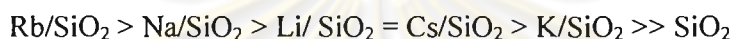
Figure 1.4 The structure of calcined MCM-22.

In 1996, Perego *et al.* [6] adopt ERB-1 catalyst in cumene synthesis by the alkylation of benzene with propylene. This reaction has been largely applied in the petrochemical industry. Cumene has been an important chemical intermediate mainly used for the production of phenol and acetone. The result showed the propylene conversion and the cumene selectivity obtained 95.40% and 90.70%, respectively.

Increasing the efficiency of ERB-1 catalyst in order to apply for large molecule, Corma *et al.* compared the catalytic activity of ITQ-2 (Delaminated MCM-22) and MCM-22 in vacuum gasoil cracking. The results indicated that the activity of ITQ-2 is extremely higher than MCM-22, in agreement with the much higher amount of accessible acid sites presented in the former. The higher ratio of “external” versus microporous surface in the case of ITQ-2 was responsible for the formation of more liquids and less gases and coke. When looking into the ratios $C_3^= / C_3$, $C_4^= / C_4$, and $iC_4^= / iC_4$, it is clear that ITQ-2 gave a higher ratio of olefins to paraffins than MCM-22, showing a lower hydrogen transfer ability of the above structures [7].

1.3 Literature reviews on the basic modification and application of catalysts

In 2006, Ziolk *et al.* [8] prepared the catalysts containing all alkali metals (from Li to Cs) located in amorphous silica as support by wetness impregnation method. The acid–base properties of the obtained materials were tested in the acetonylacetone (AcAc) cyclisation. The formation of 2,5-dimethylfuran (DMF) occurred on acidic centres, whereas in the production of 3-methyl-2-cyclopentenone (MCP) basic centres took part. On the basis of the ratio of selectivity to MCP/selectivity to DMF, the sequence of the basicity of the prepared catalysts could be estimated. The basicity of the catalyst was stated if $MCP/DMF \gg 1$. Taking into account the activity of the alkali metal located in amorphous silica, the following order was observed:



Silica based catalyst rubidium modified sample exhibited the highest basic properties concluded from MCP/DMF.

1.4 Literature reviews on transesterification reaction of triglycerides

In 1998 Papayannakos *et al.* [9] studied thermal non-catalytic transesterification of soybean oil with methanol. The experiments were conducted at 220 and 235°C at 55 and 62 bar initial pressure with various methanol/oil ratios ranged from 6/1 to 27/1. The evolution of concentration of four components in the ester phase could be very well followed by the kinetic model. It was observed that methyl ester content was 85% after 10 h reaction time at 235°C and 67 wt% after 8 h at 220°C. Following an initial increase, the content of diglyceride decreased and after 10 h at 235°C, it was less than 0.3 wt%. Monoglyceride content initially increased and reached a maximum, like diglyceride, but it decreased very slowly and even after 10 h at 235°C, a value close to 15 wt% was determined. Triglyceride content decreased with reaction time and a total conversion is observed after 10 h at 235°C. It could conclude that triglyceride and diglyceride conversion rates were much higher than the conversion rates of monoglyceride to glycerol.

A non-catalytic biodiesel production route with supercritical methanol was studied by Ayhan Demirbas [10]. Supercritical methanol has a high potential for both

transesterification of triglyceride and methyl esterification of free fatty acids to methyl ester for diesel substitution. In the supercritical method, the conversion increased to 95% in 10 min and the viscosity values of vegetable oil methyl ester were between 3.59 and 4.63 mm²/s, whereas those of vegetable oils were between 27.2 and 53.6 mm²/s. However, the presence of water and fatty acid affected positively the formation of methyl ester in supercritical method which was opposite to the alkali and acid catalysts.

Comparative studies on transesterification method were studied by Demirbas [11]. The transesterification process was catalyzed by brønsted acids, preferably by sulfon and sulfuric acids. These catalysts gave very high yields in alkyl esters, but the reactions were slow. In case of the base catalyzed transesterification, it proceeded faster than the acid catalyzed reaction. Alkali metal alkoxides (as CH₃ONa for the methanolysis) were the most active catalysts, since they gave very high yield (>98%) in short reaction time (30min) even if they were applied at low molar concentrations (0.5 mol%). In the supercritical alcohol method, the yield of conversion rose to 50-95% for the first 8 min and in the catalytic supercritical methanol method, the yield of conversion rose to 60-90% for the first 1 min.

Leung and Guo [12] were studied the characteristics and performance of three commonly used homogeneous catalysts (NaOH, KOH and CH₃ONa) used for alkaline-catalyzed transesterification of edible Canola oil and used frying oil (UFO) in 2006. The transesterification of the UFO with methanol was carried out with a 7.5:1 molar ratio of methanol to oil at 70°C for 30 min. The three catalysts exhibited similar trends on the conversion of triglycerides to esters but different amounts of catalyst were required for achieving the same conversion. Maximum ester content was reached at 1.1, 1.3 and 1.5 wt% of the catalyst concentration for NaOH, CH₃ONa and KOH, respectively. Comparing the performance and cost of the three catalysts, NaOH was found to be more superior than CH₃ONa and KOH due to its lower price and smaller amount of catalyst required. Therefore, NaOH was chosen for this research. Moreover, the process variables that influence the transesterification of triglycerides, such as catalyst concentration, molar ratio of methanol to raw oil, reaction time, reaction temperature and free fatty acids content of raw oil in the reaction system were investigated and optimized. Optimal reaction for transesterification of

commercial edible Canola oil with a 0.25% free fatty acid content, the optimal conditions were 40–45 °C for 60 min, 1.0 wt% NaOH and 6:1 molar ratio of methanol/oil. For UFO with an acid value of 2 could be achieved at 60 °C for a reaction time of 20 min, 1.1 wt% NaOH and 7:1 molar ratio of methanol/UFO. But the maximum biodiesel yield is 88.8 wt%, much lower than 93.5 wt% for neat Canola oil.

In this recent, many heterogeneous catalysts have been developed to catalyze the transesterification because these catalysts can be regenerated many times. For example, NaX zeolite, soybean oil methyl esters preparation using NaX zeolites loaded with KOH was studied by Xie *et al.* [13]. The soybean conversion reached the maximum value of 85.6% after reaction had been a methanol/oil molar ratio 10:1, 3 wt% catalyst amount at 65°C for 8 h. In order to study the stability of KOH/NaX catalyst, it was regenerated before use in the next experiment. A decline was observed in the conversion to methyl esters from 85.6% to 48.7%, thereby indicating the decrease of catalytic activity. Such a decrease in the catalytic activity was, probably, responsible for leaching of the KOH species from the supported catalyst. The cost of catalyst is significant and for the economic reason the catalyst needs to be regenerated. For this purpose, the used catalyst was regenerated by impregnating catalysts in an aqueous solution of 5% KOH. The results showed that the regenerated catalyst could give a good conversion of 84.3%.

The transesterification of soybean oil with methanol were performed with NaX zeolite, ETS-10 and metal catalysts. The NaX and ETS-10 were exchanged with potassium and cesium whereas NaX also containing occluded sodium oxide and sodium azide. The reactions were carried out at 60°C, 120°C and 150°C for 24 h and mol ratio of oil to alcohol was 1:6. The result showed that the increased conversions were attributed to the higher basicity of ETS-10 and large pore structures that improved intra-particle diffusion. Conversion to methyl esters in excess of 90% were achieved at temperatures of 150°C and 120°C with residence times of 24 h. Pretreating the ETS-10 catalyst at 500°C for 4 h was instrumental in increasing the activity of the ETS-10 catalyst. Methyl ester yield increased with an increase in temperature and the catalyst was reused without observed loss of activity. Moreover, potassium and cesium exchanged ETS-10 provided lower methyl ester yield than ETS-10 in all temperature [14].

Furthermore, the activity and selectivity of a variety of commercial alkali and alkali-earth metals compounds as catalysts for the methanolysis of sunflower oil at 323 K had been investigated by Gandia *et al.* in 2008 [15]. The hydroxide of alkali metals (Li, Na, K, Rb and Cs) were completely soluble in methanol and behaved as homogeneous catalysts. These were very active methanolysis catalysts that at the very low concentration equivalent to 0.1% NaOH, taken as reference, achieved sunflower oil conversions above 90% after 100 min of reaction. Selectivities for methyl esters (biodiesel) were also high. Differences in performance among the several alkali metals hydroxides were not significant so there was no advantage in using lithium, rubidium or cesium compounds in place of the conventional NaOH or KOH. As concerns the remainder catalysts, some of them showed negligible activity, they were NaHCO_3 , Na_2HPO_4 , NaH_2PO_4 , KHCO_3 , K_2HPO_4 , CaCO_3 , calcined CaO, fresh and calcined MgO as well as $\text{Mg}(\text{OH})_2 \cdot 4\text{MgCO}_3$. However, K_2CO_3 , Na_2CO_3 and Na_3PO_4 resulted moderately active thus evidencing the effect of the basic strength of the anions in these compounds in the formation of active methoxide species. This explained the higher methanolysis activity of carbonates or phosphates than bicarbonates, hydrogen phosphates or dihydrogen phosphates. Potassium carbonate at a concentration equivalent to 0.2% NaOH required only 108 min to achieve 90% oil conversion. Sodium carbonate and phosphate exhibited a very similar behaviour and achieved 90% oil conversion after 8 h. However, these compounds were moderately soluble in the reaction mixture which could also contribute to their higher activity. The percentage of catalyst dissolved at reaction completion amounted up to 55% for K_2CO_3 , 20% for Na_2CO_3 and 15% for Na_3PO_4 .

From literatures that were mentioned above, the heterogeneous base catalyst was suitable for transesterification reaction both in catalytic activity and separation process. Thus in this research, the modified ERB-1 catalysts were chosen as catalyst in transesterification reaction. The reaction was started with palm oil and methanol to produce fatty acid methyl ester (biodiesel). The catalytic activities of used and Na-reloaded catalysts were also investigated.

1.5 Objectives

- 1.5.1 To synthesize and characterize ERB-1 catalyst.
- 1.5.2 To increase the activity of ERB-1 by delamination.
- 1.5.3 To modify the basic strength of ERB-1 and delaminated ERB-1 (Del-ERB-1) by loading with alkali hydroxide solution.
- 1.5.4 To study the catalytic activity of these catalysts in transesterification reaction of palm oil.
- 1.5.5 To investigate the optimum condition in transesterification reaction.
- 1.5.6 To study the catalytic activity of used and reloaded catalyst.

1.6 Scope of work

ERB-1 catalyst is synthesized by piperidine (PD) as the structure directing agent and is delaminated to the delaminated ERB-1 (Del-ERB-1). Both ERB-1 and del-ERB-1 are loaded with hydroxide of alkali ions (Na, K, Rb and Cs) in order to increase the basic strength of catalyst that has the potential to increase the methyl esters yield. Then, these catalysts are tested in transesterification of palm oil by studying the effects of temperature, time, methanol to oil molar ratio and catalyst amount to biodiesel production. Furthermore, the catalytic activities of used and Na-reloaded catalysts are also investigated.

CHAPTER II

THEORY

2.1 The phenomenon catalysis [16]

Catalysis is the key to chemical transformations. Most industrial syntheses and nearly all biological reactions require catalysts. Furthermore, catalysis is the most important technology in environmental protection, i.e., the prevention of emissions. A well-known example is the catalytic converter for automobiles.

While it was formerly assumed that the catalyst remained unchanged in the course of the reaction, it is now known that the catalyst is involved in chemical bonding with the reactants during the catalytic process. Thus catalysis is a cyclic process: the reactants are bound to one form of the catalyst and the products are released from another, regenerating the initial state.

In simple terms, the catalytic cycle can be described as shown in Figure 2.1. The intermediate catalyst complexes are in most cases highly reactive and difficult to detect.

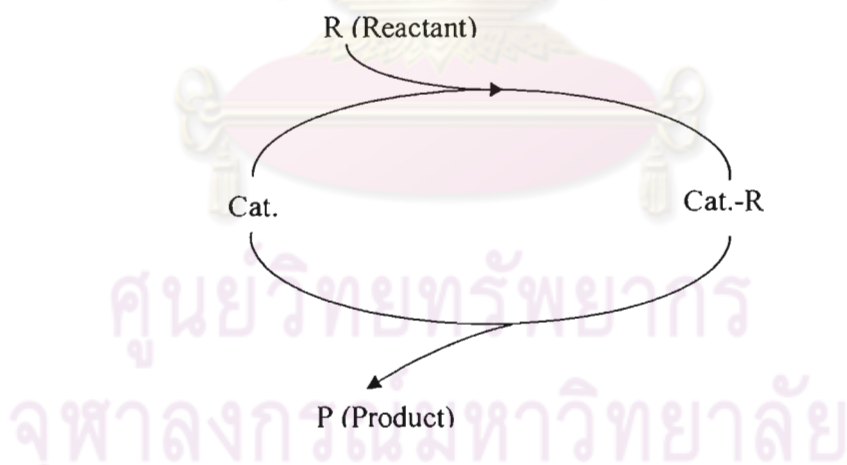


Figure 2.1 Catalytic cycle.

In theory, an ideal catalyst would not be consumed but this is not the case in practice. Owing to competing reactions, the catalyst undergoes chemical changes and its activity becomes lower (catalyst deactivation). Thus catalysts must be regenerated or eventually replaced.

Apart from accelerating reactions, catalysts have another important property: they can influence the selectivity of chemical reactions. This means that completely different products can be obtained from a given starting material by using different catalyst systems. Industrially, this targeted reaction control is often even more important than the catalytic activity.

Most of the process involved in crude-oil processing and petrochemistry, such as purification stage, refining and chemical transformations, require catalysts. Environmental protection measures such as automobile exhaust control and purification of off-gases from power stations and industrial plant would be inconceivable without catalysts.

2.2 Definition of catalysis

The usually accepted definition of a catalyst is that it is a substance that increases the rate at which a chemical system approaches equilibrium, without being consumed in the process. Catalysis is the phenomenon of a catalyst in reaction.

2.3 Mode of action of catalysts

2.3.1 Activity

Activity is a measure of how fast one or more reactions proceed in the presence of the catalyst. Activity can be defined in term of kinetics or from a more practically oriented viewpoint.

The primary effect of a catalyst on a chemical reaction is thus to increase its rate and this must mean to increase its rate coefficient. According to the collision theory, the rate coefficient k is given by

$$k = PZ \exp(- E/RT) \quad (2.1)$$

where P is the so-called steric factor, Z the collision frequency, R the gas constant and T the absolute temperature.

In terms of the absolute rate theory, the rate coefficient is given by

$$k = \frac{kT}{h} \exp(-\Delta G^\ddagger/RT) \quad (2.2)$$

where k is the Boltzmann constant, ΔG^\ddagger is the Gibbs free energy of activation and h is Planck's constant and so the effect of a catalyst must be to decrease the free energy of activation of the reaction. This in turn is composed of an entropy and an enthalpy of activation. Now the entropy of activation in a catalyzed reaction will usually be less than in the corresponding uncatalyzed reaction because the transition state is immobilized on the catalyst surface with consequent loss of translational freedom. There must therefore be a corresponding decrease in the enthalpy of activation to compensate for this or more than to compensate if efficient catalysis is desired. Thus according to either theory, the activation energy for a catalyzed reaction ought to be less than for the same uncatalyzed reaction.

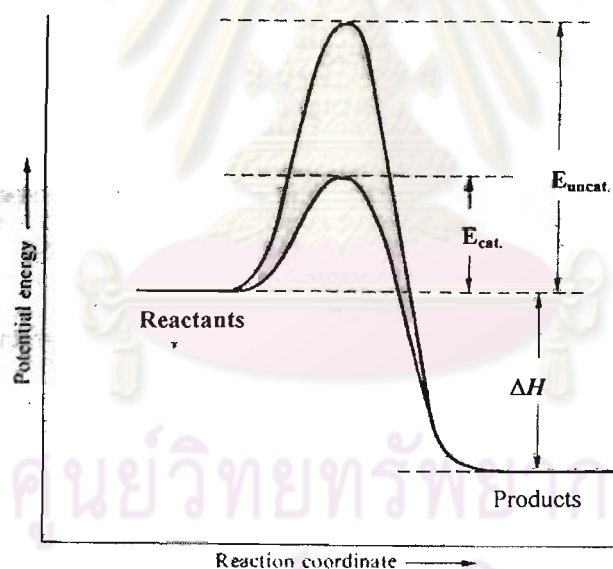
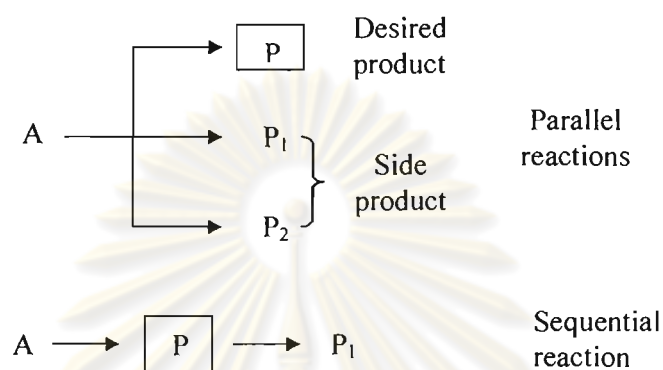


Figure 2.2 Potential energy profile for an exothermic reaction, showing the lower activation energy of the catalyzed reaction.

2.3.2 Selectivity

The selectivity of a reaction is the fraction of the starting material that is converted to the desired product. It is expressed by the ratio of the amount of desired product to the reacted quantity of a reaction partner and therefore gives information about the course of the reaction. In addition to the desired reaction, parallel and sequential reactions can also occur.



Scheme 2.1 Parallel and sequential reactions.

2.3.3 Stability

The chemical, thermal and mechanical stability of a catalyst determines its lifetime in industrial reactors. Catalyst stability is influenced by numerous factors, including decomposition, coking and poisoning. Catalyst deactivation can be followed by measuring activity or selectivity as a function of time.

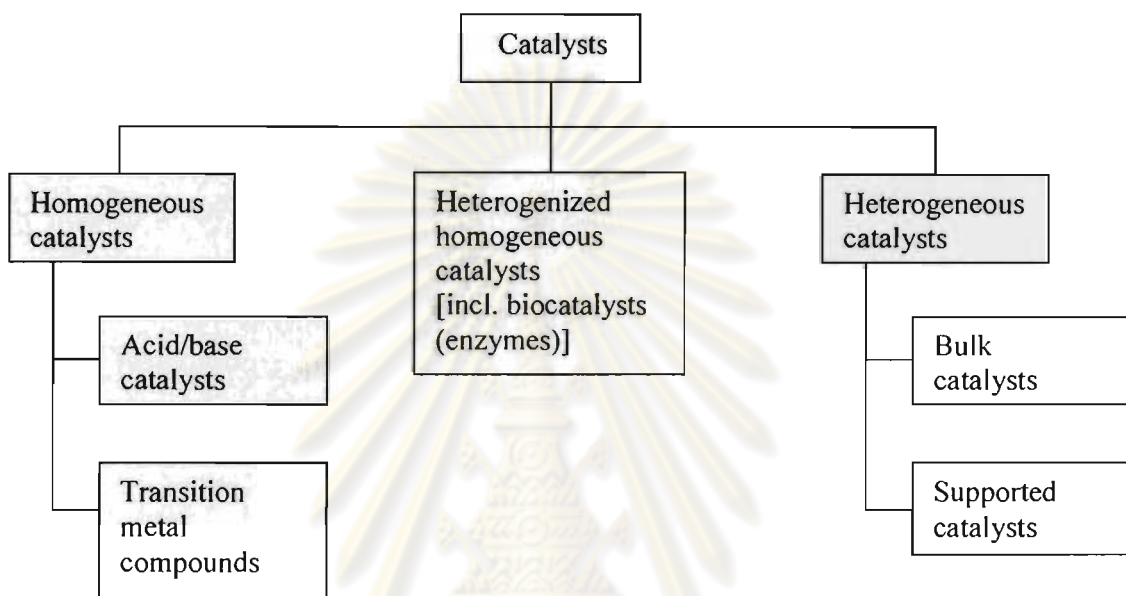
Catalysts that lose activity during a process can often be regenerated before they ultimately have to be replaced. The total catalyst lifetime is of crucial importance for the economics of a process.

Today the efficient use of raw materials and energy is of major importance and it is preferable to optimize existing processes than to develop new ones. For various reasons, the target quantities should be given the following order of priority:

$$\text{Selectivity} > \text{stability} > \text{activity}$$

2.4 Classification of catalytic systems

In fact, it is possible to divide catalytic systems into two distinct categories: homogeneous catalysts and heterogeneous catalysts (solid-state catalysts). There are also intermediate forms such as homogeneous catalysts attached to solid (supported catalysts), also known as immobilized catalysts. The well-known biocatalysts (enzymes) also belong to this class



Scheme 2.2 Classification of catalysts.

When the catalyst is of the same phase as the reactants and no phase boundary exists, it is spoken of *homogeneous catalysis*. This may take place either:

- (i) in the gas phase, as, for example, when nitrogen oxide catalyses the oxidation of sulphur dioxide; or
- (ii) in the liquid phase, as when acids and bases catalyze the mutarotation of glucose.

When a phase boundary separates the catalyst from the reactants, it is spoken of *heterogeneous catalysis*. A number of phase combinations can then occur, as shown in Table 2.1. Other possible phase combinations rarely arise in catalysis.

Table 2.1 Phase combinations for heterogeneous catalysis

Catalyst	Reactant	Example
Liquid	Gas	Polymerization of alkenes catalyzed by phosphoric acid
Solid	Liquid	Decomposition of hydrogen peroxide catalyzed by gold
Solid	Gas	Ammonia synthesis catalyzed by iron
Solid	Liquid+Gas	Hydrogenation of nitrobenzene to aniline catalyzed by palladium

There is however one extremely important group of substances which cannot be accommodated within this classification. Enzymes are neither a homogeneous nor heterogeneous system but something in between.

Enzymes are the driving force for biological reactions. They exhibit remarkable activities and selectivities. For example, the enzyme catalase decomposes hydrogen peroxide 10^9 times faster than inorganic catalysts. The enzymes are organic molecules that almost always have a metal as the active center. Often the only difference to the industrial homogeneous catalysts is that the metal center is ligated by one or more proteins, resulting in a relatively high molecular mass.

Apart from high selectivity, the major advantage of enzymes is that they function under mild conditions, generally at room temperature in aqueous solution at pH values near 7. Their disadvantage is that they are sensitive, unstable molecules which are destroyed by extreme reaction conditions. They generally function well only at physiological pH values in very dilute solutions of the substrate.

Enzymes are expensive and difficult to obtain in pure form. With the increasing importance of biotechnological processes, enzymes will also grow in importance.

2.5 Comparison of homogeneous and heterogeneous catalysis

Whereas for heterogeneous catalysts, phase boundaries are always present between the catalyst and the reactants, in homogeneous catalysis, catalyst, starting materials and products are present in the same phase. Homogeneous catalysts have a higher degree of dispersion than heterogeneous catalysts since in theory each individual atom can be catalytically active. In heterogeneous catalysts only the surface atoms are active.

Due to their high degree of dispersion, homogeneous catalysts exhibit a higher activity per unit mass of metal than heterogeneous catalysts. The high mobility of the molecules in the reaction mixture results in more collisions with substrate molecules. The reactants can approach the catalytically active center from any direction and a reaction at an active center does not block the neighboring centers. This allows the use of lower catalyst concentrations and milder reaction conditions.

The most prominent feature of homogeneous transition metal catalysts are the high selectivities that can be achieved. Homogeneously catalyzed reactions are controlled mainly by kinetics and less by material transport because diffusion of the reactants to the catalyst can occur more readily. Due to the well-defined reaction site, the mechanism of homogeneous catalysis is relatively well understood. In contrast, processes occurring in heterogeneous catalysis are often obscure.

In industrial use, both types of catalyst are subjected to deactivation as a result of chemical or physical processes. Table 2.2 summarizes the advantages and disadvantage of the two classes of catalyst.

The major disadvantage of homogeneous transition metal catalysts is the difficulty of separating the catalyst from the product. Heterogeneous catalysts are either automatically removed in the process or they can be separated by simple methods such as filtration or centrifugation. In the case of homogeneous catalysts, more complicated processes such as distillation, liquid-liquid extraction and ion exchange must often be used.

Table 2.2 Comparison of homogeneous and heterogeneous catalysts

	Homogeneous	Heterogeneous
<i>Effectivity</i>		
Active centers	all metal atoms	only surface atoms
Concentration	low	high
Selectivity	high	lower
Diffusion problems	practically absent	present (mass-transfer-controlled reaction)
Reaction conditions	Mild (50-200°C)	severe (often > 250°C)
Applicability	limited	wide
Activity loss	irreversible reaction with products (cluster formation); poisoning	Sintering of the metal crystallite; poisoning
<i>Catalyst properties</i>		
Structure/stoichiometry	defined	undefined
Modification possibilities	high	low
Thermal stability	low	high
<i>Catalyst separation</i>	sometimes laborious (chemical decomposition, distillation, extraction)	fixed-bed: unnecessary suspension: filtration
<i>Catalyst recycling</i>	Possible	unnecessary (fixed-bed) or easy (suspension)
<i>Cost of catalyst losses</i>	high	low

2.6 Porous materials [18]

Porous materials have found wide applications in many technological fields such as adsorption and environmental technology including catalysis because of their high surface area, large pore volume and uniformity in pore size. The design and processing of novel porous materials are driven by the rapidly growing demands of emerging applications such as separation, purification, immobilization of biological

molecules, drug delivery and gas storage, etc. Porous materials can be classified based on the IUPAC pore diameter into three groups that is shown in Table 2.3.

Table 2.3 IUPAC classification of porous materials

Porous material	Pore diameter (nm)
Microporous	Up to 2
Mesoporous	2-50
Macroporous	50 to up

2.7 Shape-Selective catalysis: Zeolites

2.7.1 Composition and structure of zeolites

Zeolites are crystalline, hydrated aluminosilicates of group I and group II elements, in particular, sodium, potassium, magnesium, calcium, strontium and barium. Structurally the zeolites are “framework” aluminosilicates which are based on an infinitely extending three-dimensional network of AlO_4^- and SiO_4 tetrahedra linked to each other by sharing all of the oxygens.

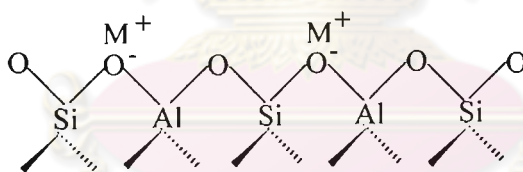
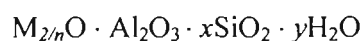


Figure 2.3 Framework of zeolite.

Zeolites may be represented by the empirical formula



In this oxide formula, x is generally equal to or greater than 2 since AlO_4^- tetrahedra are joined only to SiO_4 tetrahedra, n is the cation valence. The framework contains channels and interconnected voids which are occupied by the cation and water

molecules. The cations are quite mobile and may usually be exchanged, to varying degrees, by other cations. Intracrystalline “zeolitic” water in many zeolites is removed continuously and reversibly. In many other zeolites, mineral and synthetic, cation exchange or dehydration may produce structural changes in the framework.

The structural formula of a zeolite is best expressed for the crystallographic unit cell as: $M_{x/n}[(AlO_2)_x(SiO_2)_y] \cdot wH_2O$ where M is the cation of valence n , w is the number of water molecules and the ratio y/x usually has values of 1-5 depending upon the structure. The sum $(x+y)$ is the total number of tetrahedra in the unit cell. The composition is characterized by the Si/Al atomic ratio or by the molar ratio R

$$R = \frac{SiO_2}{Al_2O_3}$$

and the pore size of zeolites by the type (A, X, Y).

Zeolites are mainly distinguished according to the geometry of the cavities and channels formed by the grid framework of SiO_4 and AlO_4^- tetrahedra. The tetrahedra are the smallest structural units into which zeolites can be divided. Linking these primary building units together leads to 16 possible secondary building blocks (polygons), the interconnection of which produces hollow three-dimensional structures. The entrances to the cavities of the zeolites are formed by 6-, 8-, 10- and 12-ring apertures (small-, medium- and widepore zeolites).

2.7.2 Production of zeolites

Zeolite syntheses start from alkaline aqueous mixtures of aluminum and silicon compounds. The reactions are sometimes carried out at atmospheric pressure but more often in a high-pressure autoclave. The controlled crystallization of a particular zeolite requires careful control of the concentration and stoichiometry of the reaction partners, the temperature and the shearing energy of the stirrer. After mixing of the liquid phase and formation of a gel, a transition of the gel phase in to the liquid aqueous phase occurs, whereby crystalline zeolites are formed from the amorphous particles.

The silicon-rich pentasils are mainly synthesized in the presence of organic cations. Their open structures seem to be formed around hydrated cations or other

cations such as NR_4^+ . In particular, templates such as tetrapropylammonium hydroxide are used and are of decisive importance for the crystallization of the zeolite structures. The C, H and N of the tertiary ammonium cation are removed in the subsequent calcination of the microcrystalline product.

2.8 Catalytic properties of the zeolites

In 1962 the zeolites were introduced by Mobil Oil Corporation as new cracking catalysts in refinery technology. They were characterized by higher activity and selectivity in cracking and hydrocracking. At the end of the 1960s, the concept of shape-selective catalysis with zeolites was introduced to petrochemistry and the zeolites became of increasing importance in catalysis research and applied catalysis.

Due to the outstanding catalytic properties of the zeolites, no other class of catalysts offers so much potential for variation and so many advantages in application. Their advantages over conventional catalysts can be summarized as follows:

- Crystalline and therefore precisely defined arrangement of SiO_4 and AlO_4^- tetrahedral. This results in good reproducibility in production.
- Shape selectivity: only molecules that are smaller than the pore diameter of the zeolite undergo reaction.
- Controlled incorporation of acid centers in the intracrystalline surface is possible during synthesis and/or by subsequent ion exchange.
- Catalytically active metal ions can be uniformly applied to the catalyst by ion exchange or impregnation. Subsequent reduction to the metal is also possible.
- Zeolite catalysts are thermally stable up to 600°C and can be regenerated by combustion of carbon deposits.

Let us first take a closer look at the most important properties of the zeolites:

- Shape selectivity
- Acidity

2.8.1 Shape selectivity

The inner pore system of the zeolites presents a well-defined crystalline surface. The structure of the crystalline surface is predetermined by the composition and type of the zeolite and is clearly defined. Such conditions are otherwise found only with single-crystal surfaces.

The accessibility of the pores for molecules is subject to definite geometric or steric restrictions. The shape selectivity of zeolites is based on the interaction of reactants with the well-defined pore system. A distinction is made between three variants, which can, however, overlap:

- Reactant selectivity
- Product selectivity
- Restricted transition state selectivity

Figure 2.4 shows these schematically with examples of reactions.

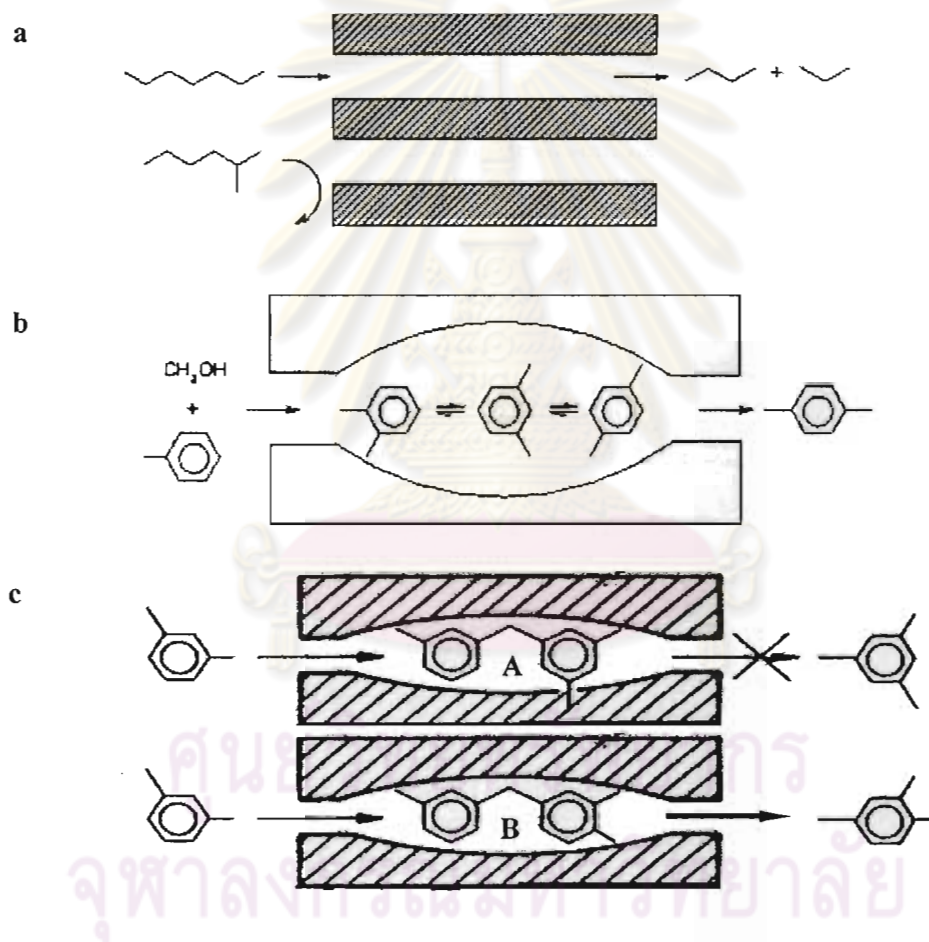


Figure 2.4 Shape selectivity of zeolites with examples of reactions.

- a) Reactant selectivity: cleavage of hydrocarbons
- b) Product selectivity: methylation of toluene
- c) Restricted transition state selectivity: disproportionation of m-xylene

2.8.1.1 Reactant selectivity

Reactant selectivity means that only starting materials of a certain size and shape can penetrate into the interior of the zeolite pores and undergo reaction at the catalytically active sites. Starting material molecules that are larger than the pore apertures can not react (Figure 2.4 a). Hence the term “molecular sieve” is justified.

2.8.1.2 Product selectivity

Product selectivity arises when, corresponding to the cavity size of a zeolite, only products of a certain size and shape that can exit from the pore system are formed. Well-known examples of product selectivity are the methylation of toluene (Figure 2.4 b) and the disproportion of toluene on ZSM-5.

2.8.1.3 Restricted transition state selectivity

This third form of shape selectivity depends on the fact that chemical reactions often proceed via intermediates. Owing to the pore system, only those intermediates that have a geometrical fit to the zeolite cavities can be formed during catalysis. This selectivity occurs preferentially when both monomolecular and bimolecular rearrangements are possible. In practice, it is often difficult to distinguish restricted transition state selectivity from product selectivity.

2.8.2 Acidity of zeolites

Zeolites in the H form are solid acids whose acid strength can be varied over a wide range by modification of the zeolites (ion exchange, partial dealumination and isomorphic substitution of the framework Al and Si atoms). Direct replacement of the alkali metal ions by protons by treatment with mineral acids is only possible in exceptional cases (e.g., the high-silicon zeolite ZSM-5). The best method is exchange of the alkali metal ions by NH_4^+ ions, followed by heating the resulting ammonium salts to 500-600°C (deammonization).

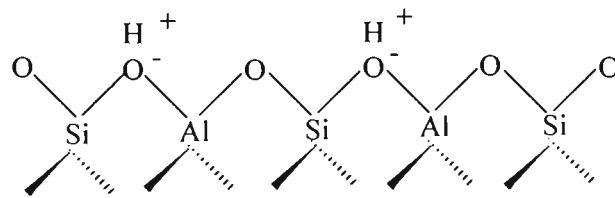


Figure 2.5 Zeolite in the H form.

2.9 Structure of ERB-1 catalyst

The synthesis of the borosilicate molecular sieve, hereafter referred to as ERB-1 (EniRicercheBoralite-1) and isostructural with the aluminosilicate PSH-1, was claimed by Bellussi *et al.* in 1988.

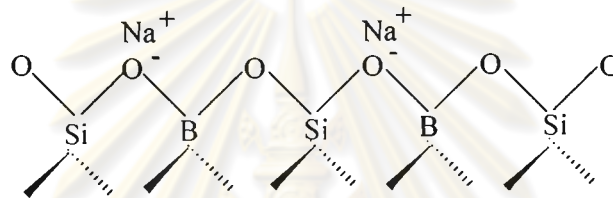


Figure 2.6 Framework of ERB-1 catalyst.

The framework topology of ERB-1, MWW structure, is characterized by two independent non-interconnected pore systems both having ten-membered ring openings. One system is defined by two-dimensional sinusoidal channels with slightly folded elliptical apertures, and the other consists of large supercages, with the internal diameter defined by twelve-membered rings, interconnected by slightly elliptical apertures.

ศูนย์วิทยทรัพยากร
จุฬาลงกรณ์มหาวิทยาลัย

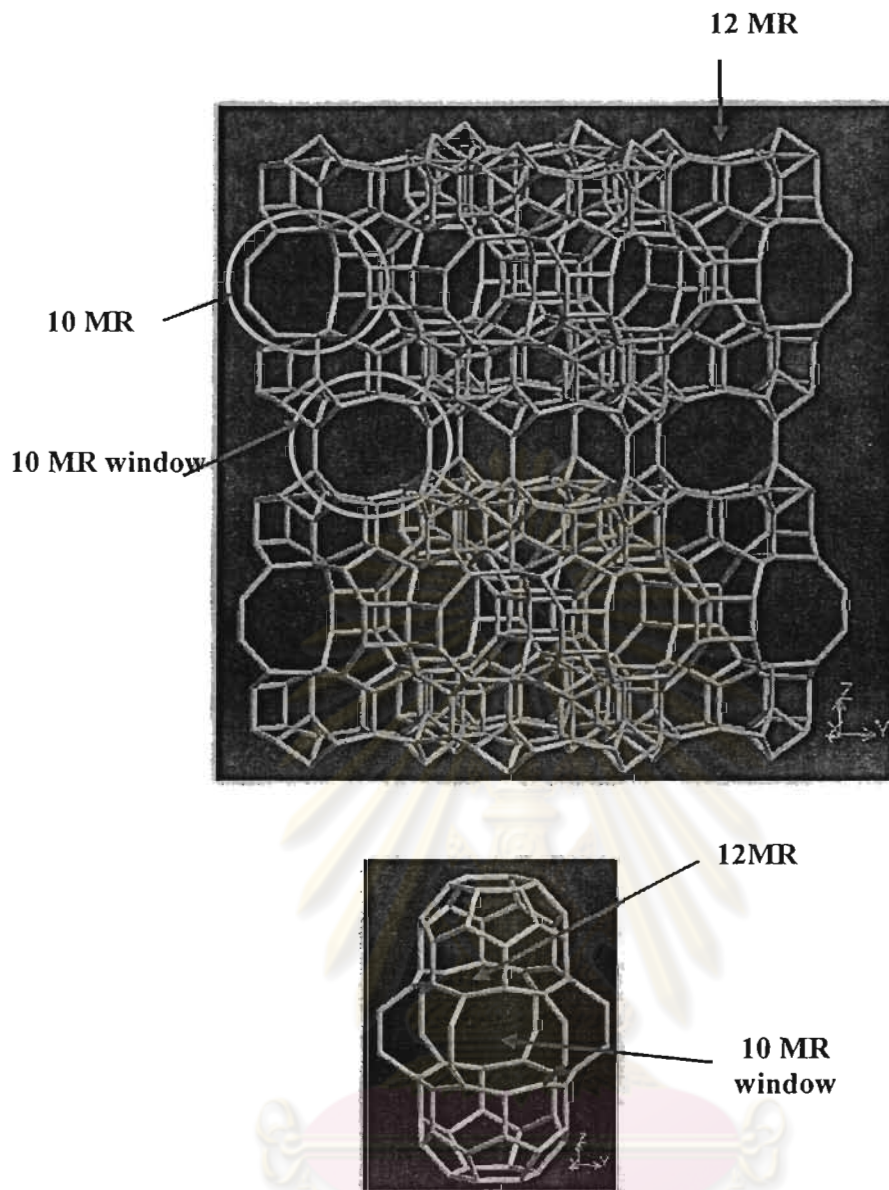


Figure 2.7 MWW structure of ERB-1 catalyst.

The crystallization of molecular sieves usually takes place under hydrothermal conditions in the presence of organic molecules (templates) which are responsible for the microporous structure formed. The crystalline solid (precursor) recovered has a bi-dimensional (2D) layered structure and contains the template molecules which are subsequently eliminated by calcination. The precursor already possesses a three-dimensional (3D) framework of $[TO_4]$ tetrahedra and little or no structural variation occurs during calcination. Surprisingly, this is not the case for ERB-1. In fact, a

number of investigations allowed us to conclude for a layered structure of ERB-1 precursor, the 3D structure being formed only upon calcination.

Details about some representative syntheses of ERB-1, the $\text{SiO}_2/\text{B}_2\text{O}_3$ molar ratio appears to be a critical parameter; in fact, ERB-1 is preferably obtained with this molar ratio ranging between 1.5 and 3. At higher boron concentration new phases, probably non-porous borosilicates, appear; at low concentration ($\text{SiO}_2/\text{B}_2\text{O}_3 > 10$) amorphous materials were obtained together with quartz or other compact silicates. ERB-1 is formed in the absence of sodium ions from gels containing only piperidine as structure-directing agent. However, if sodium is added to the starting gel it is retained only in minor amounts in the recovered solid. This indicates a negligible, if any, role played by the alkali metal ion in directing the formation of ERB-1.

2.10 Preparation of del-ERB-1

Delaminated ERB-1 (Del-ERB-1) has been prepared by swelling and delaminating an as-synthesized ERB-1. Del-ERB-1 consists of thin sheets with an extremely high external surface area. After calcination, these sheets consist of a hexagonal array of “cups” that penetrate into the sheet from both sides. These cups form by a 12-member ring (12MR) and meet at the centre of the layer, forming a double 6-member ring window that connects the cups, bottom to bottom. As a result, a smooth, 10-member ring (10MR) channel system runs in between the cups, inside the sheet.

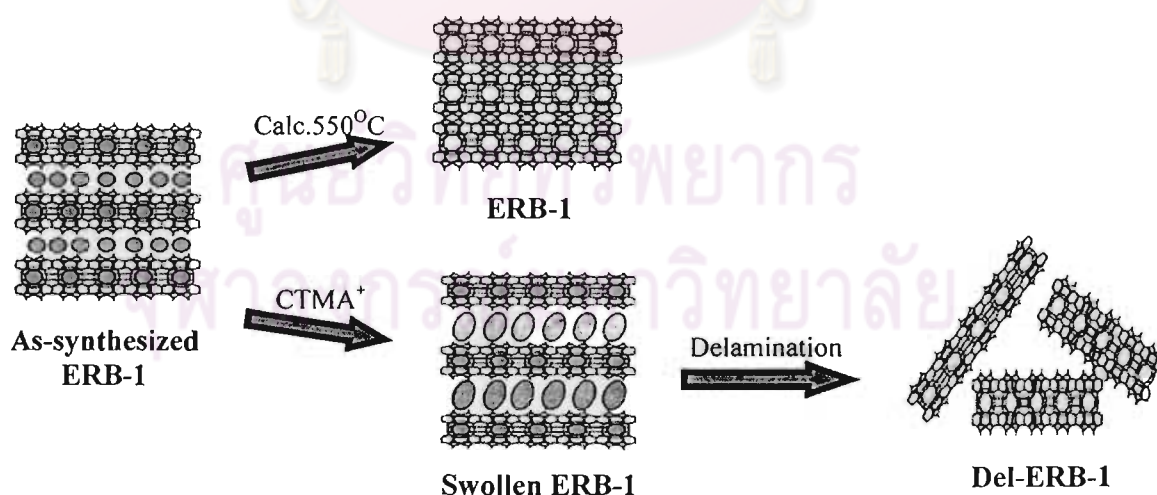


Figure 2.8 Preparation of del-ERB-1 from as-synthesized ERB-1.

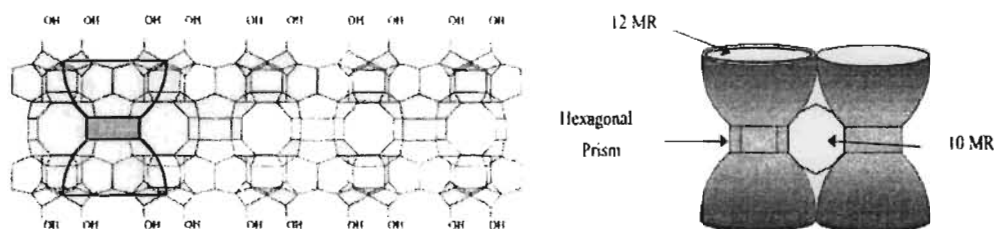
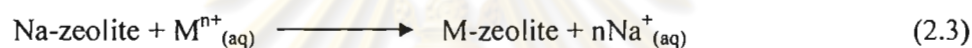


Figure 2.9 Proposed structural model for del-ERB-1.

2.11 Ion-exchange

The efficiency way of modifying the acidity and basicity of catalyst is ion-exchange. Ion-exchange is often an essential procedure in the preparation and/or manufacture of zeolites for use either as sorbents or catalysts. Metal ion and cationic complexes can occupy framework cationic sites of zeolite as shown in equation 2.3.



The interaction is stronger than that the case of physisorption. This method provides stronger coulombic interaction between species and zeolite anionic framework. These exchange reactions obey the same kinetic laws as the reaction of heterogeneous catalysis. They take place in two consecutive stages, the diffusion of solute to be exchanged at the surface and the ionic exchange itself. When the support is a porous solid, as are most catalyst supports, the diffusion limitation can be extragranular or intragranular.

2.12 Catalyst deactivation and regeneration

Catalysts have only a limited lifetime. Some lose their activity after a few minutes, others last for more than ten years. The maintenance of catalyst activity for as long as possible is of major economic importance in industry. A decline in activity during the process can be the result of various physical and chemical factors, for example:

- Blocking of the catalytically active sites
- Loss of catalytically active sites due to chemical, thermal or mechanical processes

2.13 Characterization of materials

2.13.1 X-ray powder diffraction (XRD)

An electron in an alternating electromagnetic field will oscillate with the same frequency as the field. When an X-ray beam hits an atom, the electrons around the atom start to oscillate with the same frequency as the incoming beam. In almost all directions we will have destructive interference, that is, the combining waves are out of phase and there is no resultant energy leaving the solid sample. However, the atoms in a crystal are arranged in a regular pattern, in a very few directions we will have constructive interference. The waves will be in phase and there will be well defined X-ray beams leaving the sample at various directions. Hence, a diffracted beam may be described as a beam composed of a large number of scattered rays mutually reinforcing one another.

Let us consider an X-ray beam incident on a pair of parallel planes P1 and P2, separated by an interplanar spacing d .

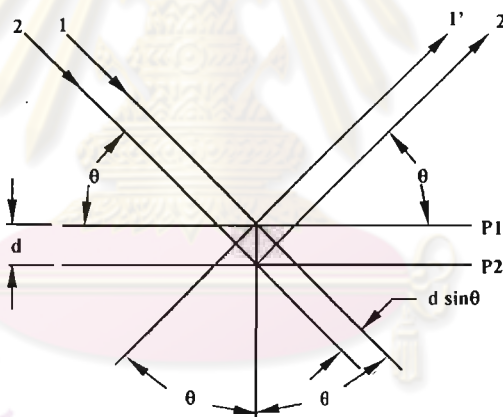


Figure 2.10 Diffraction of X-rays by a crystal.

The two parallel incident rays 1 and 2 make an angle (THETA; θ) with these planes. A reflected beam of maximum intensity will result if the waves represented by 1' and 2' are in phase. The difference in path length between 1 to 1' and 2 to 2' must then be an integral number of wavelengths, (LAMBDA; λ). We can express this relationship mathematically in Bragg's law.

$$2d\sin\theta = n\lambda \quad (2.4)$$

The process of reflection is described here in terms of incident and reflected (or diffracted) rays, each making an angle THETA with a fixed crystal plane. Reflections occurs from planes set at angle THETA with respect to the incident beam and generates a reflected beam at an angle 2-THETA from the incident beam.

The possible d-spacing defined by the indices h, k, l are determined by the shape of the unit cell. Rewriting Bragg's law we get :

$$\sin \theta = \lambda/2d \quad (2.5)$$

Therefore the possible 2-THETA values where we can have reflections are determined by the unit cell dimensions. However, the intensities of the reflections are determined by the distribution of the electrons in the unit cell. The highest electron density is found around atoms. Therefore, the intensities depend on what kind of atoms we have and where in the unit cell they are located. Planes going through areas with high electron density will reflect strongly, planes with low electron density will give weak intensities.

2.13.2 Nitrogen adsorption-desorption technique

Adsorption is the process by which atoms or molecules become attached to a surface. In principle adsorption can occur at any surface but it has particular significance when a gas or liquid is in contact with a porous solid such as charcoal or alumina.

The forces that bind an adsorbed molecule (*adsorbate*) to the surface may be physical or chemical in nature (though the dividing line between the two is not sharp), giving rise to the phenomena of *physisorption* and *chemisorption* respectively. In practical terms, the two types of adsorption are normally distinguished on the basis of the strength of the bond formed between adsorbate and surface - weak Van der Waals bonds are deemed to give rise to physisorption, while shared electron bonds are responsible for chemisorption.

Adsorption is described using an *adsorption isotherm*; this shows the amount of gas adsorbed as a function of pressure, at constant temperature. The simplest

isotherm is due to Langmuir and can readily be derived with the following assumptions:

1. In the gas phase, the adsorbate behaves ideally.
2. Adsorbed molecules are confined to a monolayer and never form multilayers.
3. Every part of the surface has the same energy of adsorption (the energy that is released as the adsorbate bonds to the surface).
4. No adsorbate-adsorbate interaction takes place.
5. Every site is equivalent.
6. The adsorbed molecules are immobile.

Let us consider each of these assumptions: The first is often reasonable, but the second is unreasonable for physisorption, since multiple layers are common. The next three assumptions are never correct - no surface is ever uniform and even for a noble gas, the interaction between adsorbed molecules may account for as much as 25% of the measured heat of adsorption at half coverage of the surface. The final assumption is usually true at low temperature but not at room temperature for physisorption, since, although the bonds joining each molecule to the surface have an energy usually greater than kT , it is not true that $e^{-E/RT} \ll 1$. Quite recent work has shown that many molecules are in fact highly mobile when “stuck” onto the surfaces of solids.

Especially at low temperatures, multilayer adsorption is common, and the BET (Brunauer, Emmett and Teller) isotherm is more useful under these conditions. The BET isotherm makes the same assumptions as the Langmuir isotherm, except that multilayer adsorption is permitted. The derivation of the Langmuir and BET isotherms is given in standard physical chemistry texts (derivation of the Langmuir isotherm frequently appears in physical chemistry exam papers); we shall quote only the final BET result here:

$$\frac{x}{V(1-x)} = \frac{1}{V_m C} + \frac{(C-1)x}{V_m C} \quad (2.6)$$

In equation (2.6), x is the relative pressure (p/p_0) at which a volume of gas V , measured at room temperature and pressure, is adsorbed. p is the pressure of the gas, and p_0 its saturation vapour pressure at the temperature of the vessel containing the adsorbent. In this experiment nitrogen is the gas, and the adsorbent alumina is held at 77K, the normal boiling point of liquid nitrogen where, by definition, its vapour pressure p_0 equals atmospheric pressure. V_m is the volume of adsorbed gas required to form a monolayer on the adsorbent, and is a constant for a given temperature. Equation (2.6) demonstrates that a plot of $x/[V(1-x)]$ against x should give a straight line, whose intercept is $1/V_m C$ and slope is $(C-1)/V_m C$. Thus from the slope and intercept, C and V_m can be found.

The constant C is given by:

$$C = \frac{a_1 b_2}{a_2 b_1} \times e^{-(E_1 - E_L)/RT} \quad (2.7)$$

where $(E_1 - E_L)$ is the difference between the average enthalpy of adsorption in the first layer and the enthalpy of liquefaction of the adsorbate. a_1 , a_2 , b_1 and b_2 are constants connected with the formation and evaporation of the first and higher layers of adsorbed molecules.

Brunauer and his co-workers have suggested that in certain circumstances $a_1 b_2 / a_2 b_1$ should be close to unity. If this is so, it would be possible to determine E_1 from a measurement of C from the isotherm. The BET method yields a value for V_m , the volume of gas required to form a monolayer. Brunauer and Emmett suggested that the area of each adsorbed molecule could be found from the density of the liquid adsorbate according to the equation:

$$\text{Molecular area} = 4(0.866) \left\{ \frac{M}{4(2)^2 N d} \right\}^{\frac{2}{3}} \quad (2.8)$$

where M is the molecular weight of the adsorbate, N is Avogadro's number and d the density of the liquefied adsorbent, which equals 0.808 g cm^{-3} for liquid nitrogen. Knowing V_m , the surface area can then be found. Adsorption amount depends on gas

pressure, adsorption temperature and properties of adsorptive gas and adsorbent solid. In nitrogen adsorption isotherm measurement, temperature is constant and gas is limited, thus the isotherm changes according to the property of solid. The surface area of a solid includes both the external surface and the internal surface of the pores. Several forms of isotherm besides the langmuir type have been shown in Figure 2.12. According to the IUPAC definition, microporous materials exhibit a type I adsorption-desorption isotherm. Nonporous or macroporous exhibit types II, III and VI and mesoporous exhibits type IV and V.

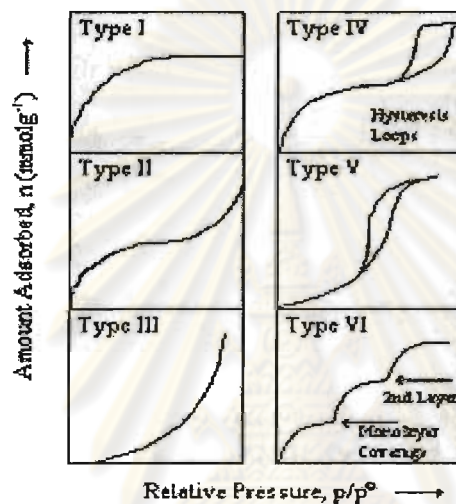


Figure 2.11 The IUPAC classification of adsorption isotherm.

Adsorption isotherms are described as shown in Table 2.4 based on the strength of the interaction between sample surface and gas adsorbate.

ศูนย์วิทยทรัพยากร
จุฬาลงกรณ์มหาวิทยาลัย

Table 2.4 Features of adsorption isotherms

Type	Features	
	Interaction between sample surface and gas adsorbate	Porosity
I	Relatively strong	Microporous
II	Relatively strong	Nonporous
III	Weak	Nonporous
IV	Relatively strong	Mesoporous
V	Weak	Microporous or Mesoporous
VI	Relatively strong	Nonporous

2.13.3 Inductively coupled plasma-atomic emission spectrometry (ICP-AES)

This method describes multi-elemental determinations by ICP-AES using sequential or simultaneous optical systems and axial or radial viewing of the plasma. The instrument measures characteristic emission spectra by optical spectrometry. Samples are nebulized and the resulting aerosol is transported to the plasma torch. Element-specific emission spectra are produced by a radio-frequency inductively coupled plasma. The spectra are dispersed by a grating spectrometer and the intensities of the emission lines are monitored by photosensitive devices. Background correction is required for trace element determination. Background correction is not required in cases of line broadening where a background correction measurement would actually degrade the analytical result. Additional interferences and matrix effects must be recognized and appropriate corrections made; tests for their presence are described. Alternatively, users may choose multivariate calibration methods. In this case, point selections for background correction are superfluous since whole spectral regions are processed.

2.14 Diesel oil [19]

Diesel or diesel fuel is a specific fractional distillate of petroleum fuel oil or a washed form of vegetable oil that is used as fuel in a diesel engine invented by German engineer Rudolf Diesel.

2.14.1 Petroleum diesel

Petroleum diesel or petrodiesel is produced from petroleum and is a hydrocarbon mixture, obtained in the fractional distillation of crude oil between 200°C and 350°C at atmospheric pressure.

The density of petroleum diesel is about 850 g/l whereas gasoline has a density of about 720 g/l, about 15% less. When burnt, diesel typically releases about 40.9 MJ/l, gasoline releases 34.8 MJ/l, about 15% less. Diesel is generally simpler to refine from petroleum than gasoline.

2.14.2 Chemical composition

Petroleum-derived diesel is composed of about 75% saturated hydrocarbons (primarily paraffins including *n*, *iso*, and cycloparaffins) and 25% aromatic hydrocarbons (including naphthalenes and alkylbenzenes). The average chemical formula for common diesel fuel is $C_{12}H_{23}$, ranging from approx. $C_{10}H_{20}$ to $C_{15}H_{28}$

2.14.3 Alternative diesel fuels

They are developed for securing the supply of future transportation fuels and for cleaner fuel utilization. Alternative fuels for diesel engines include synthetic middle distillates from natural gas, liquefied petroleum gas (LPG), compress natural gas (CNG), dimethyl ether (DME), biodiesel and other.

2.15 Natural palm oil

Palm oil is a form of edible vegetable oil obtained from the fruit of the oil palm tree. Previously the second-most widely produced edible oil, after soybean oil, 28 million metric tons were produced worldwide in 2004. It may have now surpassed soybean oil as the most widely produced vegetable oil in the world. Palm oil has two species of oil palm, the better known one is originating from Guinea, Africa. The palm fruit is the source of both palm oil (extracted from palm fruit) and palm kernel oil (extracted from the fruit seeds). Palm oil itself is reddish because it contains a high amount of beta-carotene. It is used as cooking oil to make margarine and is a component of many processed foods. Palm oil is one of the few vegetable oils relatively high in saturated fats (such as coconut oil) and thus semisolid at room temperature. It is also an important component of many soap, washing powders and

personal care products and has controversially found a new use as a feedstock for biofuel.

2.16 Palm oil composition

Palm oil extracted from the mesocarp of the fruit of the palm *Elaeis guineensis*. The mesocarp comprises about 70-80% by weight of the fruit and about 45-50% of this mesocarp is oil. The rest of the fruit comprises the shell, kernel, moisture and other non fatty fiber. The extracted oil is known as crude palm oil (CPO) which until quite recently was known as the golden commodity.

Palm oil like all natural fats and oils comprises mainly mono-, di- and triglycerides. Free fatty acids, moisture, dirt and minor components of non oil fatty matter referred to collectively as unsaponifiable matter.

2.16.1 Triglyceride

It is a chemical compound of one molecule of glycerol bound to three molecules of fatty acid.

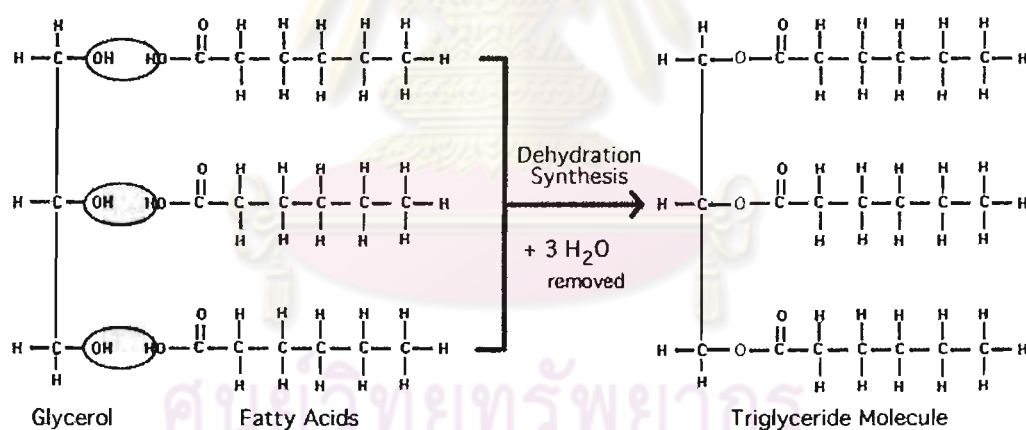


Figure 2.12 Formation of triglyceride.

The fatty acids could be of the same type or they could be different. The property of a triglyceride will depend on the different fatty acids that combine to form the triglyceride. The fatty acids themselves are different depending on their chain length and degree of saturation. The short chain fatty acids are of lower melting point and are more soluble in water; whereas, the longer chain fatty acids have higher melting

points. The melting point is also dependent on degree of non-saturation. Unsaturated acids will have a lower melting point compared to saturated fatty acids of similar chain length. The two most predominant fatty acids in palm oil are C16:0 (saturated) palmitic acid and C18:1 (unsaturated) oleic acid. Typical fatty acid composition of palm oil is given in Table 2.5.

Table 2.5 Typical fatty acid composition of palm oil

C. No.: DB	Fatty acid	%Weight
C12:0	Lauric acid	0.2
C14:0	Myristic acid	1.1
C16:0	Palmitic acid	44.0
C18:0	Stearic acid	4.5
C18:1	Oleic acid	39.2
C18:2	Linoleic acid	10.1
C18:3	Linolenic acid	0.4
C20:0	Arachidic acid	0.4

C: carbon, DB: double bond

2.16.2 Mono- and diglycerides and free fatty acid (FFA)

In the presence of heat and water the triglycerides break up by a process known as hydrolysis to form free fatty acids thus yielding mono- and diglycerides and FFA which is of crucial importance to the refiners. Mono- and diglycerides account for about 3 to 6% by weight of the glycerides in the oil. Good oils having lower amount of mono and diglycerides is said to be of great importance in the fractionation process because they act as emulsifying agents inhibiting crystal formation and making filtration difficult. The amount of mono- and diglycerides and FFA is reduced in the process of refining as can be seen from their concentration in the DFA (Distillate Fatty Acid).

2.16.3 Moisture and dirt

This is a result of milling practice. Good milling will reduce moisture and dirt in palm oil but normally it is in the range of 0.25%.

2.16.4 Minor component

These are classified into one category because they are fatty in nature but are not really oils. They are referred to as unsaponifiable matter and they include that are caroteneoids, tocopherols, sterols, polar lipids, impurities.

2.17 The production of biodiesel

There are several generally accepted ways to make biodiesel some more common than others, e.g. blending and transesterification and several others that are more recent developments, e.g. reaction with supercritical method. An overview of these processes is as follows;

2.17.1 Direct use and blending

The direct use of vegetable oils in diesel engines is problematic and has many inherent failings. It has only been researched extensively for the past couple of decades but has been experimented with for almost a hundred years. Although some diesel engines can run pure vegetable oils engines, turbocharged direct injection engines such as trucks are prone to many problems. Energy consumption, with the use of pure vegetable oils, was found to be similar to that of diesel fuel. For short term use ratios of 1:10 to 2:10 oil to diesel have been found to be successful. The difficulties may be grouped into three key areas.

2.17.2 Microemulsions

Microemulsions are defined as a colloidal equilibrium dispersions of optically isotropic fluid microstructures with dimensions generally in the 1-150 nm range. These are formed spontaneously from two normally immiscible liquids and one or more ionic or non-ionic amphiphiles. A microemulsion is designed to tackle the problem of the high viscosity of pure vegetable oils by reducing the viscosity of oils with solvents such as simple alcohols. The performances of ionic and non-ionic microemulsions were found to be similar to diesel fuel, over short term testing. They also achieved good spray characteristics with explosive vaporization which improved the combustion in performance was observed however significant injector needle sticking, carbon deposits, incomplete combustion and increasing viscosity of lubricating oils were reported.

2.17.3 Thermal cracking (Pyrolysis)

Pyrolysis is the conversion of one substance into another by means of applying heat, i.e. heating in the absence of air or oxygen with temperatures ranging from 450°C – 850°C. In some situations this is with the aid of a catalyst leading to the cleavage of chemical bonds to yield smaller molecules. Unlike direct blending, fats can be pyrolysed successfully to produce many smaller chain compounds. The pyrolysis of fats has been investigated for over a hundred years, especially in countries where there is a shortage of petroleum deposits. Typical catalyst that can be employed in pyrolysis are SiO₂ and Al₂O₃. The ratios of light to heavy compounds are temperature and time dependent. Typical breakdown of compounds found from pyrolysis of safflower and soybean oil are listed in Table 2.6.

Table 2.6 Compositional data of pyrolysis of oils

	Percent by weight	
	*HO Safflower	Soybean
Alkanes	40.9	29.9
Alkenes	22.0	24.9
Alkadienes	13.0	10.9
Aromatics	2.2	1.9
Unresolved unsaturates	10.1	5.1
Carboxylic acids	16.1	9.6
Unidentified	12.7	12.6

*HO High oleic safflower oil

The equipment for pyrolysis or thermal cracking is expensive for modest throughputs. Although the products are chemically similar to pyrochemically based diesel, oxygen removal from the process decreases the products benefits of being an oxygenated fuel. This decreases its environmental benefits and generally produces more fuel similar in properties of gasoline than diesel with the addition of some low value materials.

2.17.4 Transesterification (Alcoholysis)

Transesterification is the reaction of a lipid with an alcohol to form esters and a by-product, glycerol. It is in principle the action of one alcohol displacing another from an ester, the term alcoholysis (cleavage by an alcohol). The reaction, as shown in Figure 2.14 is reversible and thus an excess of alcohol is usually used to force the equilibrium to the product side. The stoichiometry for the reaction is 3:1 alcohol to lipids however in practice this is usually increased to 6:1 to increase product yield. A catalyst is usually used to speed up the reaction and may be basic, acid or enzymatic in nature. The alkalis that are generally used include NaOH, KOH, carbonates and corresponding sodium and potassium alkoxides such as sodium methoxide, ethoxide, propoxide and butoxide. Sodium hydroxide is the most common alkali catalyst that is used, due to economical reasons and availability. Alkali catalysed reactions are used more often commercially than acid catalysts, as the reactions are faster.

Only simple alcohols can be used in transesterification such as methanol, ethanol, propanol, butanol and amyl alcohol. Methanol is most often used for commercial and process reasons related to its physical and chemical nature (shortest chain alcohol and is polar). The type of catalyst, the reaction conditions and the concentration of impurities in a transesterification reaction determine the path that the reaction follows.

For alkali catalysed transesterification, water and free fatty acid (FFA) are not favourable to the reaction, so anhydrous triglycerides and alcohol are necessary to minimise the production of soap. Soap production decreases the amount of esters and renders the separation of glycerol and esters difficult. In current commercial processes using crude feed stock, excess alkali is added to remove all the FFAs.

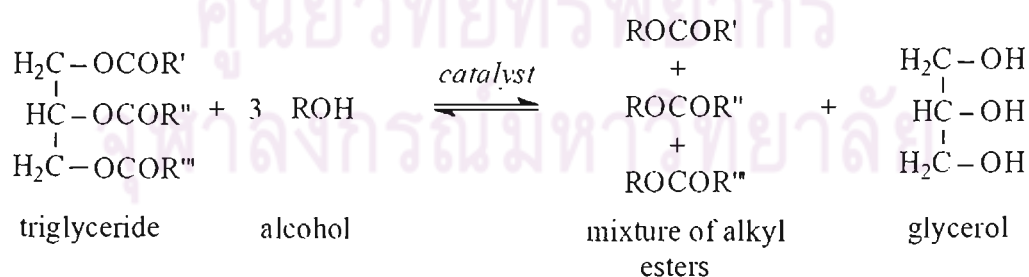


Figure 2.13 Transesterification of triglycerides with alcohol.

2.17.4.1 Esterification

The formation of esters occurs through a condensation reaction known as esterification. This requires two reactants, carboxylic acids (fatty acids) and alcohols. Esterification reactions are acid catalysed and proceed slowly in the absence of strong acids such as H_2SO_4 , H_3PO_4 and HCl . The equation for an esterification reaction can be seen in Figure 2.15.

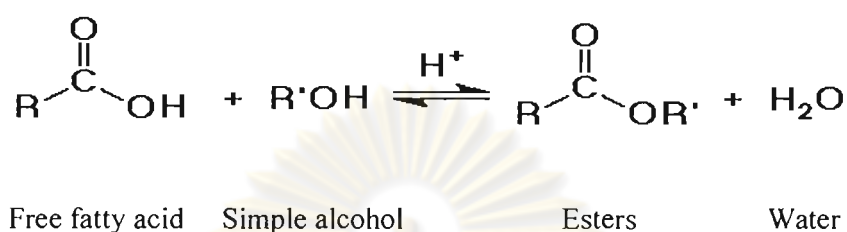


Figure 2.14 Esterification.

2.17.4.2 Saponification

The production of soap sometimes called alkaline hydrolysis, converts triacylglycerols to glycerol and a mixture of salts of long-chain carboxylic acids. As can be seen from Figure 2.16, the reaction can be carried out with an ester (i.e. triglycerides) or with carboxylic acids (i.e. free fatty acids). However, the production of fatty acids is an intermediate step when triglycerides are directly used for saponification. The commercial production of soap is usually conducted in two phases. The first phase is the conversion of lipids into FFAs by boiling with aqueous NaOH until hydrolysis is complete and then adding NaCl to precipitate the soap.

ศูนย์วิทยทรัพยากร
จุฬาลงกรณ์มหาวิทยาลัย

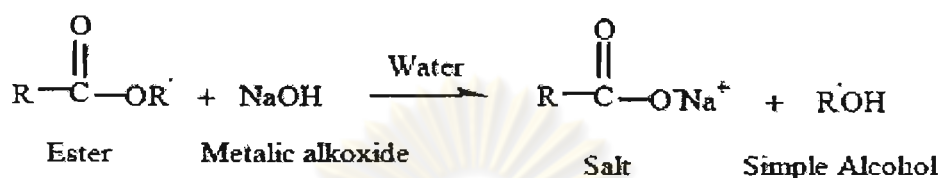
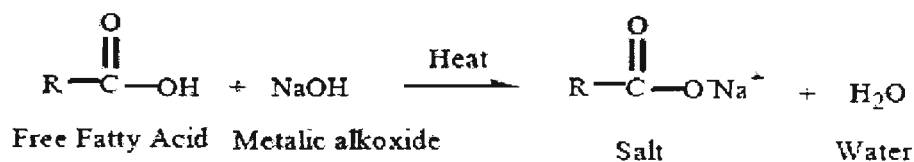


Figure 2.15 Saponification from free fatty acid and ester.

2.17.4.3 Hydrolysis

The hydrolysis of lipids forms a heterogeneous reaction system made up of two liquid phases. The dispersed aqueous phase consists of water and glycerol; the homogeneous lipid phase consists of fatty acids and glycerides. The hydrolysis of glycerides takes place in the lipid phase in several stages via partial glycerides (diglycerides and monoglycerides). Acid catalysts are very effective at accelerating the hydrolysis reaction. However, at high temperatures substantial material corrosion occurs. Basic metal oxides have a higher activity than more strongly alkaline monobasic metal oxides. Zinc oxide in its soap form has been suggested to be the most active catalyst for hydrolysis reactions. Reaction without a catalyst is not economical below 210°C, thus requiring the implication of high temperature, pressure techniques. Modern continuous plants operate at pressures between 0.6-1.2 MPa at 210-260°C without a catalyst. This increased pressure allows the mutual solubility of the two phases to increase to a point where the formation of continuous phase occurs.

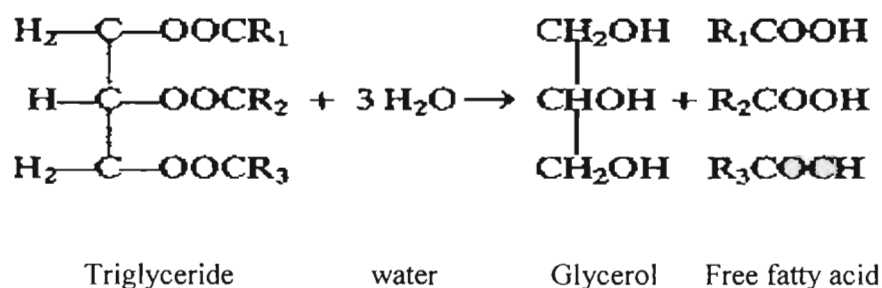


Figure 2.16 Hydrolysis of triglycerides.

2.17.5 Other forms of catalysis

2.17.5.1 Biocatalysts

Biocatalysts are usually lipases; however conditions need to be well controlled to maintain the activity of the catalyst. Hydrolytic enzymes are generally used as biocatalysts as they are readily available and are easily handled. They are stable, do not require co-enzymes and will often tolerate organic solvents. “Their potential for regioselective and especially for enantioselective synthesis makes them valuable tools”. Recent patents and articles have shown that reaction yields and times are still unfavourable compared to base-catalysed transesterification for commercial application.

2.17.5.2 Supercritical methanol

The study of the transesterification of rapeseed oil with supercritical methanol was found to be very effective and gave conversion of >95% within 4min. A reaction temperature of 350°C, pressure of 30MPa and a ratio of 42:1 of methanol to rapeseed oil for 240s were found to be the best reaction conditions. The rate was substantially high from 300 to 500°C but at temperatures above 400°C, it was found that thermal degradation takes place. Supercritical treatment of lipids with a suitable solvent such as methanol relies on the relationship between temperature, pressure and the thermophysical properties such as dielectric constant, viscosity, specific weight and polarity.

2.17.5.3 Catalyst free

Transesterification will occur without the aid of a catalyst; however, at temperatures below 300°C the rate is very low. There are two methods to produce biodiesel and that is with and without a catalyst. A comparison of supercritical methanol production and alcoholysis can be seen in Table 2.7.

Table 2.7 Comparison between production of biodiesel

	Common method	*SC MeOH method
Reaction time (h)	1-6	0.067
Reaction condition (MPa and °C)	0.1, 30-65	35, 350
Catalyst	Acid or alkali	None
Free fatty acids	Saponified products	Methyl esters
Yield (%)	97	98.50
Removal for purification	Methanol, catalyst and saponified products	Methanol
Process	Detailed	Simple

*SC MeOH method – Supercritical methanol

2.18 Transesterification kinetic and mechanism

Transesterification of triglyceride (TGs) with alcohol proceeds via three consecutive and reversible reactions where the FFA ligands combine with alcohol to produce a fatty acid alkyl ester, diglyceride and monoglyceride intermediates and finally glycerol by-product. The stoichiometric reaction requires 1 mole of TG and 3 moles of methanol to produce 3 moles of linear ester and 1 mole of glycerol. In presence of excess alcohol, the forward reaction is pseudo-first order and the reverse reaction is found to be second-order. It was observed that transesterification is faster when catalyzed by alkali. The mechanism of acid and alkali-catalyzed transesterification is described in Figure 2.18 and 2.19, respectively.

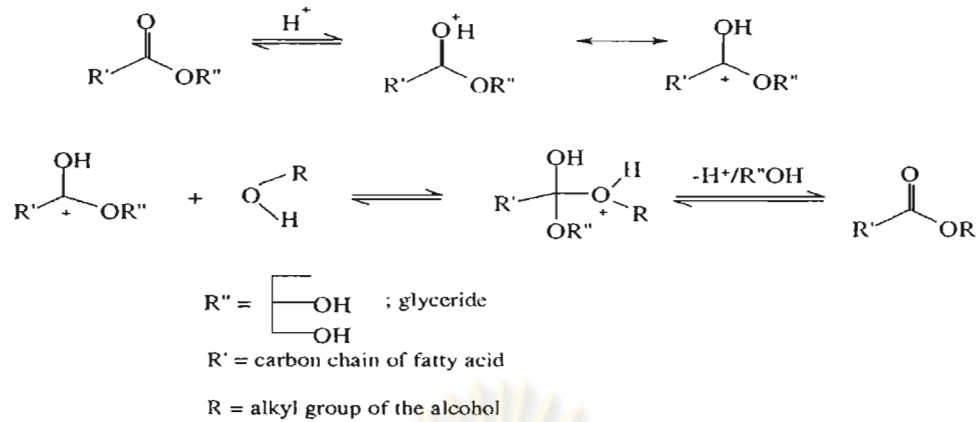


Figure 2.17 Mechanism of the acid-catalyzed transesterification.

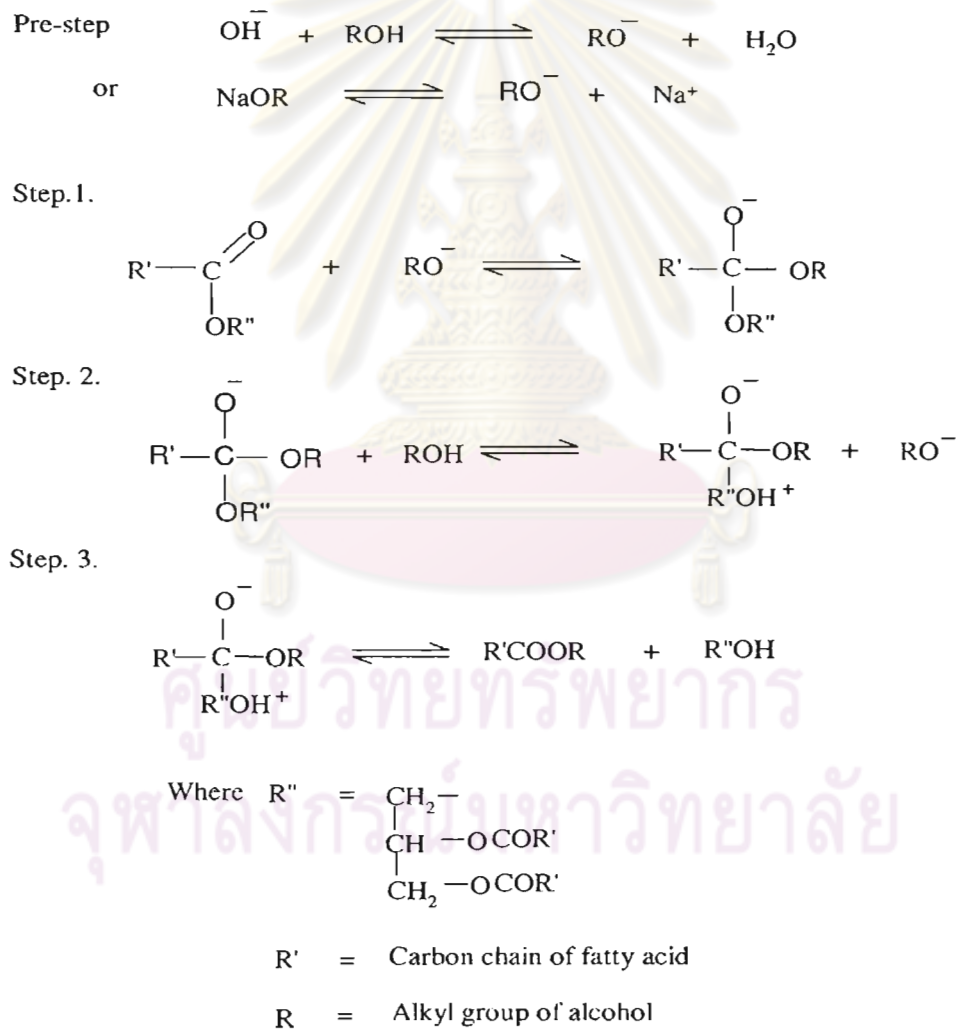


Figure 2.18 Mechanism of the base-catalyzed transesterification [2].

2.19 Transesterification parameters

The most relevant variables that influence the transesterification reactions are the following

2.19.1 Moisture and free fatty acid

The glyceride should have an acid value less than 1 and all materials should be substantially anhydrous. If the acid value is greater than 1, more NaOH is required to neutralize the free fatty acids. Water also causes soap formation, which consumes the catalyst and reduced catalyst efficiency.

2.19.2 Reaction time

The conversion rate increases with reaction time. The di- and monoglycerides increase at the beginning and then decrease. At the end, the amount of monoglycerides is higher than that of diglycerides.

2.19.3 Reaction temperature

Transesterification can occur at different temperatures, depending on the oil used and catalyst types. Temperature clearly influences the reaction rate and yield of esters.

2.19.4 Molar ratio of alcohol to oil

One of the most important variables affecting the yield of ester is the molar ratio of alcohol to triglyceride. The molar ratio is associated with the type of catalyst used. Methanol present in amounts of above 1.75 equivalents tended to prevent the gravity separation of glycerol, thus adding more cost to the process. Higher molar ratios result in greater ester conversion in a shorter time.

2.20 Silylation

Silylation is the most widely used derivatization technique. Nearly all functional groups which present a problem in gas chromatographic separation (hydroxyl, carboxylic acid, amine, thiol, phosphate) can be derivatized by silylation reagents such as N-methyl-N-trimethylsilyltrifluoroacetamide (MSTFA). MSTFA is an effective trimethylsilyl donor which reacts to place labile hydrogens of hydroxyl compound with $-\text{Si}(\text{CH}_3)_3$ group. The derivatives are generally less polar, more

volatile and more thermally stable. One advantage of MSTFA over other silylating reagents is the volatility of its byproduct, N-methyltrifluoroacetamide. N-methyltrifluoroacetamide has an even lower retention time than MSTFA.

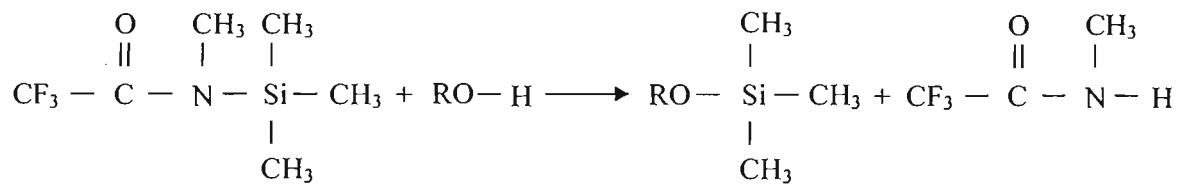


Figure 2.19 Silylation of alcohol with MSTFA.



คุนยวทยทรพยากร
จุพาลงกรณมหาวิทยาฬย

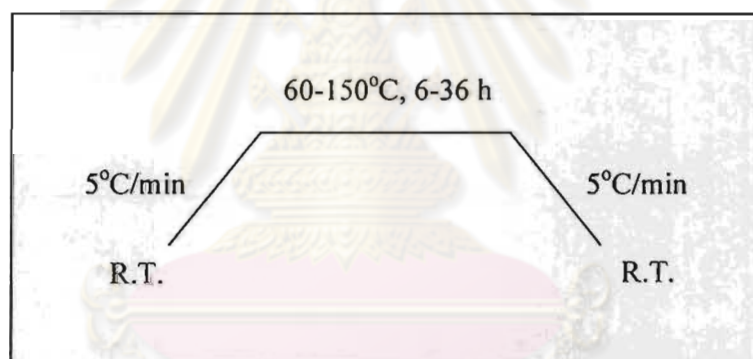
CHAPTER III

EXPERIMENTAL

3.1 Instrument and apparatus

3.1.1 Pressure reactor

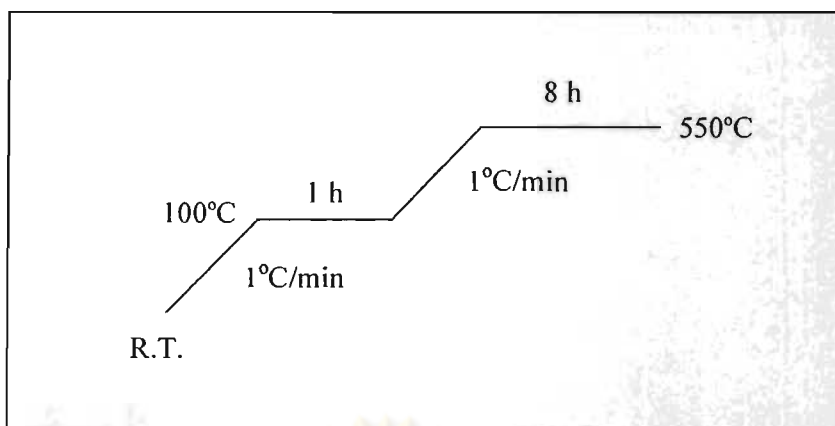
Crystallization of ERB-1 during the synthesis was performed at 175°C using a Parr series 4560, 300 and 600 ml Mini Bench Top reactors and transesterification reaction which also carried out in a Parr series 4560, 100 ml Mini Bench Top reactor, together with 4840 Modular Controller. The used temperature program for reaction was shown in Scheme 3.1.



Scheme 3.1 The temperature program for transesterification reaction.

3.1.2 Furnace

Calcination of the solid catalysts at elevated temperature was achieved in a Carbolite RHF 1600 muffle furnace. The temperature program for calcination was shown in Scheme 3.2.



Scheme 3.2 The temperature program for calcination.

3.1.3 X-Ray powder diffractometer

XRD patterns were obtained with a Rigaku, Dmax 2200/ultima plus X-ray powder diffractometer. Data were collected stepwise over $2^\circ < 2\theta < 40^\circ$, with a step size of $0.02^\circ 2\theta$, using Cu target X-ray tube.

3.1.4 Inductively coupled plasma-atomic emission spectrometer

Boron content in the catalysts was analyzed using the Perkin Elmer Plasma-1000 inductively coupled plasma-atomic emission spectrometer (ICP-AES).

3.1.5 Atomic absorption spectrometer

Sodium and potassium contents in the catalysts were analyzed using the Varian, 280FS atomic absorption spectrometer (AAS).

3.1.6 Surface area analyzer

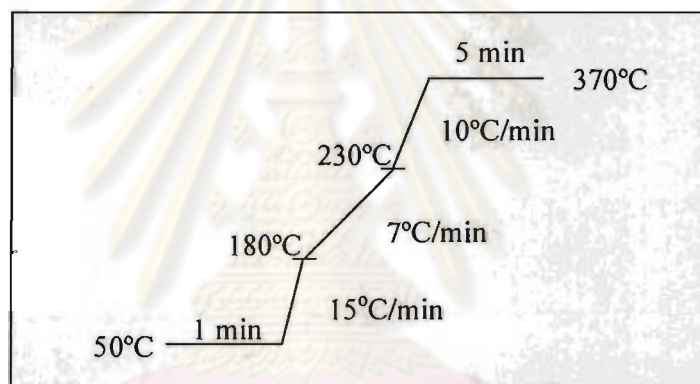
Characterization of catalyst porosity in terms of nitrogen adsorption-desorption isotherms, BET specific surface area, and pore size distribution of the catalysts were carried out using a BEL Japan, BELSORP-mini instrument. The sample weight was near 40 mg and weighed exactly after pretreatment at 400°C for 3 h before each measurement.

3.1.7 Scanning electron microscope

Scanning electron micrographs were obtained on a JEOL JSM-5410 LV scanning electron microscope. The samples were sputtered with gold before taking the images. The coupled EDX mode was used in determination of the alkali (Na, K, Rb and Cs) content in different alkali ions loaded on ERB-I catalysts.

3.1.8 Gas chromatography

Methyl esters, total glycerol, mono-, di- and triglyceride contents were analyzed using a Varian, GC CP 3800 model, gas chromatograph equipped with a 10 m length \times 0.32 mm inner diameter select biodiesel for glycerides column (High temperature type). GC detector was flame ionization detectors (FID). The GC heating program was shown in Scheme 3.3.



Scheme 3.3 The GC heating program for methyl esters, free glycerol, mono-, di- and triglyceride contents analysis.

3.2 Chemical reagents

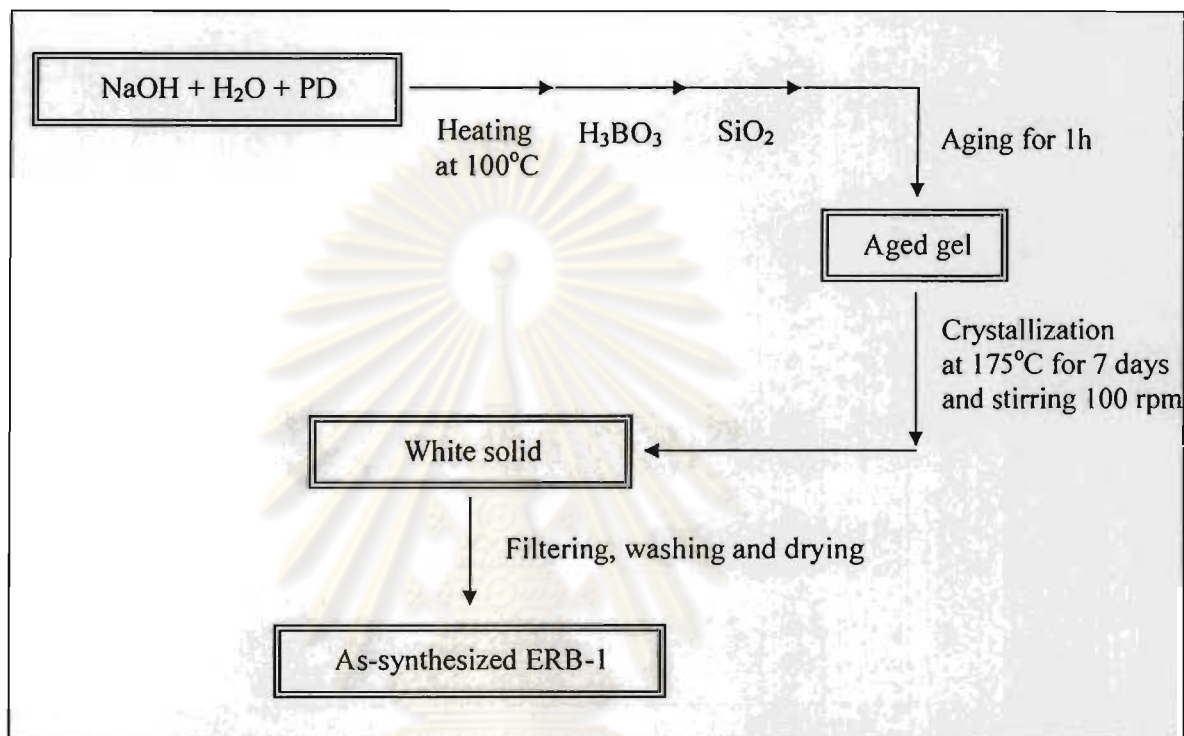
1. Fumed silica (Cab-osil®M-5) (Riedel-de Haën)
2. Sodium hydroxide, NaOH ($\geq 99\%$, Lab-Scan)
3. Boric acid, H_3BO_3 ($\geq 99.5\%$, Merck)
4. Hexamethylenimine, HMI ($\geq 97.0\%$, Fluka)
5. Piperidine ($\geq 99.5\%$, Sigma)
6. Hexadecyltrimethylammonium bromide, CTMABr ($\geq 96.0\%$, Fluka)
7. Tetrapropylammonium hydroxide, TPAOH (1.0 M in water, Aldrich)

8. Hydrochloric acid, HCl (37%, Carlo Erba)
9. Potassium hydroxide, KOH ($\geq 85.0\%$, Analar)
10. Cesium hydroxide monohydrate, CsOH.H₂O ($\geq 95.0\%$, Fluka)
11. Rubidium hydroxide, RbOH (99%, Aldrich)
12. Refined palm oil (OLEEN, Co. Ltd., commercial grade)
13. Methanol, CH₃OH (99.9%, Merck)
14. Heptane, C₇H₁₆ (99%, Scharlau)
15. Eicosane, C₂₀H₄₂ ($\geq 97\%$, Fluka)
16. Methyl palmitate, C₁₇H₃₄O₂ ($\geq 97.0\%$, Fluka)
17. Methyl oleate, C₁₉H₃₆O₂ (Aldrich, 99%)
18. Methyl linoleate, C₁₈H₃₄O₂ ($\geq 98.5\%$, Fluka)
19. Methyl stearate, C₁₈H₃₈O₂ (99.5%, Fluka)
20. Monoolein standard (5000 μ l/ml in pyridine, Restek)
21. Diolein standard (5000 μ l/ml in pyridine, Restek)
22. Triolein standard (5000 μ l/ml in pyridine, Restek)
23. 1,2,4-butanetriol standard (1000 μ l/ml in pyridine, Restek)
24. 1,4-butanediol, C₄H₁₀O₂ (99%, Sigma)
25. Tricaprin standard, (8000 μ l/ml in pyridine, Restek)
26. N-methyl-N-(trimethylsilyl)trifluoro acetamide, MSTFA (97.0%, Fluka)
27. Hydrofluoric acid, HF (48%, Merck)
28. Nitric acid, HNO₃ (65%, Lab-Scan)
29. Acetone, C₃H₆O (99.5%, Merck)

3.3 Synthesis procedure of ERB-1

The modified ERB-1 synthesis was followed by the reported method of Millini et al. and piperidine was used as the template. ERB-1 was synthesized from a gel of the following composition: 1.50 SiO₂ : B₂O₃ : 0.60 NaOH : 1.80 piperidine (PD) : 28.50 H₂O. A typical synthesis procedure was follows: Into a 2000-cm³ 4-necked round bottom flask, a 10.97 g of NaOH was dissolved in 209.75 g of deionized water and 81.58 g of piperidine was added. 56.51 g of H₃BO₃ was added at 50°C. After total dissolution of boric acid, 41.19 g of SiO₂ was added gradually over 1 h with stirring. After that, the clear solution was aged for 1 h, cooled at room

temperature and charged into a Parr reactor. Crystallization was achieved after seven days at 175°C with stirring at 100 rpm. The obtained white solid was separated by filtration and washed with water for several times, finally dried overnight at 120°C. The procedure for preparing the ERB-1 was shown in Scheme 3.4.



Scheme 3.4 Preparation diagram for ERB-1.

ศูนย์วิทยทรัพยากร
จุฬาลงกรณ์มหาวิทยาลัย

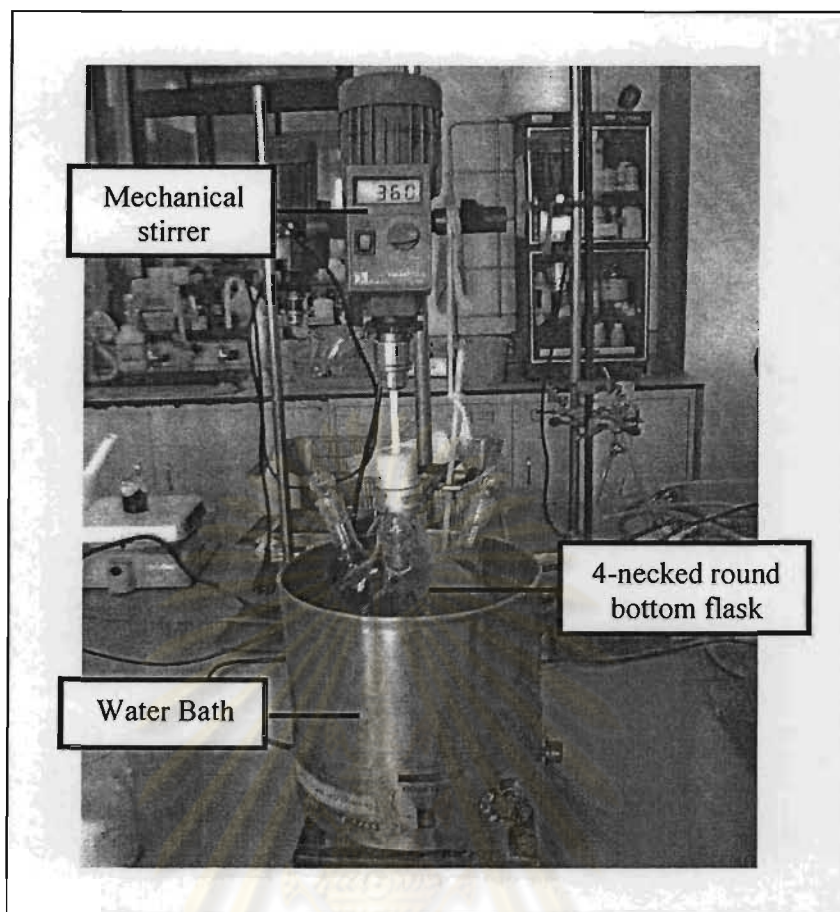


Figure 3.1 Apparatus for ERB-1 synthesis.

3.4 Organic template removal

To remove the template, the solid sample was calcined in a muffle furnace from room temperature to 550°C for 8 h as shown in Scheme 3.2.

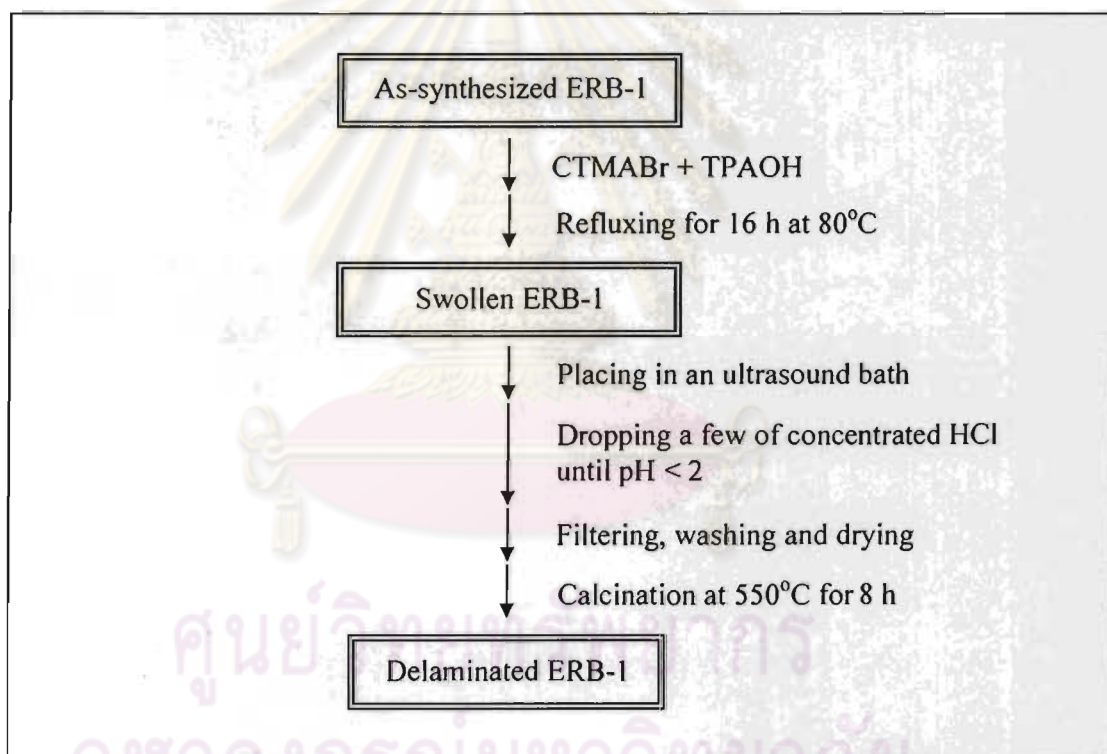
3.5 Preparation of delaminated ERB-1 (del-ERB-1)

The del-ERB-1 sample was obtained by swelling the precursor with CTMABr. Typically, dried ERB-1 precursor was mixed with an aqueous solution of CTMABr surfactant and an aqueous solution of 1.0 M TPAOH and refluxed for 16 h at 80°C. The layers were forced apart by placing the slurry in an ultrasound bath. Subsequently, it was added a few drops of concentrated hydrochloric acid (HCl), until the pH was below 2 and harvested the solid by centrifugation. Then, it was removed the organic material by calcination at 550°C to achieve del-ERB-1. The preparation

preparation conditions were shown in Table 3.1 and the delamination procedure was shown in Scheme 3.5.

Table 3.1 Conditions of del-ERB-1 preparation [20-23]

Sample Code	Composition (g)				Sonication time (h)
	Precursor	H ₂ O	CTMABr	TPAOH	
D1	1.00	32.36	5.60	2.40	1
D2	1.00	11.36	5.60	6.00	1
D3	1.00	45.94	19.44	6.11	1
D4	1.00	11.90	5.64	12.02	3



Scheme 3.5 Preparation diagram for del-ERB-1.

3.6 Loading of XERB-1 (X = Na, K, Rb or Cs)

The NaERB-1 was prepared that 1 g of calcined ERB-1 was stirring at RT or refluxing at 60°C with 30 ml of 0.05-0.50 M NaOH solutions for 3 h. After loading, NaERB-1 was filtered, dried and calcined at 550°C for 8h. All loaded catalysts were adopted in transesterification reaction of palm oil. The conditions of NaERB-1 preparation were shown in Table 3.2.

Table 3.2 Conditions of NaERB-1 preparation

Sample Code	Concentration of NaOH solution (M)	Temperature (°C)
NaERB-1(0.05, RT)	0.05	RT
NaERB-1(0.05, 60)	0.05	60
NaERB-1(0.10, RT)	0.10	RT
NaERB-1(0.10, 60)	0.10	60
NaERB-1(0.30, RT)	0.30	RT
NaERB-1(0.30, 60)	0.30	60
NaERB-1(0.50, RT)	0.50	RT
NaERB-1(0.50, 60)	0.50	60

The ERB-1 catalysts were stirred with 0.10 M of KOH, RbOH and CsOH·H₂O aqueous solutions under same condition as NaERB-1(0.10, RT) to obtain KERB-1(0.10, RT), RbERB-1(0.10, RT) and CsERB-1(0.10, RT), respectively.

3.7 ICP-AES and AAS analysis

3.7.1 CsCl stock solution, 1000 ppm

A 1000 mg of CsCl was accurately weighed approximately in a 1000 ml volumetric flask and made up to the mark with de-ionized water.

3.7.2 Sample preparation

A 40 mg of calcined sample was soaking with 10 ml of conc. HCl and subsequently 10 ml of 48% hydrofluoric acid was added dropwise to get rid of silica

in the form of volatile SiF_4 . The sample was heated on a hot plate until dryness and repeated three times. An amount of 10 ml of a mixture of 6 M HCl : 6 M HNO_3 at a ratio of 1:3 was added slowly and warmed until dryness again. Then an amount of 10 ml de-ionized water was added and warmed for 5 min to complete dissolution. The solution was transferred to a 50-ml polypropylene volumetric flask and made with CsCl stock solution. The solution in the flask was brought to the mark with de-ionized water. The flask was capped and shaken thoroughly. The solution was transferred into a plastic bottle with a treaded cap lined under with a polyethylene seal.

3.8 Transesterification reaction procedure

A 10 g of commercial palm oil and methanol (with molar ratio of methanol to palm oil 9:1) were added into the reactor with 1 g of catalyst. The system temperature was raised to 120°C under stirring speed 200 rpm. After 24 h, the reactor was cooled to room temperature. After cooling, the catalyst was separated from the methyl ester products by centrifugation. The used catalyst was washed with acetone, separated by centrifuge again and drying overnight at 120°C . The calcination heating program for the used catalyst was shown in Scheme 3.2. The products were analyzed by gas chromatography. Commercial Oleen palm oil was used as the starting material, which the composition of fatty acids in triglycerides was shown in Table 3.3.

Table 3.3 Fatty acid composition (wt%) of commercial Oleen palm oil

Fatty acid	Composition (wt%)
Oleic acid (C18:1)	45.2
Palmitic acid (C16:0)	37.9
Linoleic acid (C18:2)	10.9
Stearic acid (C18:0)	3.8
Myristic acid (C14:0)	1.2
Lauric acid (C12:0)	0.7
Linolenic acid (C18:3)	0.3

Data from Oleen Company.

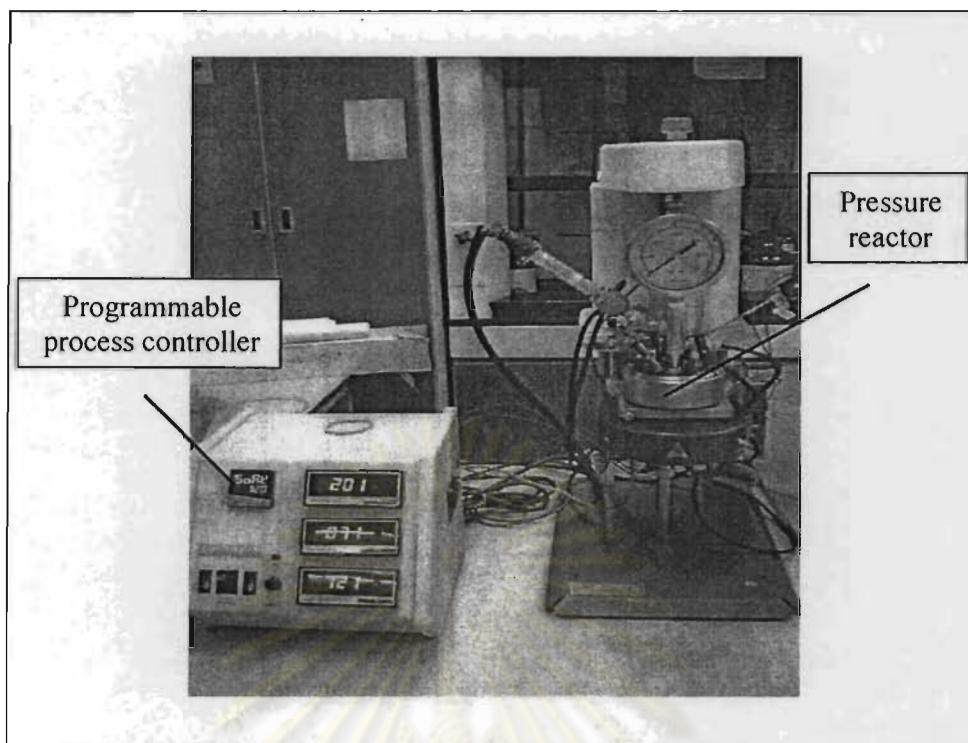


Figure 3.2 Apparatus for transesterification reaction.

3.8.1 Effect of reaction time

The reaction was performed at different reaction time of 6, 12, 24, 30 and 36 h.

3.8.2 Effect of methanol/palm oil molar ratio

In order to study the effect of molar ratio on methyl ester yield of the transesterification, experiments were conducted with various molar ratios of methanol to oil in range of 6:1 to 15:1.

3.8.3 Effect of catalyst amount

The transesterification reaction was carried out using a catalyst quantity equivalent to 5 wt%, 10 wt%, and 15 wt% of palm oil.

3.8.4 Effect of reaction temperature

To examine the temperature dependency on conversion, reactions were conducted at 90 to 120°C

3.9 Determination of free and total glycerol and mono-, di- and triglyceride contents [37]

The purified methyl esters were evaluated in a series of tests to determine if the biodiesel produced met the British Standard EN 14105:2003. This European Standard specified a method to determine the glycerol and residual mono-, di- and triglyceride contents in fatty acid methyl ester (FAME).

3.9.1 Internal stand No.1 stock solution, 1 mg/ml.

A 10 mg of 1,4-butanediol was accurately weighed approximately in a 10 ml volumetric flask and made up to the mark with pyridine.

3.9.2 Internal stand No.2 stock solution, 8 mg/ml.

A 80 mg of 1,2,3-tricaproylglycerol was accurately weighed approximately in a 10 ml volumetric flask and made up to the mark with pyridine.

3.9.3 Glycerol stock solution, 0.5 mg/ml.

A 5 mg of glycerol was accurately weighed in a 10 ml volumetric flask and made up to the mark with pyridine. Using a pipette, a 1 ml of this solution was transferred into a 10 ml volumetric flask and made up to the mark with pyridine.

3.9.4 Calibration solutions

Daily four calibration solutions were prepared by transferring into a series of vials. The volumes of stock solutions of reference substances and of internal standards given in Table 3.4., using microsyringe.

Table 3.4 Preparation of calibration solutions

Calibration solution	1	2	3	4
Glycerol solution (μl)	10	40	70	100
Monoolein solution (μl)	50	120	190	250
Diolein solution (μl)	10	40	70	100
Triolein solution (μl)	10	30	60	80
1,2,4-Butanetriol solution (Internal standard No.1) (μl)	80	80	80	80
1,2,3-Tricaproylglycerol solution (Internal standard No.2) (μl)	100	100	100	100

3.9.5 Preparation and analysis of the calibration solutions

Using a microsyringe, a 100 μl of N-methyl-N-trimethylsilyltrifluoroacetamide (MSTFA) was added to each of the four calibration solutions, the vials were hermetically closed and vigorously shaken and avoided contact with moisture. They were stored 15 minutes at room temperature, then 8 ml of heptane was added.

A 1 μl of each reaction mixture was analysed by GC under the condition defined above. Samples were stable for one day after derivatisation.

3.10 Determination of methyl ester contents

Determination of methyl ester contents was simulated from the British Standard EN 14105:2003 method.

3.10.1 Internal standard No.3 stock solution, 10 mg/ml.

A 500 mg (to the nearest 0.1 mg) of eicosane was accurately weighed approximately in a 50 ml volumetric flask and made up to the mark with heptane.

3.10.2 Methyl ester calibration solutions

Five calibration solutions were prepared by transferring into a series of vials. The volumes of stock solutions of reference substances and of internal standards given in Table 3.6, using microsyringe.

Table 3.5 Preparation of calibration solutions

Calibration solution	1	2	3	4	5
Methyl oleate (μl)	46.6	31.0	20.7	10.3	5.3
Methyl palmitate (μl)	40.0	26.8	17.8	8.9	4.5
Methyl linoleate (μl)	11.0	7.3	4.9	2.5	1.1
Methyl stearate (μl)	0.0035	0.0023	0.0015	0.0008	0.0004
Eicosane solution (Internal standard No.3) (ml)	1.00	1.00	1.00	1.00	1.00

3.10.3 Preparation and analysis of the calibration solutions

Each of the five calibration solutions, 8 ml of heptane was added into the vials. A 1 μl of each reaction mixture was analysed by GC under the conditions defined above.

3.11 The stability and regeneration of catalyst

The single used catalyst was separated from liquid layer by centrifugation, washed with acetone, dried at 120°C overnight, calcined at 550°C and characterized by XRD, ICP-AES, AAS, SEM and nitrogen adsorption-desorption. For Na-reloaded sample, 1 g of the used catalyst was refluxed with 30 ml of 0.10 M aqueous solution of NaOH at room temperature for 3 h. Finally, it was dried and calcined before testing activity at the same condition as previous.

3.12 Analysis of leached Na content

0.50 g of NaERB-1(0.10, RT) or Na-reloaded ERB-1 was stirred in 5.00 ml of methanol at 120°C for 24 h and filtered. The filtrate was analyzed by AAS and used in transesterification without catalyst to observe leaching of Na ions from the catalyst.

CHAPTER IV

RESULTS & DISCUSSION

4.1 ERB-1 catalyst

4.1.1 X-ray powder diffraction (XRD)

XRD patterns of the as-synthesized and calcined ERB-1 are shown in Figure 4.1. By comparing, one can observe that the angular position of some reflections remain practically unchanged (2θ about 7.2° , 25.4° and 26.4°). Other peaks, such as those located at 2θ about 3.3° and 6.6° [(001) and (002), respectively], refer to lamella structure of as-synthesized ERB-1 disappear after calcination. Furthermore, all peaks become more intense, resulting from the removal of organic template. It is now well documented that as-synthesized ERB-1 is formed of layers and upon calcination, the layers condense to form a fully connected framework.

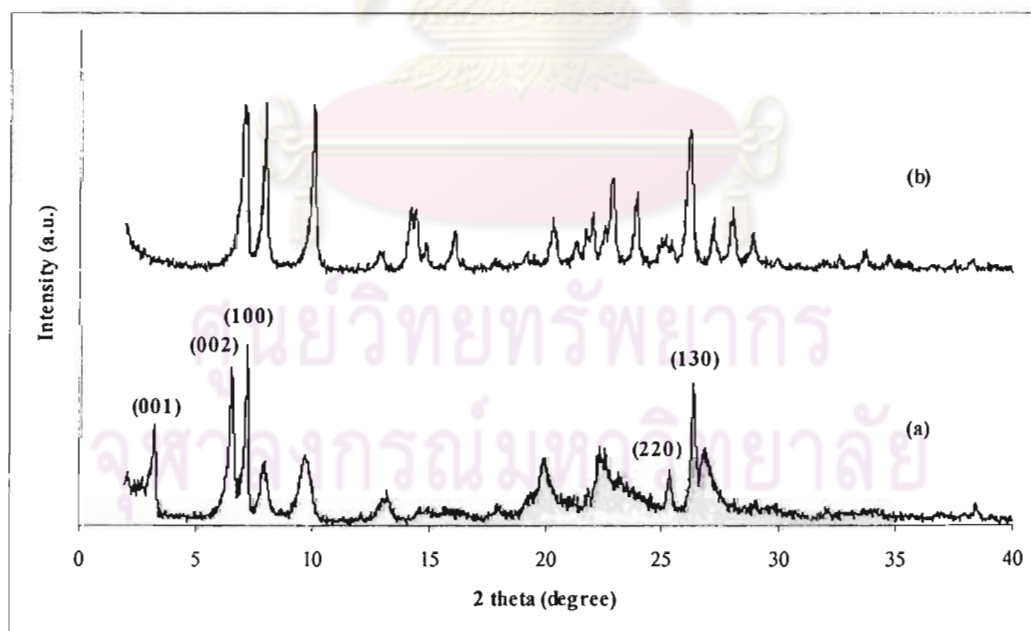


Figure 4.1 XRD patterns of as-synthesized (a) and calcined (b) of ERB-1.

4.1.2 Sorption properties

N₂ adsorption-desorption isotherms of calcined ERB-1 are shown in Figure A-1 (in Appendices). Isotherm exhibits a type I, characteristic of micropores. The total specific surface area, external surface area, micropore volume and micropore distribution are 474 m²/g, 27 m²/g, 0.17 cm³/g and 0.60 nm, respectively.

4.1.3 Elemental analysis

The obtained results from ICP-AES and AAS techniques, the SiO₂/B₂O₃, Na/SiO₂ and B/Na ratios in catalyst are 52.01, 0.01 and 3.25, respectively. The SiO₂/B₂O₃ ratio is negligible, since acidity of catalyst is not required. While the Na/SiO₂ ratio is the important parameter because Na amount reveals basic strength. Millini *et al.*'s research showed that if sodium was added to the starting gel, it was retained only in minor amounts in the recovered solid (the Na/SiO₂ ratio = 0.01) [4]. Therefore, the catalyst must be modified to increase basic strength. For B/Na ratio is more than 1, probably due to non-framework site of boron.

4.2 Alkali ion loaded on ERB-1

After the synthesis, basic strength of catalyst was modified by loading of various alkali ions (Na, K, Rb and Cs) in order to obtain the most efficient basic catalyst.

4.2.1 Na loaded ERB-1

4.2.1.1 X-ray powder diffraction (XRD)

In order to obtain the optimum condition of alkali ion loaded on ERB-1; firstly, ERB-1 was stirred at room temperature or refluxed at 60°C by various concentrations of NaOH solution. The concentration was varied by being 0.05, 0.10, 0.30 and 0.50 M, respectively. They are denoted as NaERB-1(x, RT) and NaERB-1(x, 60), where x is a concentration (molar) of NaOH solution. Figure 4.2 and 4.3 show the XRD patterns of various ERB-1 materials which loaded with various NaOH solution concentrations by stirring at RT and refluxing at 60°C, respectively. Compared to calcined ERB-1, the XRD patterns of base modified ERB-1 indicate reducing of XRD peak intensity, but no new crystalline phase is detected. Using the equal NaOH solution concentration, NaERB-1(x, 60) is observed that the intensity of

diffraction peaks slightly decreases by comparing with NaERB-1(x, RT). In case of the same temperature, when concentration of NaOH solution was increased, the intensity of all diffraction peaks obviously decrease especially NaERB-1(0.30, RT), NaERB-1(0.50, RT), NaERB-1(0.30, 60) and NaERB-1(0.50, 60), because of their damaged structure. Thus, these NaERB-1 samples do not adopt to be catalysts.

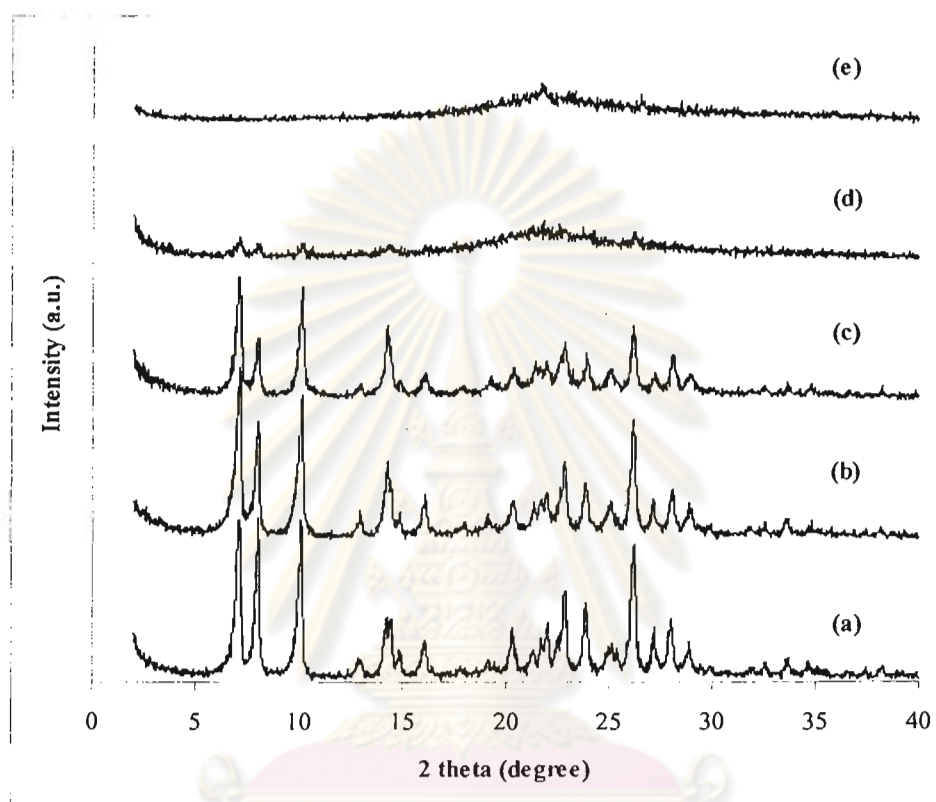


Figure 4.2 The XRD patterns of various NaOH solution concentrations loaded on ERB-1 catalysts by stirring at RT: calcined ERB-1 (a), NaERB-1(0.05, RT) (b), NaERB-1(0.10, RT) (c), NaERB-1(0.30, RT) (d) and NaERB-1(0.50, RT) (e).

จุฬาลงกรณ์มหาวิทยาลัย

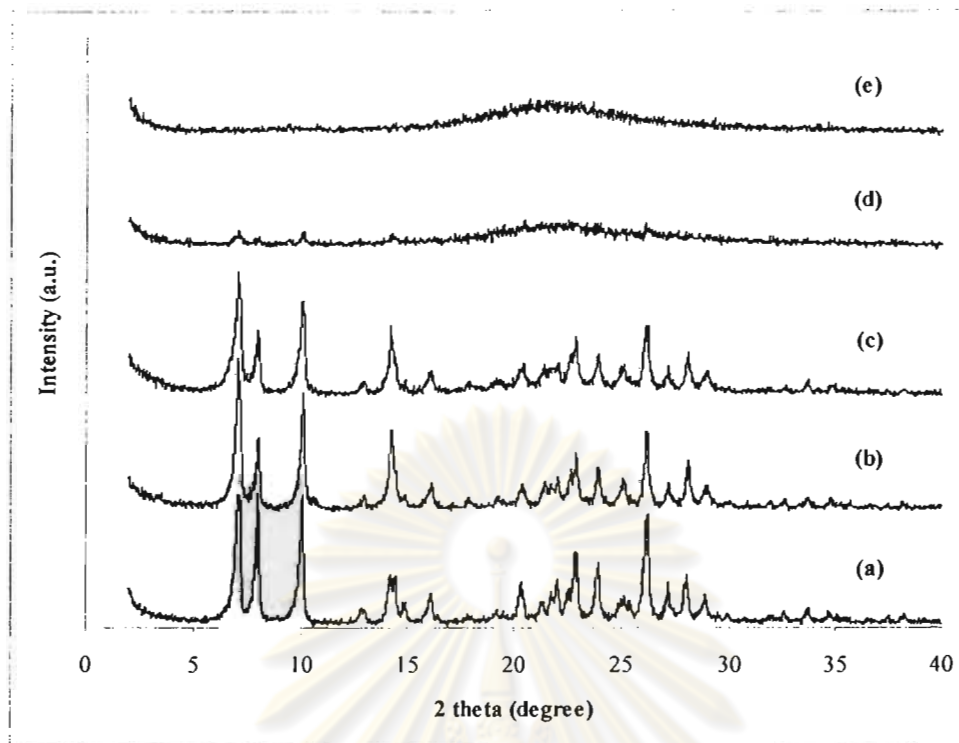


Figure 4.3 The XRD patterns of various NaOH solution concentrations loaded on ERB-1 catalysts by refluxing at 60°C: calcined ERB-1 (a), NaERB-1(0.05, 60) (b), NaERB-1(0.10, 60) (c), NaERB-1(0.30, 60) (d) and NaERB-1(0.50, 60) (e).

ศูนย์วิทยทรัพยากร
จุฬาลงกรณ์มหาวิทยาลัย

4.2.1.2 Sorption properties

Na doped samples exhibit N_2 adsorption isotherms of type I like ERB-1 (Figure A-2 and A-3 in appendices). Table 4.1 and 4.2 show textural properties of various NaOH solution concentrations loaded on ERB-1 by stirring at RT and refluxing at 60°C. The higher Na loading amount leads to the lower total specific surface area on account of increasing Na ion on surface. Moreover, the micropore volume decreases, it may be concerned with sodium species transfer into pore of catalyst.

Table 4.1 Textural properties of various NaOH solution concentrations loaded on ERB-1 by stirring at RT

Sample	Total specific surface area ^a (m ² /g)	External surface area ^b (m ² /g)	Micropore volume ^b (cm ³ /g)	Micropore distribution ^c (nm)
ERB-1	471	27	0.17	0.60
NaERB-1(0.05, RT)	419	34	0.15	0.60
NaERB-1(0.10, RT)	298	27	0.10	0.60

^acalculated using the BET plot method

^bcalculated using the t-plot method

^ccalculated using the MP-plot method

Table 4.2 Textural properties of various NaOH solution concentrations loaded on ERB-1 by refluxing at 60°C

Sample	Total specific surface area ^a (m ² /g)	External surface area ^b (m ² /g)	Micropore volume ^b (cm ³ /g)	Micropore distribution ^c (nm)
ERB-1	471	27	0.17	0.60
NaERB-1(0.05, 60)	335	24	0.12	0.60
NaERB-1(0.10, 60)	224	33	0.08	0.60

^acalculated using the BET plot method

^bcalculated using the t-plot method

^ccalculated using the MP-plot method

4.2.1.3 Elemental analysis

The Na/SiO₂ ratios of various NaOH solution concentrations on loaded ERB-1 by stirring at RT and refluxing at 60°C are shown in Table 4.3 and 4.4, respectively. The Na/SiO₂ ratio increases according to increasing Na loading amount. NaERB-1(0.10, RT) shows highest Na/SiO₂ ratio, this implies to highest content of Na ion in catalyst. Thus, the optimum condition for Na loading on ERB-1 is 1g of ERB-1 with 30 ml of 0.10 M NaOH solution stirring at RT for 3 h. Then, this condition will be adapted to the other alkali metals (K, Rb and Cs) loading on ERB-1 catalysts.

Table 4.3 The Na/SiO₂ ratio of various NaOH solution concentrations loaded on ERB-1 by stirring at RT

Sample	Na/SiO ₂ ^a
ERB-1	0.01
NaERB-1(0.05, RT)	0.17
NaERB-1(0.10, RT)	0.19

^aobtained sodium content by AAS

Table 4.4 The Na/SiO₂ ratio of various NaOH solution concentrations loaded on ERB-1 by refluxing at 60°C

Sample	Na/SiO ₂ ^a
ERB-1	0.01
NaERB-1(0.05, 60)	0.17
NaERB-1(0.10, 60)	0.18

^aobtained sodium content by AAS

4.2.2 The different alkali ions loaded ERB-1

4.2.2.1 X-ray powder diffraction (XRD)

For the other alkali ions (K, Rb and Cs) loading on ERB-1, the optimum condition for alkali loading was adopted that was stirring with 0.10 M alkali metal hydroxide solution at RT. Figure 4.5 shows the XRD patterns of alkali catalysts. The result shows the intensity of diffraction peaks reduces when samples were loaded by the alkali ions. Furthermore, the larger size of alkali metal causes more reduction

of diffraction line than the smaller one because of its higher basic strength. The high basic strength affects to the damaged structure.

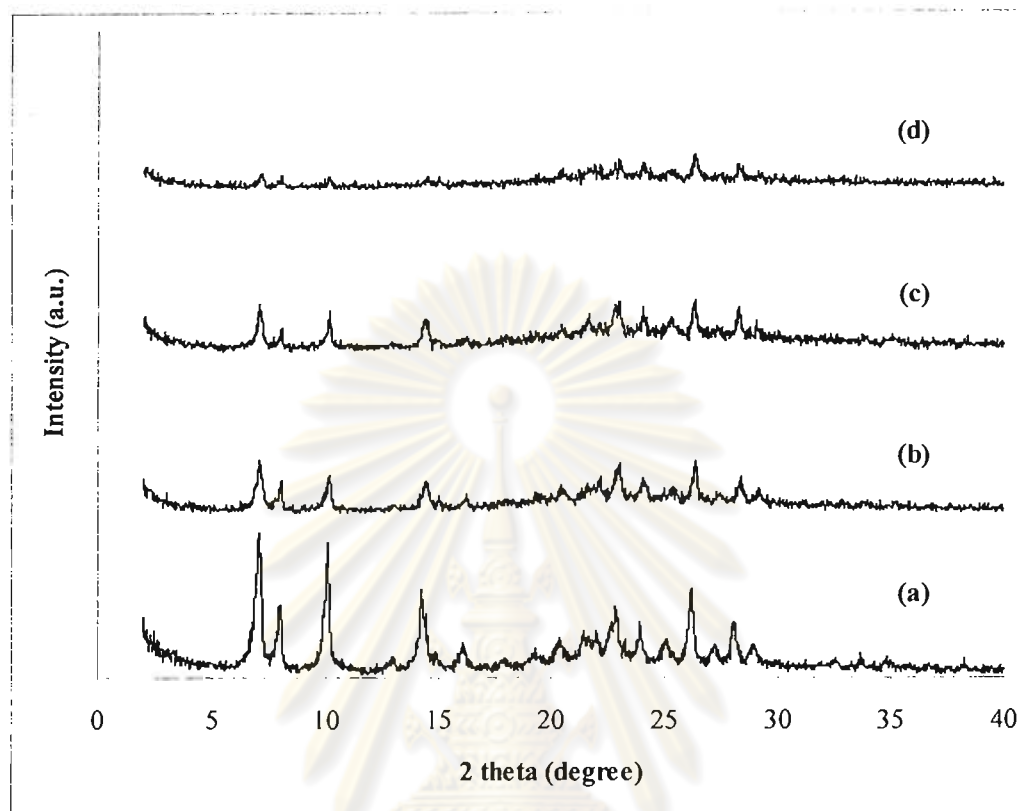


Figure 4.4 The XRD patterns of different alkali ions loaded on ERB-1 catalysts: NaERB-1(0.10, RT) (a), KERB-1(0.10, RT) (b), RbERB-1(0.10, RT) (c) and CsERB-1(0.10, RT) (d).

4.2.2.2 Sorption properties

N_2 adsorption isotherms of catalysts are shown in Figure A-4. Table 4.5 shows textural properties of different alkali ions loaded on ERB-1 samples. Pore size of ERB-1 is nearly $7.1 \text{ \AA} \times 7.1 \text{ \AA}$, while ionic radius of Na, K, Rb and Cs ions are 1.0, 1.4, 1.5 and 1.7 \AA , respectively [46]. Then these alkali cations can transfer into pore and distribute upon surface. Total specific surface area, external surface area and micropore volume become lower because of damaged ERB-1 structure and the larger alkali ionic size. This observation is corresponding to Xie's research [13].

Table 4.5 Textural properties of different alkali metals loaded on ERB-1 catalysts

Sample	Total specific surface area ^a (m ² /g)	External surface area ^b (m ² /g)	Micropore volume ^b (cm ³ /g)	Micropore distribution ^c (nm)
ERB-1	471	27	0.17	0.60
NaERB-1(0.10, RT)	298	27	0.10	0.60
KERB-1(0.10, RT)	17	9	3.21×10 ⁻³	0.90
RbERB-1(0.10, RT)	13	8	1.80×10 ⁻³	0.70
CsERB-1(0.10, RT)	10	8	1.02×10 ⁻³	1.00

^acalculated using the BET plot method

^bcalculated using the t-plot method

^ccalculated using the MP-plot method

4.2.3.3 Elemental analysis

SEM-EDX was used in the measurement of alkali contents. The Na, K, Rb and Cs contents in alkali ion loaded on ERB-1 catalysts are shown in Table 4.6. The order of alkali content in each catalyst is in order K > Cs ≈ Na > Rb, respectively.

Table 4.6 Alkali contents in alkali ion loaded on ERB-1 catalysts

Catalyst	Alkali content (atomic%)			
	Na	K	Rb	Cs
NaERB-1(0.10, RT)	7.24	-	-	-
KERB-1(0.10, RT)	-	10.27	-	-
RbERB-1(0.10, RT)	-	-	5.08	-
CsERB-1(0.10, RT)	-	-	-	7.65

4.2.3.4 Scanning electron microscopy (SEM)

SEM images of different alkali ions on loaded ERB-1 samples are shown in Figure 4.5. The calcined ERB-1 particles are aggregated sheets [Figure 4.5 (a)]. After alkali ion loading [Figure 4.5 (b-e)], no important differences are observed between calcined ERB-1 and other catalysts, except for the presence of small aggregated particles in the alkali ion loaded on ERB-1. By drawing on the results, after being loaded with alkali ion, ERB-1 retains its structure where alkali ion is

homogeneously distributed upon the surface of the support. The same phenomena of alkali ion loading on catalyst used to be reported by Xie *et al.* [3] and [13].

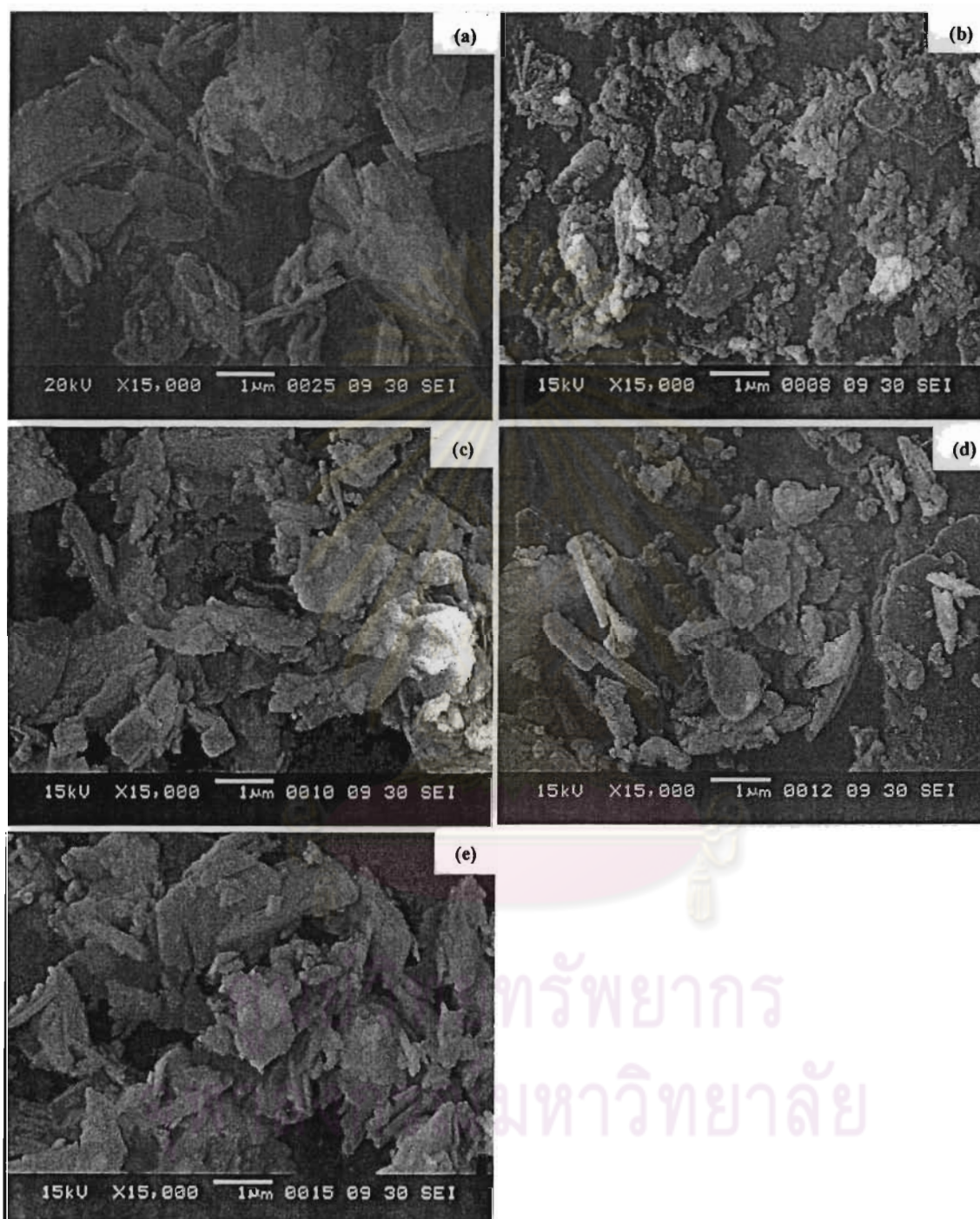


Figure 4.5 SEM images of different alkali ions loaded on ERB-1 catalysts: calcined ERB-1 (a), NaERB-1(0.10, RT) (b), KERB-1(0.10, RT) (c), RbERB-1(0.10, RT) (d) and CsERB-1(0.10, RT) (e).

4.3 Reaction mixture qualitative analysis

Troublesome compounds for GC analysis are physically large i.e. free and bound glycerol and triglycerides. In the case of the hydroxyl groups, silylation is employed to derivatise free and bound glycerol. This converts any hydroxyl groups into trimethylsilyl ether groups $[-OSi(CH_3)_3]$, which are more volatile and do not interact with the stationary phase of the capillary column.

A gas chromatogram of silylated palm oil methyl ester is shown in Figure A-7. Peak identification is achieved by comparison with reference substances or chromatograms. Since 1,2,4-butanetriol is not available, 1,4-butanediol is instead used for sample analysis. 1,4-butanediol and glycerol elute in advance of the fatty acid methyl esters at column temperatures lower than 100°C. Mono-, di- and triglycerides are mainly separated according to carbon number (CN). The analysis of the calibration solutions under the same operating condition as those used for the analysis of the sample allows the identification of the peaks by comparison of the retention times. For monoglycerides, the peak with the relative retention time (RRT) of 0.77 (2-Mono-C18:1,2,3) and 0.78 (1-Mono-C18:1,2,3) with respect to the internal standard tricaprin clearly dominate and correspond to the signals of monoolein (C18:1), monolinolein (C18:2) and monolinolenin (C18:3). The asymmetric peak shape is due to the superimposition of these monoglyceride peaks with equal carbon number (CN = 18) but different number of double bonds. In addition, the signals of monopalmitin (CN = 16; RRT=0.70) and monostearin (CN = 18; RRT=0.79) can be identified.

The diglycerides are also primarily separated according to carbon number and appear in groups of peaks corresponding to 1,2- and 1,3- isomers or to diglycerides with equal carbon number but different number of double bonds. The individual diglyceride peaks can not be reliably identified. Nevertheless, the signals with relative retention times from 1.09 to 1.13 can clearly be assigned to diglycerides with carbon numbers of 34 and 36 by comparison of chromatograms of samples with high and low degrees of transesterification and reference chromatograms.

At the end of the chromatogram, the triglycerides form a group of peaks separate only according to carbon number. Signals with relative retention time 1.34 to 1.39 corresponding to triglycerides with carbon numbers of 50 and 54 are included in quantitation [38].

For peak of each methyl ester, it obviously separates from others, except for methyl linoleate and methyl oleate. Both peaks slightly overlap but can be identified.

4.4 Reaction mixture quantitative analysis

For the quantitative determination of methyl esters, free glycerol, mono-, di- and triglycerides in palm oil methyl ester, a calibrations with the reference substances methyl oleate (MO), methyl palmitate (MP), methyl linoleate (ML), methyl stearate (MS), glycerol, mono-, di- and triolein are carried out. Due to structural differences between the individual analytic classes and to partial thermal degradation observe for the high boiling di- and triglycerides, calibration is of great importance for a reliable quantification. Freshly prepared standard solutions (5 concentration levels for methyl esters and 4 levels for others), containing known amounts of the reference substances four methyl esters, glycerol, mono-, di- and triolein and three internal standards are analyzed. A corresponding gas chromatogram is shown in Figure A-5 for methyl esters and Figure A-6 for glycerol, mono-, di- and triglycerides, respectively. The calibration curves of methyl esters are shown in Figure A-8 to A-10 and A-11 to A-14 of glycerol, mono-, di- and triglycerides. Moreover, the calculation of the percentage of methyl esters, free glycerol, glycerides and total glycerol is shown in 2.2, 3.3 to 3.5 in appendices.

4.5 Catalytic activities of ERB-1 in transesterification reaction

The values of % conversion and product yield obtained by transesterification reaction of palm oil over non-catalyst and ERB-1 catalyst at 120 and 150°C are compared in Table 4.7. Desired product is methyl esters and by-products are glycerol, mono-, di- and triglycerides. MO, MP, ML and MS are abbreviation of methyl oleate, methyl palmitate, methyl linoleate and methyl stearate, respectively. Without addition of a catalyst, the conversion and product yield, except for total glycerol, increase by rising temperature from 120 to 150°C. Considering free and bound parts in total glycerol, free glycerol increases but bound glycerol, consists of mono-, di- and triglycerides, decreases. Bound glycerol is the main part of glycerol, it highly affects to reduction of total glycerol, although methyl esters yield doubly increases. Comparing to the blank test at 120°C, the conversion over ERB-1 catalyst is decreased, which is possibly due to the lack of strong basic sites and the rise of a mixing problem of reactants and solid catalyst. For non-catalyst reaction at 150°C, the conversion over ERB-1 shows the same trend as reaction at 120°C. Considering conversion with addition of ERB-1 catalyst, it increases because of increasing reaction temperature but methyl ester yield is nearly equal. That means that the

mixing problem of reactants and solid catalyst. For non-catalyst reaction at 150°C, the conversion over ERB-1 shows the same trend as reaction at 120°C. Considering conversion with addition of ERB-1 catalyst, it increases because of increasing reaction temperature but methyl ester yield is nearly equal. That means that the increasing reaction temperature to 150°C does not promote methyl ester yield. From this experiment, ERB-1 seems to retard palm oil transesterification. Then next step, ERB-1 has to be improved its activity by base loading.

Table 4.7 Conversion and product yield in transesterification reaction of palm oil over non-catalyst and ERB-1 catalyst at 120 and 150°C
(Condition: 10 wt% catalyst, MeOH to oil molar ratio of 9:1 for 24 h)

	Reaction temperature (°C)			
	120		150	
	None	ERB-1	None	ERB-1
Conversion (%)	26.01	22.13	34.36	31.88
Product yield (%)				
1. Methyl esters	6.63	5.85	13.96	5.80
MO and ML	47.51	41.55	42.83	44.60
MP	45.91	50.13	45.40	40.68
MS	6.59	8.32	11.78	14.72
2. Total glycerol	9.20	9.10	5.68	9.57
Free	0.07	0.06	0.68	0.03
Bound	99.93	99.94	99.32	99.97
3. Monoglycerides	0.78	0.22	1.16	1.31
4. Diglycerides	9.40	6.97	10.59	15.20
Triglycerides (%)	73.99	77.87	65.64	68.12

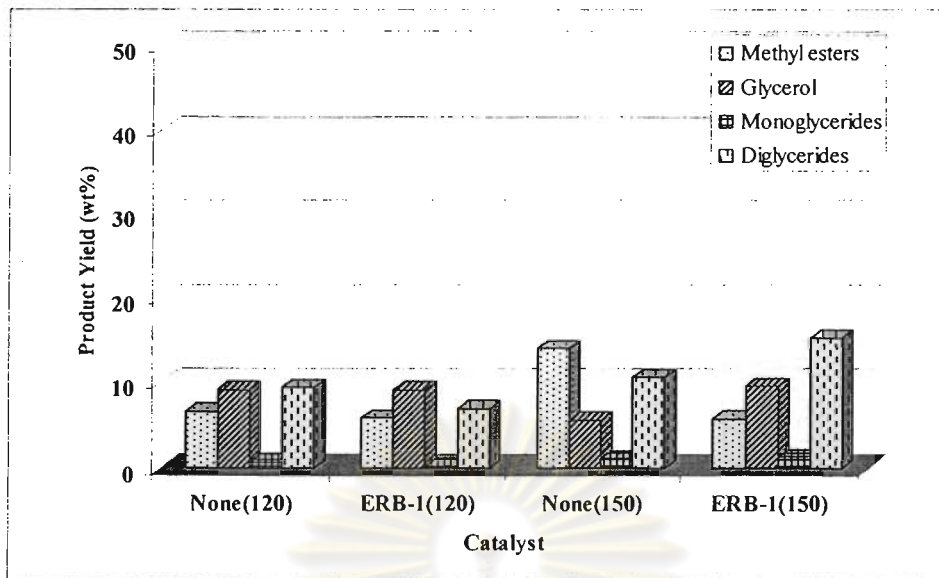


Figure 4.6 Product yield from transesterification reaction of palm oil over non-catalyst and ERB-1 at 120°C and 150°C (Condition: 10 wt% catalyst, MeOH to oil molar ratio of 9:1 for 24 h).

4.6 Catalytic activities of alkali ion loaded ERB-1 in transesterification reaction

4.6.1 Na loaded ERB-1

Loading of NaOH onto the catalyst produces a dramatic increment of basic strengths on the NaERB-1 catalyst and resulting in an increase in the conversion and methyl esters yield. Thus, the production of biodiesel in transesterification reaction of palm oil needs basic sites.

Concentration of NaOH solution and temperature refluxing were investigated. Table 4.8 shows conversion and product yield in transesterification reaction of palm oil over two NaOH solution concentrations loaded on ERB-1 by stirring at RT. When NaOH concentration was increased from 0.05 to 0.10 M, conversion and diglyceride yield highly raise from 58.48 to 74.03% and 5.26 to 16.29%, respectively, because of basic site increasing. It is confirmed by the value of Na/SiO₂ ratio in Table 4.3. For methyl ester yield gives a slight increasing from 39.33 to 42.45%.

For refluxing ERB-1 at 60°C, conversion increases due to containing Na ion in ERB-1. However, concentration was increased from 0.05 to 0.10 M, conversion is

nearly similar. Now that the Na/SiO₂ ratio of NaERB-1(0.10, 60) is slightly higher but total surface area is lower than NaERB-1(0.05, 60).

Using the same concentration, stirring ERB-1 catalyst at RT gives the conversion and methyl ester yield higher than refluxing at 60°C on account of higher surface area.

These results can conclude that NaERB-1(0.10 RT) catalyst leads to the highest conversion and methyl esters yield. Therefore, this condition for Na loading on ERB-1 will be adapted to the other alkali ions (K, Rb and Cs) loaded on ERB-1 catalysts.

Table 4.8 Conversion and product yield in transesterification reaction of palm oil over various NaOH solution concentrations loaded on ERB-1 by stirring at RT (Condition: 10 wt% catalyst, MeOH to oil molar ratio of 9:1 at 120°C for 24 h)

	Catalyst		
	ERB-1	NaERB-1 (0.05, RT)	NaERB-1 (0.10, RT)
Conversion (%)	22.13	58.48	74.03
Product yield (%)			
1. Methyl esters	5.85	39.33	42.45
MO and ML	41.55	49.41	50.17
MP	50.13	45.58	42.78
MS	8.32	5.01	7.05
2. Glycerol	9.10	7.15	8.16
Free	0.06	5.44	15.76
Bound	99.94	94.56	84.24
3. Monoglyceride	0.22	6.73	7.13
4. Diglyceride	6.97	5.26	16.29
Triglyceride (%)	77.87	41.52	25.97

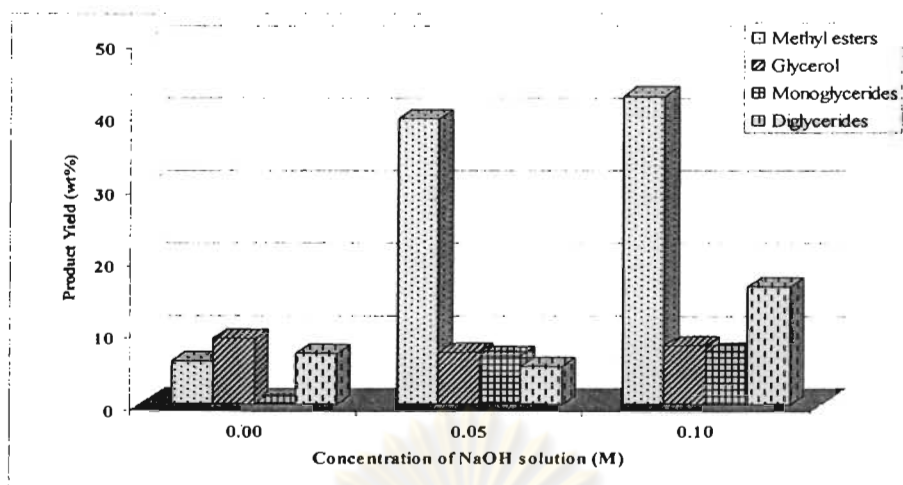


Figure 4.7 Product yield from transesterification reaction of palm oil over various NaOH solution concentrations loaded on ERB-1 by stirring at RT (Condition: 10 wt% catalyst, MeOH to oil molar ratio of 9:1 at 120°C for 24 h).

Table 4.9 Conversion and product yield in transesterification reaction of palm oil over various NaOH solution concentrations loaded on ERB-1 by refluxing at 60°C (Condition: 10 wt% catalyst, MeOH to oil molar ratio of 9:1 at 120°C for 24 h)

	Catalyst		
	ERB-1	NaERB-1 (0.05, 60)	NaERB-1 (0.10, 60)
Conversion (%)	22.13	53.66	53.75
Product yield (%)			
1. Methyl esters	5.85	33.56	30.66
MO and ML	41.55	50.76	51.01
MP	50.13	44.44	43.71
MS	8.32	4.80	5.28
2. Glycerol	9.10	7.62	8.13
Free	0.06	4.23	4.85
Bound	99.94	95.77	95.15
3. Monoglyceride	0.22	6.45	7.27
4. Diglyceride	6.97	6.03	7.68
Triglyceride (%)	77.87	46.34	46.25

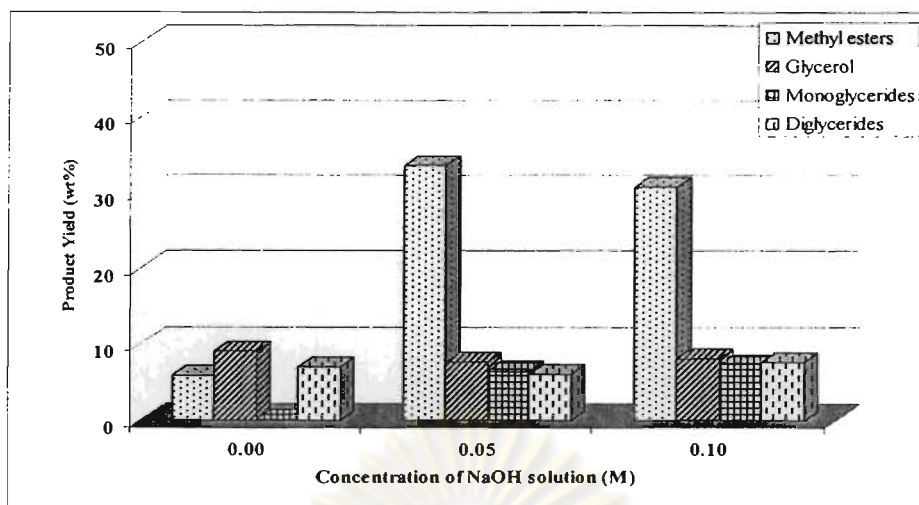


Figure 4.8 Product yield from transesterification reaction of palm oil over various NaOH solution concentrations loaded on ERB-1 by refluxing at 60°C (Condition: 10 wt% catalyst, MeOH to oil molar ratio of 9:1 at 120°C for 24 h).

4.6.2 The different alkali metal loaded ERB-1

Table 4.10 shows conversion and product yield in transesterification reaction of palm oil over different alkali ions loaded on ERB-1. The corresponding plot of product yield versus type of alkali ions is shown in Figure 4.9. Among four types of alkali ion, NaERB-1 gives highest conversion and methyl esters yield due to its highest total surface area. Although K content in KERB-1 is higher than Na content in NaERB-1, but reaction over KERB-1 exhibits lower conversion and methyl esters yield than the case of NaERB-1. Then, both conversion and methyl esters yield mainly depend on surface area of catalyst. Taking into account the activity of the alkali ion located in catalyst, the following order is NaERB-1 > KERB-1 ≈ RbERB-1 > CsERB-1.

Table 4.10 Conversion and product yield in transesterification reaction of palm oil over different alkali ions loaded on ERB-1 (Condition: 10 wt% catalyst, MeOH to oil molar ratio of 9:1 at 120°C for 24 h)

	Catalyst			
	NaERB-1 (0.10, RT)	KERB-1 (0.10, RT)	RbERB-1 (0.10, RT)	CsERB-1 (0.10, RT)
Conversion (%)	74.03	65.11	67.69	57.79
Product yield (%)				
1. Methyl esters	42.45	37.57	38.19	30.62
MO and ML	50.17	52.90	52.08	51.81
MP	42.78	42.06	42.01	42.42
MS	7.05	5.04	5.91	5.77
2. Glycerol	8.16	7.85	7.90	7.83
Free	15.76	9.24	10.48	0.27
Bound	84.24	90.76	89.52	99.73
3. Monoglycerides	7.13	6.03	5.42	5.88
4. Diglycerides	16.29	13.66	16.17	13.46
Triglycerides (%)	25.97	34.89	32.31	42.21



Figure 4.9 Product yield from transesterification reaction of palm oil over different alkali ions loaded on ERB-1 (Condition: 10 wt% catalyst, MeOH to oil molar ratio of 9:1 at 120°C for 24 h).

4.7 Catalytic activities of NaERB-1(0.10, RT) in transesterification reaction

4.7.1 Effect of reaction time

The optimum reaction time is determined by performing reactions at varying reaction time. The values of % conversion and product yield obtained by transesterification reaction of palm oil over NaERB-1(0.10, RT) for different reaction times are shown in Table 4.11. The reaction time was varied in the range of 6-36 h. The conversion and methyl esters yield increase from the reaction time range between 6 to 24 h, and thereafter kept nearly constant as a result of a nearly equilibrium conversion. It is obvious that the reaction time of 6 to 18 h is not enough for the completion of reaction at 120°C. The reaction time of 24 to 36 h makes the conversion and methyl esters yield are nearly equal value. Therefore, the suitable reaction time is 24 hours.

Table 4.11 Conversion and product yield in transesterification reaction of palm oil over NaERB-1(0.10, RT) for different reaction times
(Condition: 10 wt% catalyst, MeOH to oil molar ratio of 9:1 at 120°C)

	Time (h)					
	6	12	18	24	30	36
Conversion (%)	24.65	33.98	47.66	74.03	77.24	75.63
Product yield (%)						
1. Methyl esters	6.27	11.83	19.69	42.45	45.10	47.12
MO and ML	51.31	50.85	49.54	50.17	52.15	51.96
MP	42.65	43.74	44.37	42.78	41.71	41.57
MS	6.04	5.40	6.09	7.05	6.15	6.48
2. Glycerol	9.23	9.06	9.06	8.16	8.60	8.25
Free	0.51	1.75	6.03	15.76	24.61	25.43
Bound	99.49	98.25	93.97	84.24	75.39	74.57
3. Monoglyceride	0.74	1.70	3.35	7.13	6.45	6.27
4. Diglyceride	8.42	11.39	15.55	16.29	17.09	13.99
Triglyceride (%)	75.35	66.02	52.34	25.97	22.76	24.37

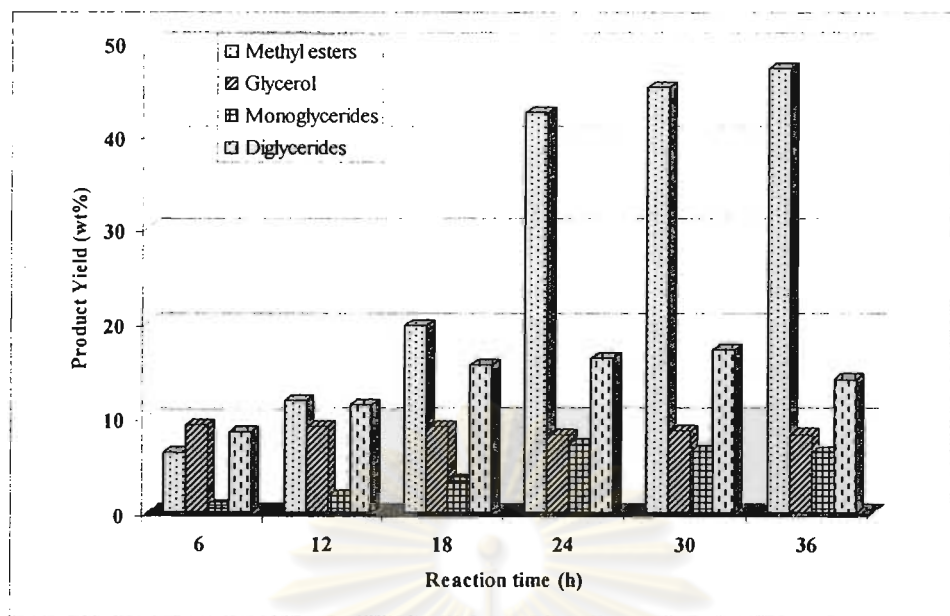


Figure 4.10 Product yield from transesterification reaction of palm oil over NaERB-1(0.10, RT) for different reaction times (Condition: 10 wt% catalyst, MeOH to oil molar ratio of 9:1 at 120°C).

4.7.2 Effect of methanol to oil molar ratio

Table 4.12 shows the effect of MeOH to oil molar ratios on the conversion. By increasing the amount of methanol loading, the methyl ester yield increases considerably. When the MeOH to oil molar ratio is very close to 9:1, the conversion and methyl esters yield reach the maximum value. However, beyond the molar ratio of 9:1, the excessively added methanol (MeOH to oil of 15:1) has no significant effect on the conversion. Therefore, the optimum molar ratio of MeOH to oil to produce methyl esters is approximately 9:1.

The stoichiometric ratio for transesterification reaction requires three moles of alcohol and one mole of triglyceride to yield three moles of fatty acid ester and one mole of glycerol. The molar ratio of methanol to vegetable oil is also one of the most important variables affecting the yield of methyl esters. In this reaction, an excess of methanol was used in order to shift the equilibrium in the direction of the products.

Table 4.12 Conversion and product yield in transesterification reaction of palm oil over NaERB-1(0.10, RT) at various ratios of methanol to oil
(Condition: 10 wt% catalyst at 120°C for 24 h)

	MeOH to oil molar ratio (mol/mol)		
	6:1	9:1	15:1
Conversion (%)	54.20	74.03	72.25
Product yield (%)			
1. Methyl esters	20.49	42.45	44.50
MO and ML	52.58	50.17	52.04
MP	42.19	42.78	43.58
MS	5.23	7.05	4.37
2. Glycerol	9.01	8.16	8.28
Free	1.61	15.76	15.85
Bound	98.39	84.24	84.15
3. Monoglyceride	4.92	7.13	11.59
4. Diglyceride	19.78	16.29	7.88
Triglyceride (%)	45.80	25.97	27.75

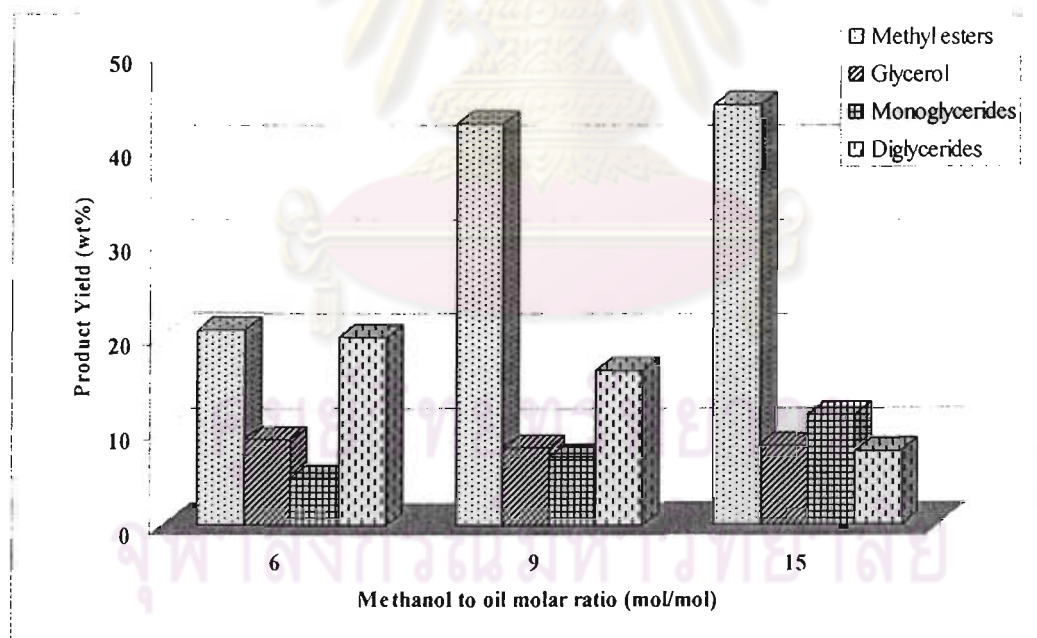


Figure 4.11 Product yield from transesterification reaction of palm oil over NaERB-1(0.10, RT) at various ratios of methanol to oil
(Condition: 10 wt% catalyst at 120°C for 24 h).

4.7.3 Effect of catalyst amount

The catalyst amount was varied in the range of 5.0 to 15.0% referred to the starting material weight, while the remaining variables keep constant. Increased catalyst amount from 5 to 10% results the increased conversion and methyl esters yield. However, with further increase in the catalyst amount, the conversion is decreased, which is possibly due to the rise of a mixing problem of reactants, products and solid catalyst. This problem corresponds to the previous report by Xie *et al.* [3] which shows lower conversion by increasing catalyst amount from 7.5 to 9.0%.

Table 4.13 Conversion and product yield in transesterification reaction of palm oil over NaERB-1(0.10, RT) at various catalyst amount
(Condition: MeOH to oil molar ratio of 9:1 at 120°C for 24 h)

	Catalyst amount (wt%)		
	5	10	15
Conversion (%)	57.18	74.03	67.96
Product yield (%)			
1. Methyl esters	25.26	42.45	41.70
MO and ML	50.73	50.17	46.64
MP	42.54	42.78	40.91
MS	6.72	7.05	12.45
2. Glycerol	7.75	8.16	10.40
Free	13.79	15.76	43.13
Bound	86.21	84.24	56.87
3. Monoglyceride	4.94	7.13	2.76
4. Diglyceride	17.45	16.29	13.10
Triglyceride (%)	42.82	25.97	32.04

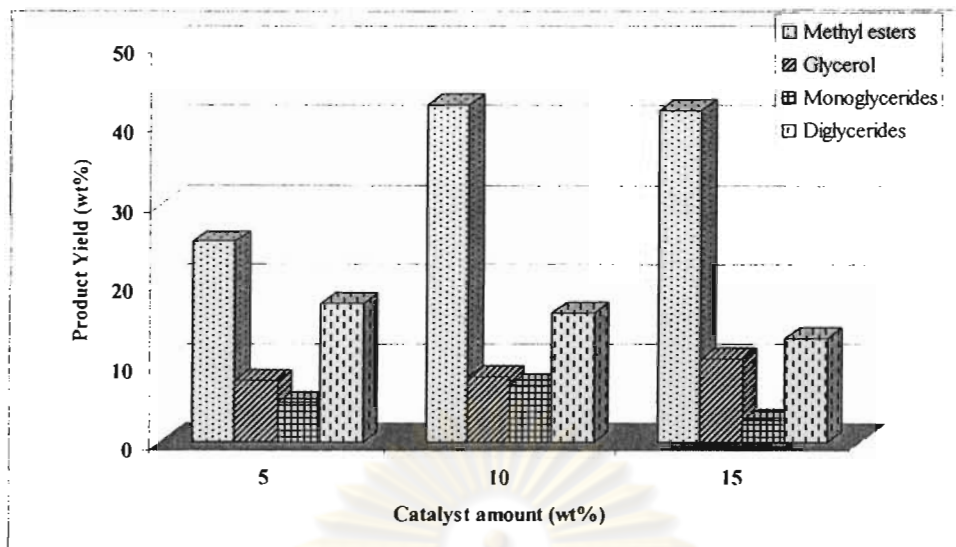


Figure 4.12 Product yield from transesterification reaction of palm oil over NaERB-1(0.10, RT) at various catalyst amounts (Condition: MeOH to oil molar ratio of 9:1 at 120°C for 24 h).

4.7.4 Effect of reaction temperature

To determine the effect of reaction temperature, the transesterification reaction was carried out under the optimal condition, obtained in the previous section (10 wt% catalyst, 9:1 methanol to oil molar ratio for 24 h). The experiments were conducted at temperatures ranging from 90 to 120°C. The effect of reaction temperature on the product yield is presented in Table 4.14 and Figure 4.13. By increasing temperature from 90 to 115°C, the conversion and methyl esters yield gradually increase. However, reaction temperature is upraised to 120°C, the conversion and methyl esters yield increases about 25%.

From all effects in transesterification reaction, these conclude that the optimum condition is 10 wt% NaERB-1(0.10, RT) catalyst, 9:1 MeOH to oil molar ratio at 120°C for 24 h. And this condition will be applied to delaminated ERB-1 catalyst (Del-ERB-1).

Table 4.14 Conversion and product yield in transesterification reaction of palm oil over NaERB-1(0.10, RT) at various reaction temperatures
(Condition: 10 wt% catalyst, MeOH to oil molar ratio of 9:1 for 24 h)

	Temperature (°C)				
	90	100	110	115	120
Conversion (%)	26.78	32.17	36.24	48.08	74.03
Product yield (%)					
1. Methyl esters	6.94	10.52	12.65	19.36	42.45
MO and ML	48.30	49.11	49.62	51.46	50.17
MP	45.35	45.19	44.94	43.89	42.78
MS	6.35	5.70	5.44	4.66	7.05
2. Glycerol	9.22	9.04	9.05	9.08	8.16
Free	0.25	0.63	1.59	5.38	15.76
Bound	99.75	99.37	98.41	94.62	84.24
3. Monoglyceride	0.92	1.43	2.00	3.48	7.13
4. Diglyceride	9.70	11.18	12.54	16.16	16.29
Triglyceride (%)	73.22	67.83	63.76	51.92	25.97



Figure 4.13 Product yield from transesterification reaction of palm oil over NaERB-1(0.10, RT) at various reaction temperatures
(Condition: 10 wt% catalyst, MeOH to oil molar ratio of 9:1 for 24 h).

4.8 Delaminated ERB-1 (Del-ERB-1)

The del-ERB-1 was made by swelling and exfoliating the as-synthesized ERB-1. The delamination process is articulated in different treatment steps:

- swelling of ERB-1 precursor [ERB-1(P)] at 80°C by CTMABr, TPAOH and H₂O (swollen product);
- ultrasound treatment (sonicated product);
- calcination (final product del-ERB-1).

4.8.1 X-ray powder diffraction (XRD)

The changing structure during delaminating treatment was followed by XRD technique. The X-ray diffraction was ensured that swelling was complete [indicated by a diffraction pattern in Figure 4.14 (c) corresponding to layer separation of approximately 4.7 nm.]. In Figure 4.14 (d), del-ERB-1 does not show the 00 l peaks [(001) and (002)] with its 2.7-nm periodicity characteristic of a MWW topology. This result indicates that basic TPAOH can cleave the linkages between layers and makes the surfactant molecules easily enter into the layer, resulting in the formation of material with expanded layers. Moreover, the solubilization of the SiO₄ species causes the partial destruction of the framework. Comparing the XRD of del-ERB-1 with that of calcined ERB-1, it can be seen the broader peaks and lower intensity for del-ERB-1 because the expanded layer structure seriously collapses.

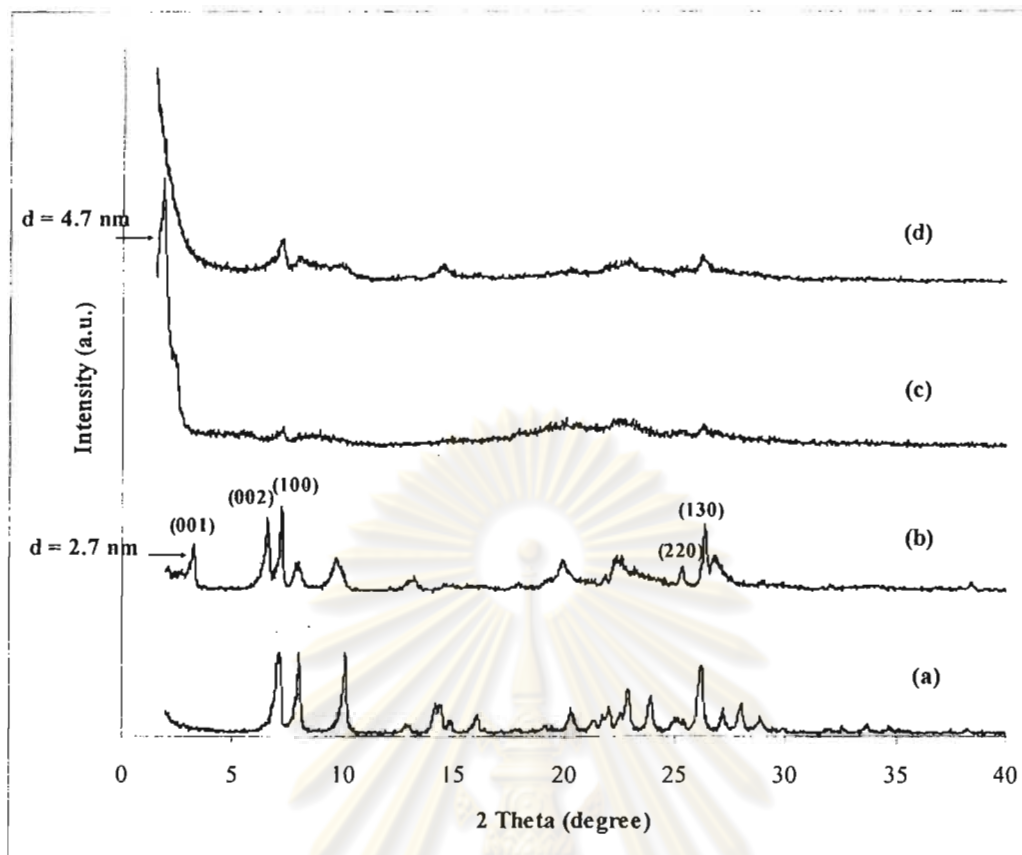


Figure 4.14 The XRD patterns of calcined ERB-1 (a), as-synthesized ERB-1 (b), swollen ERB-1 (c) and del-ERB-1 (d).

Figure 4.15 shows the XRD patterns of del-ERB-1 samples, prepared by using different amount of TPAOH base as shown in Table 3.1. The diffraction line decreases in intensity with increasing TPAOH content from 2.40 to 12.02 g. However, the excess TPAOH amount and long sonication time cause the structure of ERB-1 catalyst is destroyed to amorphous material [sample D4 in Figure 4.15 (d)]. When the weight ratio of TPAOH aqueous solution (20.10%) to ERB-1(P) is 6, the intensity of diffraction line in the XRD pattern of del-ERB-1 obviously decreases, which denoted as D2 in Figure 4.15 (b). The N_2 adsorption data of del-ERB-1 samples comparing to ERB-1 are shown in Table 4.15. It is observed that external surface area extremely increases for del-ERB-1 samples, while sample D2 provides the highest total specific surface area and external surface area. Then the suitable condition for ERB-1

delamination was 1.00g ERB-1(P) : 11.36g H₂O : 5.60g CTMABr : 6.00g TPAOH and sonicated 1 h [23].

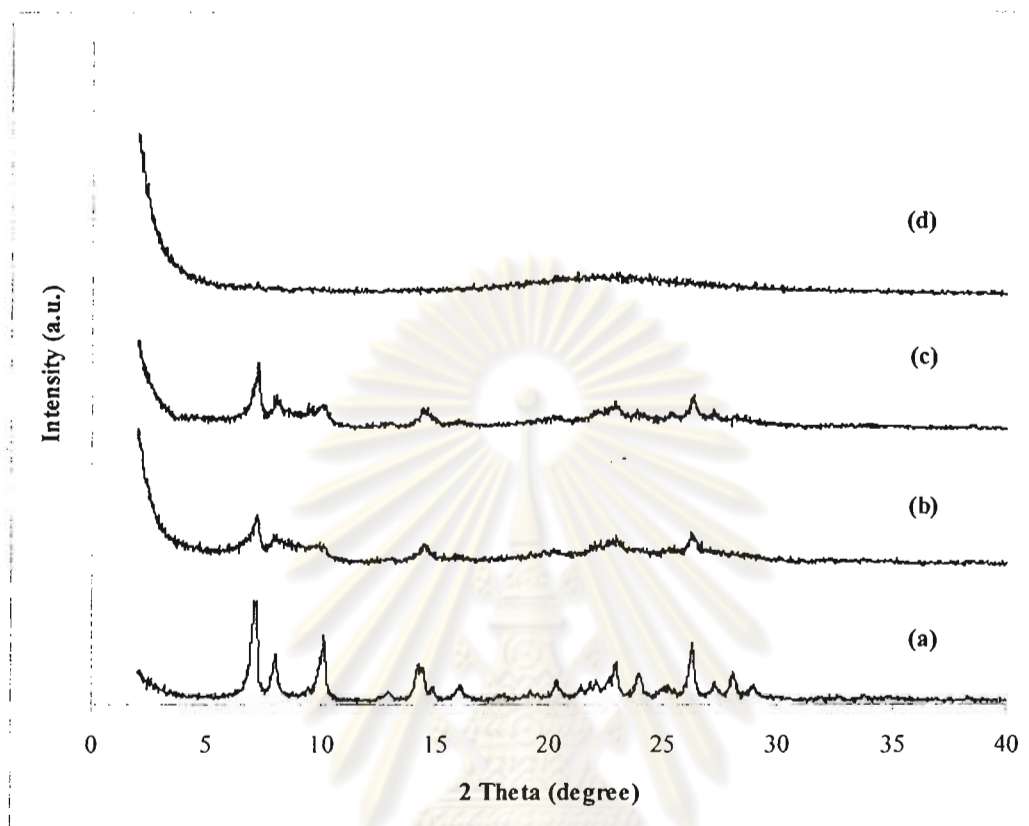


Figure 4.15 The XRD patterns of del-ERB-1 samples with various conditions: D1 (a), D2 (b), D3 (c) and D4 (d).

Table 4.15 Textural properties of ERB-1 and del-ERB-1 samples with various conditions

Sample	Total specific surface area ^a (m ² /g)	External surface area ^b (m ² /g)	Micropore volume ^b (cm ³ /g)	Micropore distribution ^c (nm)
ERB-1	471	27	0.17	0.60
D1	516	60	0.18	0.60
D2	544	357	0.07	0.60
D3	501	292	0.08	0.60

^acalculated using the BET plot method

^bcalculated using the t-plot method

^ccalculated using the MP-plot method

4.9 Na loaded delaminated ERB-1 (Na-del-ERB-1)

Del-ERB-1 can be increased the basicity by loading alkali base like ERB-1 catalyst. Therefore, the optimum condition of loading base for ERB-1 is applied to del-ERB-1, *i.e.* 1 g of del-ERB-1 stirring with 30 ml of 0.10 M NaOH solution at RT for 3 h.

4.9.1 X-ray powder diffraction (XRD)

Figure 4.16 shows the XRD pattern of del-ERB-1 and Na-del-ERB-1 (0.10, RT). After loading Na, the diffraction line of Na-del-ERB-1(0.10, RT) obviously decreases. Moreover, Table 4.16 exhibits the external surface area extremely reduced for both total specific surface area and external surface area which results are similar to NaERB-1 (4.2.2.2).

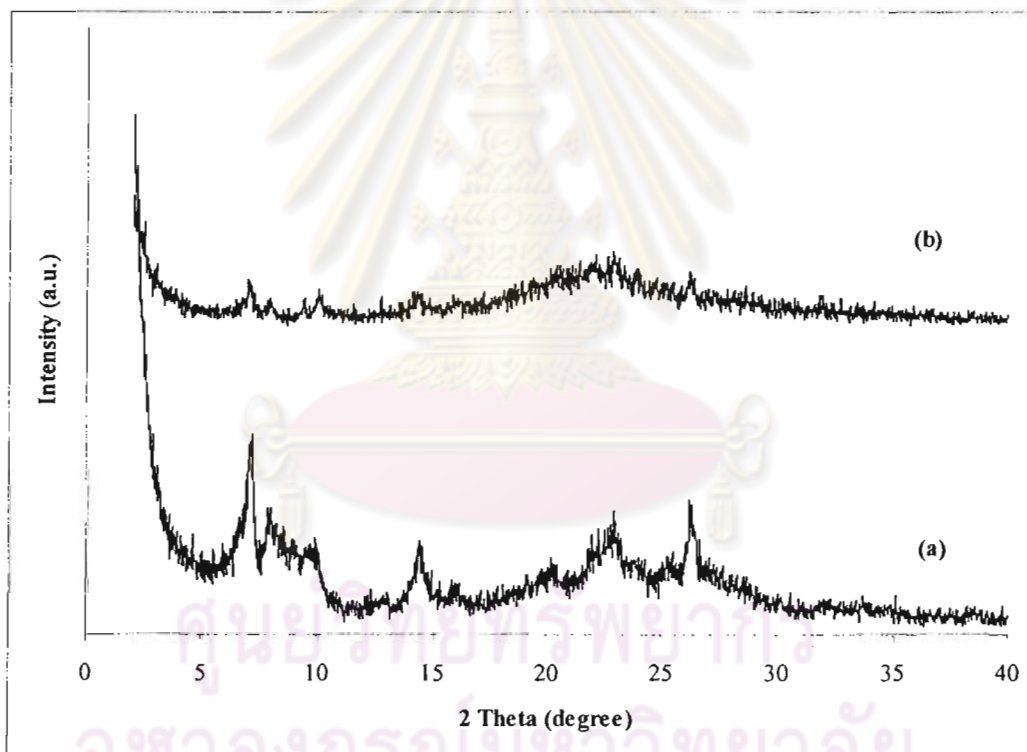


Figure 4.16 The XRD patterns of del-ERB-1 (a) and Na-del-ERB-1(0.10, RT) (b).

Table 4.16 Textural properties of del-ERB-1 and Na-del-ERB-1(0.10, RT)

Sample	Total specific surface area ^a (m ² /g)	External surface area ^b (m ² /g)	Micropore volume ^b (cm ³ /g)	Micropore distribution ^c (nm)
Del- ERB-1	544	357	0.07	0.60
Na-del-ERB-1(0.10, RT)	93	44	0.02	0.60

^acalculated using the BET plot method

^bcalculated using the t-plot method

^ccalculated using the MP-plot method

4.9.2 Elemental analysis

After Na loading, Na/SiO₂ ratio increase 12 times from 0.01 to 0.12. However, this ratio is less than NaERB-1 *i.e.* 0.19.

Table 4.17 The Na/SiO₂ ratio of del-ERB-1 and Na-del-ERB-1(0.10, RT)

Sample	Na/SiO ₂ ^a
Del-ERB-1	0.01
Na-del-ERB-1(0.10, RT)	0.12

^aobtained sodium contents by AAS

4.9.3 Scanning electron microscopy (SEM)

Figure 4.17 illustrates SEM images of calcined ERB-1 (a), NaERB-1(0.10, RT) (b), del-ERB-1 (c) and Na-del-ERB-1(0.10, RT) (d). Del-ERB-1 does not exhibit the typical platelet morphology as calcined ERB-1 particles, but shows smaller irregular particle. In case of Na-del-ERB-1, the morphology is the nearly same as del-ERB-1.

ศูนย์วิทยทรัพยากร
จุฬาลงกรณ์มหาวิทยาลัย

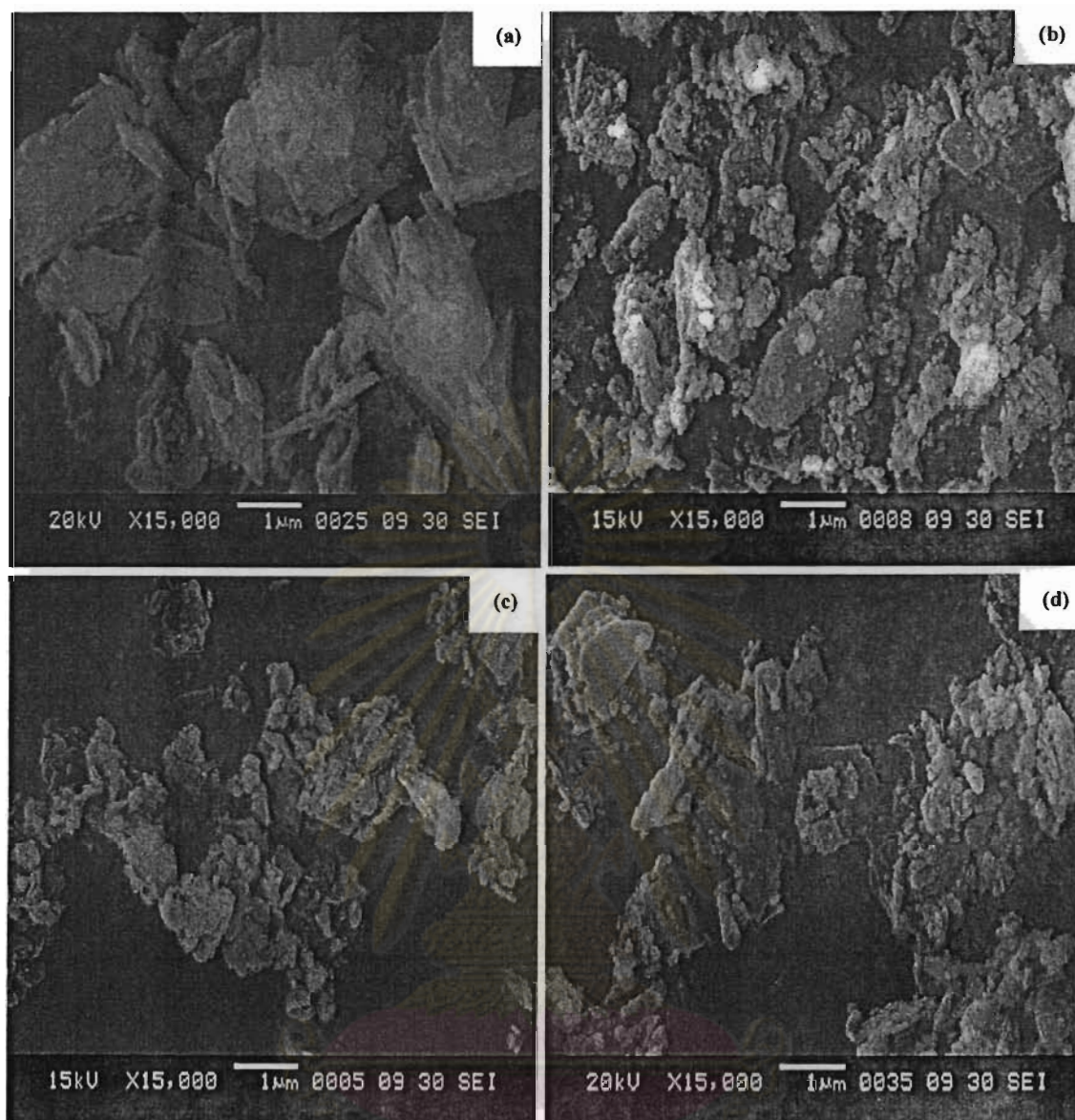


Figure 4.17 SEM images of del-ERB-I: calcined ERB-I (a), NaERB-I(0.10, RT) (b), del-ERB-I(c) and Na-del-ERB-I(0.10, RT) (d).

จุฬาลงกรณ์มหาวิทยาลัย

4.10 Catalytic activities of del-ERB-1 and Na-del-ERB-1(0.10, RT) catalysts

The values of % conversion and product yield in transesterification reaction of palm oil over ERB-1, del-ERB-1, NaERB-1(0.10, RT) and Na-del-ERB-1(0.10, RT) catalysts are shown in Table 4.18. The del-ERB-1 provides the slightly higher conversion than ERB-1 due to its higher surface area. It is observed that high surface area of catalyst hardly promotes the product amount, if basicity is not a strong enough. When del-ERB-1 was increased basic strength with Na loading, the conversion and methyl esters yield increase from 24.41 to 69.54% and 6.12 to 37.38%, respectively. However, both values are lower than that obtained from NaERB-1 since Na ion amount and total specific surface area of Na-del-ERB-1 is less than NaERB-1.



ศูนย์วิทยทรัพยากร
จุฬาลงกรณ์มหาวิทยาลัย

Table 4.18 Conversion and product yield in transesterification reaction of palm oil over ERB-1, del-ERB-1, NaERB-1(0.10, RT) and Na-del-ERB-1 (0.10, RT) (Condition: 10 wt% catalyst, MeOH to oil molar ratio of 9:1 at 120°C for 24 h)

	Catalyst			
	ERB-1	Del-ERB-1	NaERB-1 (0.10, RT)	Na-del-ERB-1 (0.10, RT)
Conversion (%)	22.13	24.41	74.03	69.54
Product yield (%)				
1. Methyl esters	5.85	6.12	42.45	37.38
MO and ML	41.55	45.69	50.17	50.77
MP	50.13	46.64	42.78	42.94
MS	8.32	7.67	7.05	6.29
2. Glycerol	9.10	9.17	8.16	8.02
Free	0.06	0.09	15.76	7.47
Bound	99.94	99.91	84.24	92.53
3. Monoglyceride	0.22	0.38	7.13	7.02
4. Diglyceride	6.97	8.74	16.29	17.11
Triglyceride (%)	77.87	75.59	25.97	30.46

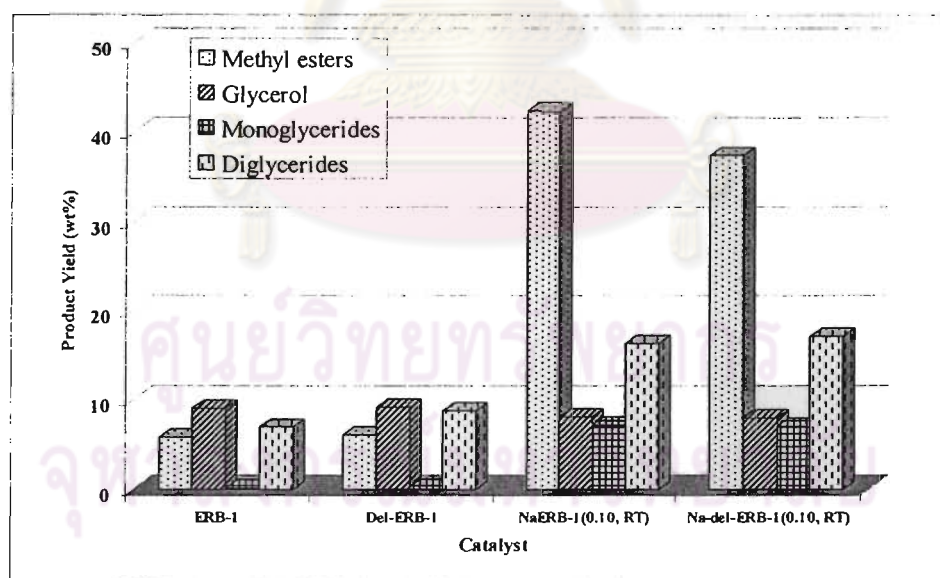


Figure 4.18 Product yield from transesterification reaction of palm oil over del-ERB-1 and Na-del-ERB-1(0.10, RT) (Condition: 10 wt% catalyst, MeOH to oil molar ratio of 9:1 at 120°C for 24 h).

4.11 Used and Na-reloaded catalysts

It is well known that the outstanding advantage of heterogeneous catalyst is the ease of separation and reuse. In this research, the spent catalyst was washed with acetone, dried at 120°C overnight and calcined at 550°C for 8 h. In addition, the used ERB-1 was refluxed with 0.10 M NaOH solution at RT for 3 h, dried and calcined at the same condition of above, which denoted as Na-reloaded ERB-1.

4.11.1 X-ray powder diffraction (XRD)

The XRD patterns of fresh, used and Na-reloaded ERB-1 catalysts are shown in Figure 4.19. XRD pattern of used ERB-1 confirms a characteristic peaks like fresh NaERB-1(0.10, RT) catalyst. The intensity of (100) peak at $2\theta \approx 7$ decreases because the catalytic structure is partially deformed during reaction. In case of Na-reloaded ERB-1, the diffraction line extremely decreases because the structure of used ERB-1 is destructed by reloaded base.

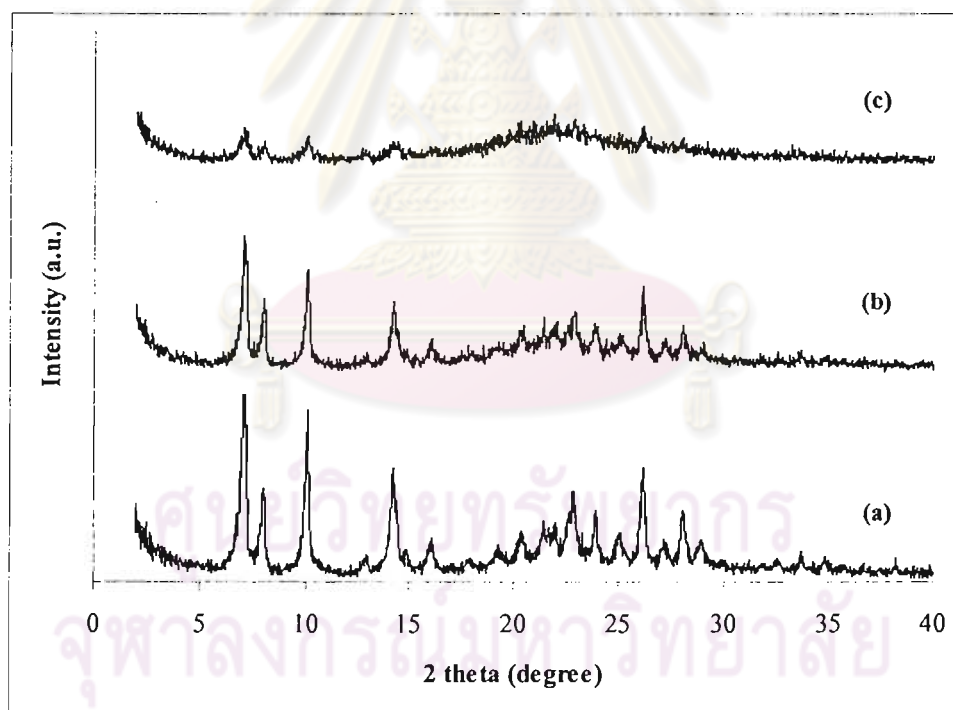


Figure 4.19 The XRD patterns of fresh NaERB-1(0.10, RT) (a), used ERB-1 (b) and Na-reloaded ERB-1 (c).

4.11.2 Sorption properties

After reaction, the total specific surface area and micropore volume of used catalyst decrease, but external surface area increases since the structure is deformed and Na ions are leached out during reaction. After loading Na ions on used ERB-1, total specific surface area, external surface area and micropore volume decrease because of increasing Na amount and the deformed EBR-1 structure as evidence from Na/SiO₂ ratio and XRD, respectively.

Table 4.19 Textural properties of used and Na-reloaded ERB-1

Sample	Total specific surface area ^a (m ² /g)	External surface area ^b (m ² /g)	Micropore volume ^b (cm ³ /g)	Micropore distribution ^c (nm)
NaERB-1(0.10, RT)	287	20	0.10	0.60
Used ERB-1	196	26	6.71x10 ⁻²	0.60
Na-reloaded ERB-1	64	23	1.73x10 ⁻²	0.60

^acalculated using the BET plot method

^bcalculated using the t-plot method

^ccalculated using the MP-plot method

Table 4.20 The Na/SiO₂ of used and Na-reloaded ERB-1

Sample	Na/SiO ₂ ^a
NaERB-1(0.10, RT)	0.19
Used ERB-1	0.09
Na-reloaded ERB-1	0.14

^aobtained sodium contents by AAS

4.11.3 Scanning electron microscopy (SEM)

Figure 4.20 shows SEM images of fresh NaERB-1(0.10, RT) (a), used ERB-1 (b) and Na-reloaded ERB-1 (c), respectively. The morphology of used and Na-reloaded ERB-1 are the aggregation of rough platelets while fresh catalyst is the aggregation of smooth sheets and covered with small particle on surface.

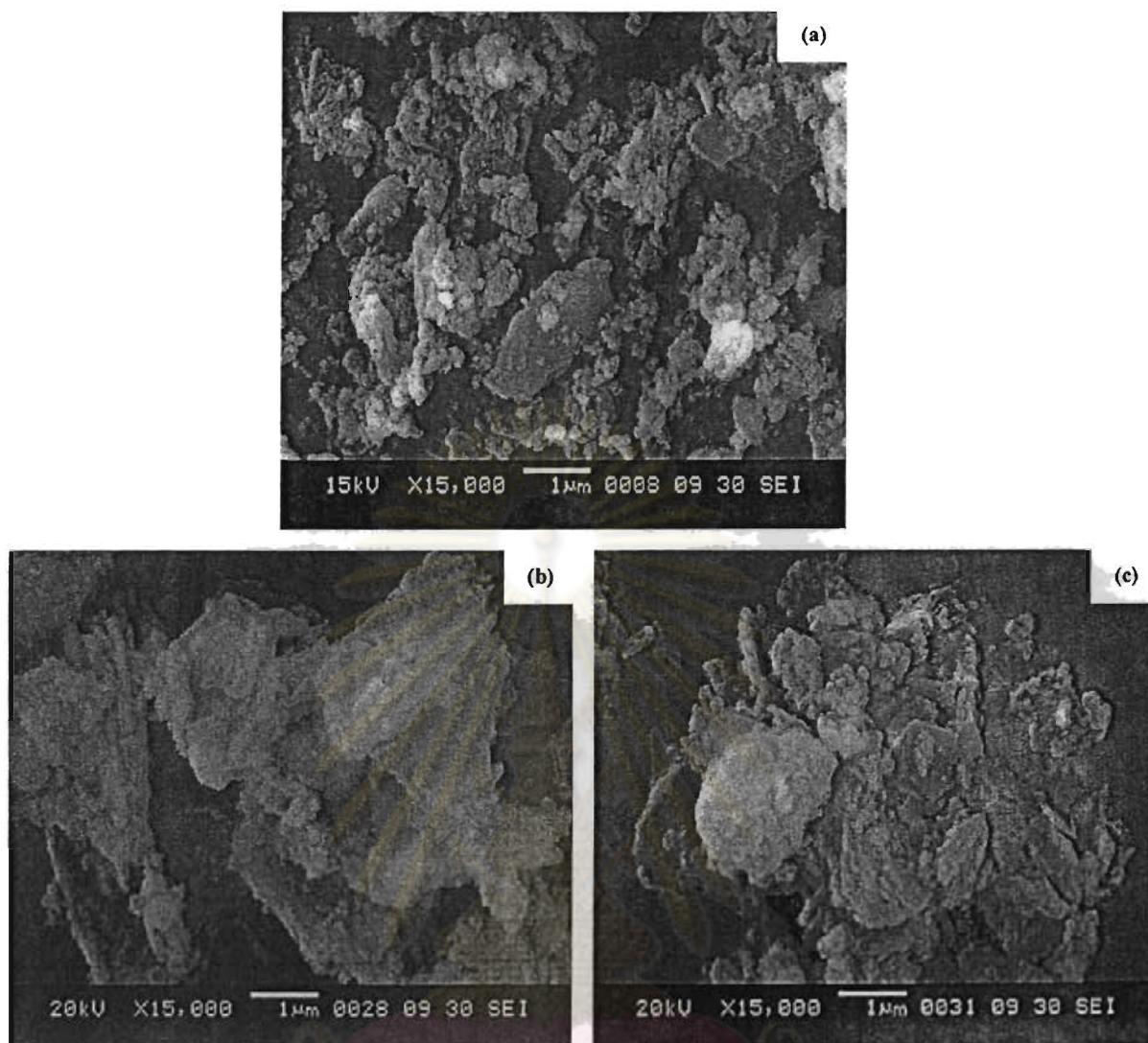


Figure 4.20 SEM images of NaERB-1(0.10, RT) (a), used ERB-1 (b) and Na-reloaded ERB-1 (c).

4.12 Catalytic activities of used and Na-reloaded catalysts

In order to study the stability of NaERB-1(0.10, RT) catalyst, it was reused by separating the catalyst, washing it thoroughly with acetone, drying overnight at 120°C and calcination at 550°C for 8h before using in the next experiment. A decline is observed in the conversion from 74.03% to 51.58%, thereby indicating the decrease of catalytic activity of used catalyst. Such a decrease in the catalytic activity is probably responsible for leaching of the Na species from ERB-1 catalyst. Then, the Na leaching experiment was conducted by stirring NaERB-1(0.10, RT) with methanol at 120°C for 24h. The filtrate was analyzed by AAS technique to confirm the Na

leaching amount during reaction, i.e. 12.55% comparing to NaERB-1 fresh catalyst. Moreover, the filtrate was adopted in transesterification without catalyst, the obtained conversion and methyl ester yield are 29.12% and 9.85%, respectively. When comparing to blank test (Table 4.7), reaction with filtrate gives slightly higher conversion and methyl esters yield about 3.11% and 3.22%, respectively. This experiment shows that methyl ester products mainly obtain from NaERB-1 catalytic performance, not only develop from leached Na ion. The cost of catalyst is significant and for the economic reason the catalyst needs to be regenerated. Moreover, the used catalyst was reloaded by stirring 0.10 M NaOH solution at RT for 3 h with hopefully increasing of activity. The catalytic results show that the Na-reloaded catalyst can give the slightly higher conversion than used ERB-1 but is lower than fresh catalyst according to effects of total specific surface area and Na amount.

Table 4.21 Conversion and product yield in transesterification reaction of palm oil over used and Na-reloaded catalysts (Condition: 10 wt% catalyst, MeOH to oil molar ratio of 9:1 at 120°C for 24 h)

	Catalyst		
	NaERB-1 (0.10, RT)	Used ERB-1	Na-reloaded ERB-1
Conversion (%)	74.03	51.58	53.53
Product yield (%)			
1. Methyl esters	42.45	21.23	25.46
MO and ML	50.17	50.77	45.90
MP	42.78	42.69	37.40
MS	7.05	6.54	16.69
2. Glycerol	8.16	9.40	8.44
Free	15.76	9.68	10.12
Bound	84.24	90.32	89.88
3. Monoglyceride	7.13	4.03	3.08
4. Diglyceride	16.29	16.93	16.55
Triglyceride (%)	25.97	48.42	46.47

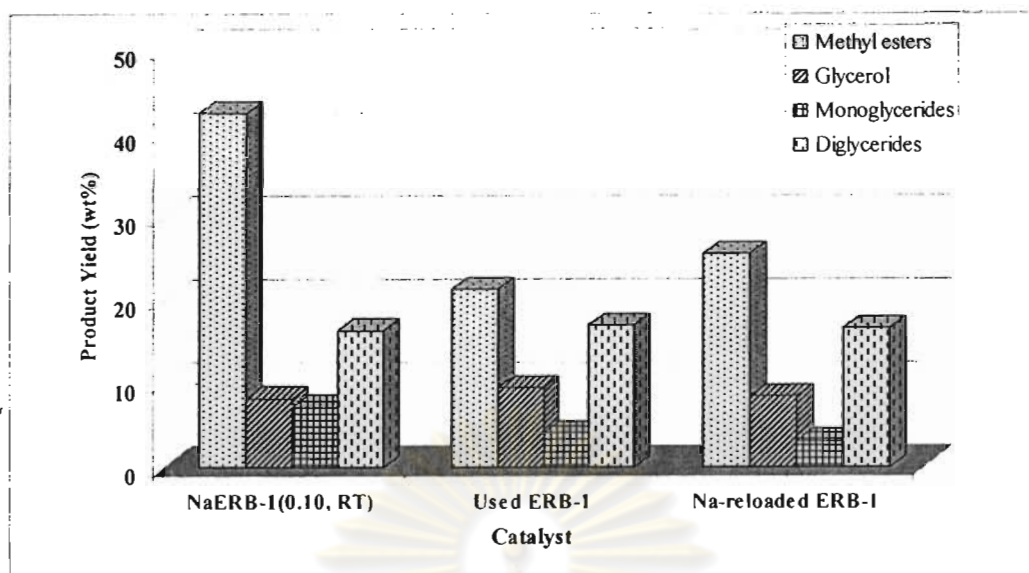


Figure 4.21 Product yield from transesterification reaction of palm oil over used and Na-reloaded catalysts (Condition: 10 wt% catalyst, MeOH to oil molar ratio of 9:1 at 120°C for 24 h).

4.13 Comparison of catalytic activity in transesterification reaction of vegetable oil over NaERB-1(0.10, RT) with other catalysts

Several studies have been described transesterification reaction of vegetable oil over different basic catalysts. Differences in the catalytic activities of these materials have usually been related to their basic properties, textural properties such as surface area and particle size and reaction condition. From Suppes, G.J. *et. al.*'s research [14], soybean transesterification was carried out at 120°C for 24 h over NaY and NaX zeolite. The soybean oil conversion and methyl esters yield were reported between 24.3-32.5% and 9.6-15.4%, respectively. These reported values are higher than the reaction carried over ERB-1 because of larger pore size of both zeolite catalysts. For another case of palm oil transesterification, it was carried out with 10 wt% of NaETS-10 catalyst at 9:1 of methanol to oil molar ratio, 120°C for 24 h [47]. NaETS-10 provides methyl esters yield about 78 wt%, which is higher than NaERB-1(0.10, RT) due to larger aperture; whereas, total specific surface area and micropore volume are nearly equal.

4.14 Transesterification mechanism for ERB-1

The mechanism was started from a framework oxide ion reacting with methanol to generate methoxide ion. Then this active species further react with triglyceride to produce methyl esters as shown in Figure 4.22.

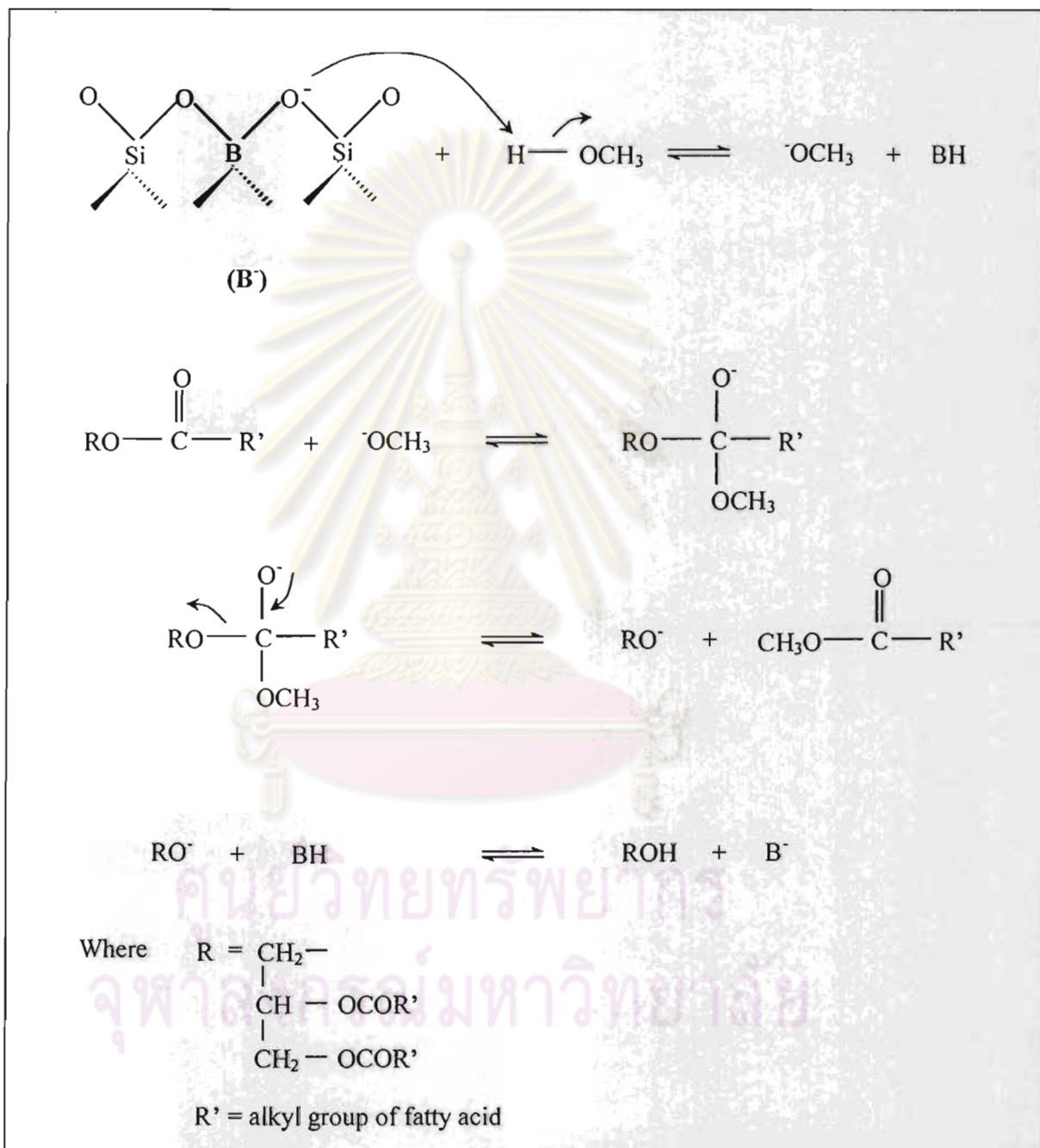


Figure 4.22 Proposed transesterification mechanism for ERB-1 catalyst.

CHAPTER V

CONCLUSION

The borosilicate molecular sieve, ERB-1 (EniRicercheBoralite-1) catalyst was synthesized by using piperidine as a structure directing agent (SDA) under hydrothermal condition. All synthesized products were characterized using XRD, ICP-AES, N₂ adsorption-desorption and SEM techniques. The XRD patterns show the characteristic peaks similar to that of ERB-1 reported by Millini *et al.* [4]. As-synthesized ERB-1 has a bi-dimensional layered structure. Upon calcination, the layers condense and form a three-dimensional microporous structure. The Na/SiO₂ ratio in catalyst is only 0.01, therefore the modification is needed to increase basic strength. Alkali bases, hydroxide solution of Na, K, Rb and Cs, were applied to increase the efficiency by loading on catalyst surface. Firstly, ERB-1 was stirred at room temperature or refluxed at 60°C by various concentrations (0.05 - 0.50 M) of NaOH solution for 3h. The optimum condition is found by stirring with a 0.10 M NaOH solution at RT, denoted as NaERB-1(0.10, RT). This makes the structure of catalyst still remains and the Na/SiO₂ ratio is the highest. This condition is adapted to other alkali bases and test catalytic activity in transesterification reaction of palm oil. The catalytic activity over NaERB-1(0.10, RT) provides the highest conversion and methyl esters yield on account of the highest Na/SiO₂ ratio of catalyst under optimum condition, i.e. 10 wt% of catalyst, 9:1 of methanol to oil molar ratio at 120°C for 24 h.

The del-ERB-1 sample was prepared by swelling and exfoliating the ERB-1 precursor. Comparing the XRD patterns of del-ERB-1 to calcined ERB-1, it can be seen that the high angle peaks decreases in intensity and broader, which indicate a reduction in number of crystal plane and the crystal size. The del-ERB-1 provides also a high external surface area.

Del-ERB-1 does not exhibit the typical platelet morphology as calcined ERB-1 particles, but shows smaller irregular particle shape. In case of Na-del-ERB-1, the morphology is the same as del-ERB-1. Adsorption-desorption isotherms of nitrogen on ERB-1 and del-ERB-1 samples exhibit a pattern of typical microporous

shape. The del-ERB-1 sample provides higher external surface area than ERB-1 sample about 13 times (from 27 to 357 m²/g). The del-ERB-1 provides the slightly higher conversion because it has higher surface area but lack of basic sites. This proves that the high surface area leads to promote the conversion and product yield. Del-ERB-1 was loaded with NaOH solution by the same condition as ERB-1. It hopes that the obtained conversion and methyl esters yield are higher than NaERB-1. In contrast, both values are lower because of less Na/SiO₂ ratio of Na-del-ERB-1 catalyst. The catalytic activities of used catalyst are decreased while after reloaded with NaOH solution, the methyl esters yield slightly increases but is not high as the fresh one according to effect of total specific surface area and Na amount of catalyst.

The suggestions for future work

The catalyst in transesterification should be adapted to improve the product yield.

1. To improve methyl esters yield by increasing reaction temperature.
2. To replace the alkali base solution with the alkali earth base solution because ERB-1 structure may remain under the weaker base condition.



ศูนย์วิทยทรัพยากร
จุฬาลงกรณ์มหาวิทยาลัย

REFERENCES

- [1] Energy information administration/the international energy outlook 2001 (IEO2001) [online]. 2002. Available from:
<http://www.eia.doe.gov/oiaf/archive/ieo01/world.html> [2002, March 3]
- [2] Meher, L.C.; Vidya Sagar, D.; Naik, S.N. Technical aspects of biodiesel production by transesterification: a review. *Renew. Sustain. E. Rev.* 10(2006) : 248.
- [3] Xie, W.; Peng, H.; Chen, L. Transesterification of soy bean oil catalyzed by potassium loaded on alumina as a solid-base catalyst. *Appl. Catal. A: Gen.* 300(2006) : 368.
- [4] Millini, R.; Perego, G.; Parker, W.O., Bellussi, G.; Carluccio, L. Layered structure of ERB-1 microporous borosilicate precursor and its intercalation properties towards polar molecules. *Micropor. Mesopor. Mater.* 4(1995) : 221.
- [5] Inagaki, S.; Kamino, K.; Kikuchi, E.; Matsukata, M. Shape selectivity of MWW-type aluminosilicate zeolites in the alkylation of toluene with Methanol. *Appl. Catal. A: Gen.* 318(2007) : 22.
- [6] Perego, C.; Amarilli, S.; Millini, R.; Bellussi, G.; Girotti, G.; Terzoni, G. Experimental and computational study of beta, ZSM-12, Y, mordenite and ERB-1 in cumene synthesis. *Microporous Mater.* 6(1996) : 395.
- [7] Corma, A.; Fornés, V.; Martínez-Triguero, J.; Pergher, S.B. Delaminated zeolites: Combining the benefits of zeolites and mesoporous materials for catalytic uses. *J. Catal.* 186(1999) : 57.
- [8] Ziolk, M.; Casilda, V.C.; Aranda, R.M.; Sobczak, I. Modification of acid-base properties of alkali metals containing catalysts by application of various supports. *Appl. Catal. A: Gen.* 303(2006) : 121.
- [9] Papayannakos, N.; Louloudi, A.; Diasakou, M. Kinetic of the non-catalytic transesterification of soybean oil. *Fuel.* 77(1998) : 1297.
- [10] Demirbas, A. Biodiesel production via non-catalytic SCF method and biodiesel fuel characteristics. *Ener. Conver. Manage.* 47(2006) : 2271.

- [11] Demirbas, A. Comparison of transesterification methods for production of biodiesel from vegetable oils and fats. *Ener. Convers. Manage.* 49(2008) : 125.
- [12] Leung, D.Y.C.; Guo, Y. Transesterification of neat and frying oil : Optimization for biodiesel production. *Fuel Process. Technol.* 87(2006) : 883.
- [13] Xie, W.; Huang, X.; Li, H. Soybean oil methyl esters preparation using NaX zeolites loaded with KOH as a heterogeneous catalyst. *Bioresour. Technol.* 98(2007) : 936.
- [14] Suppes, G.J.; Dasari, M.A.; Doskocil, E.J.; Mankidy, P.J.; Goff, M.J. Transesterification of soybean oil with zeolite and metal catalysts. *Appl. Catal. A.* 257(2004) : 213.
- [15] Arzamendi, G.; Arguinarena, E.; Campo, I.; Zabala, S.; Gandia, L.M. Alkaline and alkaline-earth metals compounds as catalysts for the methanolysis of sunflower oil. *Catal. Today.* 133-135(2008) : 305.
- [16] Bond, G.C. Heterogeneous Catalysis: Principles and Applications, Clarendon, Oxford, 1974.
- [17] Hagen, J. Industrial Catalysis: A Practical Approach, 1999.
- [18] Analysis software user's manual, BELSORP, BEL JAPAN, INC, 57.
- [19] Song, C.; Hsu, C.S.; Mochida, I. Chemistry of Diesel Fuels, New York, Taylor & Francis, 2000.
- [20] Frontera, P.; Testa, F.; Aiello, R.; Candamaro, S., Nagy, J.B. Transformation of MCM-22(P) into ITQ-2: The role of framework aluminium. *Micropor. Mesopor. Mater.* 106(2007) : 107.
- [21] Wu, P.; Fan, W.; Nuntasri, D.; Tatsumi, T. MWW-type titanosilicate: Novel preparation and high efficiency in the epoxidation of various alkenes. *Stud. Surf. Sci. Catal.* 154(2004) : 2581.
- [22] Corma, A.; Fornés, V.; Guil, J.M.; Pergher, S.; Maesen, Th.L.M.; Buglass, J.G. Preparation, characterisation and catalytic activity of ITQ-2, a delaminated zeolite. *Micropor. Mesopor. Mater.* 38(2000) : 31.
- [23] Jung, H.J.; Park, S.S.; Shin, C.H.; Park, Y.K., Hong, S.B. Comparative catalytic studies on the conversion of 1-butene and n-butane to isobutene over MCM-22 and ITQ-2 zeolites. *J. Catal.* 245(2007) : 65.

- [24] Corma, A.; Fornés, V.; Guil, J.M.; Martínez-Triguero, J.; Creyghton. Characterization and catalytic activity of MCM-22 and MCM-56 compared with ITQ-2. *J. Catal.* 191(2000) : 218.
- [25] Liu, L.; Cheng, M.; Ma, D.; Hu, G.; Pan, X.; Bao, X. Synthesis, characterization, and catalytic properties of MWW zeolite with variable Si/Al ratios. *Micropor. Mesopor. Mater.* 94(2006) : 314.
- [26] Xie, W.; Li, H. Alumina-supported potassium iodide as a heterogeneous catalyst for biodiesel production from soybean oil. *J. Mol. Catal. A: Chem.* 255(2006) : 1.
- [27] Wang, Y.; Ou, S.; Liu, P.; Xue, F.; Tang, S. Comparison of two different processes to synthesize biodiesel by waste cooking oil. *J. Mol. Catal. A: Chem.* 252(2006) : 107.
- [28] Umer, R.; Farooq, A. Production of biodiesel through optimized alkaline-catalyzed transesterification of rapeseed oil. *Fuel.* 87(2008) : 265.
- [29] Lotero, E.; Liu, Y.; Lopez, D.E.; Suwannakarn, K.; Bruce, D.A.; Goodwin, J.G. Synthesis of biodiesel via acid catalysis. *Ind. Eng. Chem. Res.* 44(2005) : 5353.
- [30] Jitputti, J.; Kitiyanan, B.; Rangsunvigit, P.; Bunyakiat, K.; Attanatho, L.; Jenvanitpanjakul, P. Transesterification of crude palm kernel oil and crude coconut oil by different solid catalysts. *Chem. Eng. J.* 116(2006) : 61.
- [31] Xie, W.; Peng, H.; Chen, L. Transesterification of soybean oil catalyzed by potassium loaded on alumina as a solid-base catalyst. *Appl. Catal. A: Gen.* 300(2006) : 67.
- [32] Liu, X.; He, H.; Wang, Y.; Zhu, S. Transesterification of soybean oil to biodiesel using SrO as a solid base catalyst. *Catal. Commun.* 8(2007) : 1107.
- [33] Demirbas, A. Biodiesel from sunflower oil in supercritical methanol with calcium oxide. *Ener. Conver. Manage.* 48(2007) : 937.
- [34] Juttu, G.G.; Lobo, R.F. Characterization and catalytic properties of MCM-56 and MCM-22 zeolites. *Micropor. Mesopor. Mater.* 40(2000) : 9.
- [35] Jung, J.J.; Park, S.S.; Shin, C.H.; Park, Y.K.; Hong, S.B. Comparative catalytic studies on the conversion of 1-butene and n-butane to isobutene over MCM-22 and ITQ-2 zeolites. *J. Catal.* 245(2007) : 65.

- [36] Díaz, U.; Fornés, V.; Corma, A. On the mechanism of zeolite growing: Crystallization by seeding with delayered zeolites. *Micropor. Mesopor. Mater.* 90(2006) : 73.
- [37] Determination of free and total glycerol and mono-, di-, triglyceride contents, BS EN 14105: 2003.
- [38] Plank, C.; Lorbeer, E. Simultaneous determination of glycerol, and mono-, di- and triglycerides in vegetable oil methyl esters by capillary gas chromatography. *J. Chromatogr. A.* 697(1995) : 461.
- [39] Azcan, N.; Danisman, A. Alkali catalyzed transesterification of cottonseed oil by microwave irradiation. *Fuel.* 86(2007) : 2639.
- [40] Mittelbach, M. Diesel fuel derived from vegetable oils, VI: specifications and quality control of biodiesel. *Bioresour. Technol.* 56(1996) :7.
- [41] Dowd, M.K. Gas chromatographic characterization of soapstocks from vegetable oil refining. *J. Chromatogr. A.* 816(1998) : 185.
- [42] Azcan, N.; Danisman, A. Microwave assisted transesterification of rapeseed oil. *Fuel.* 87(2008) : 1781.
- [43] Ngamcharussrivichai, C.; Wiwatnimit, W.; Wangnoi, S. Modified dolomites as catalysts for palm kernel oil transesterification. *J. Mol. Catal. A: Chem.* 276(2007) : 24.
- [44] Yang, Z.; Xie, W. Soybean oil transesterification over zinc oxide modified with alkali earth metals. *Fuel Process. Technol.* 88(2007) : 631.
- [45] Edgar, L.; Yijun, L.; Dora, E.L.; Kaewta, S.; David, A.B.; James, G.G. Synthesis of biodiesel via acid catalysis. *Ind. Eng. Chem. Res.* 44(2005) : 5353.
- [46] Ionic radius [online]. 2008. Available from: http://en.wikipedia.org/wiki/Ionic_radius [2008, March 11]
- [47] Satima Saranark. Transesterification of palm oil using ETS-10, ETGeS-10 and Na-loaded ETS-10 catalysts. Master' Thesis, Department of library Science, Graduate School, Chulalongkorn University, 2007.



APPENDICES

ศูนย์วิทยทรัพยากร
จุฬาลงกรณ์มหาวิทยาลัย

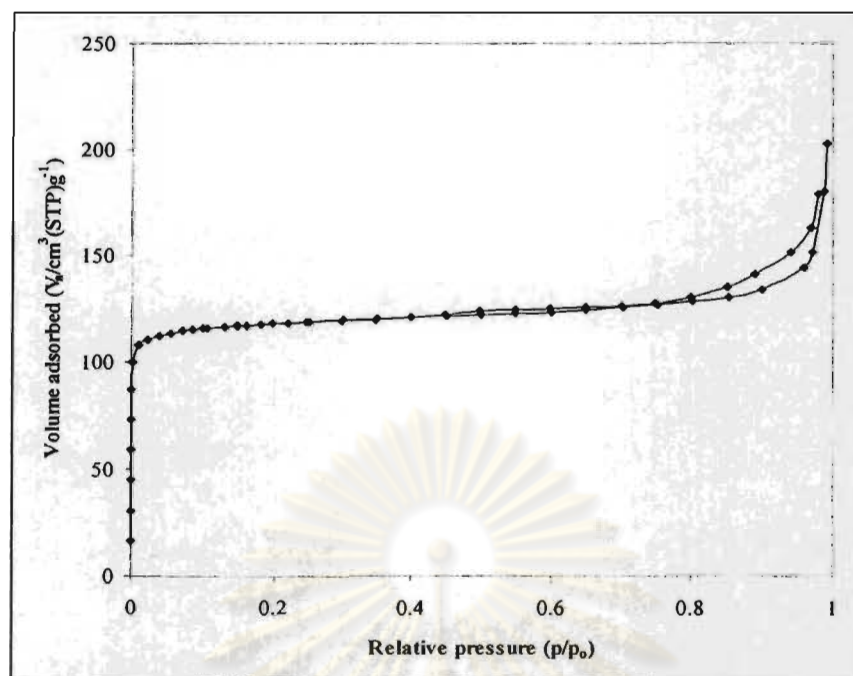


Figure A-1 N_2 adsorption-desorption isotherm of calcined ERB-1.

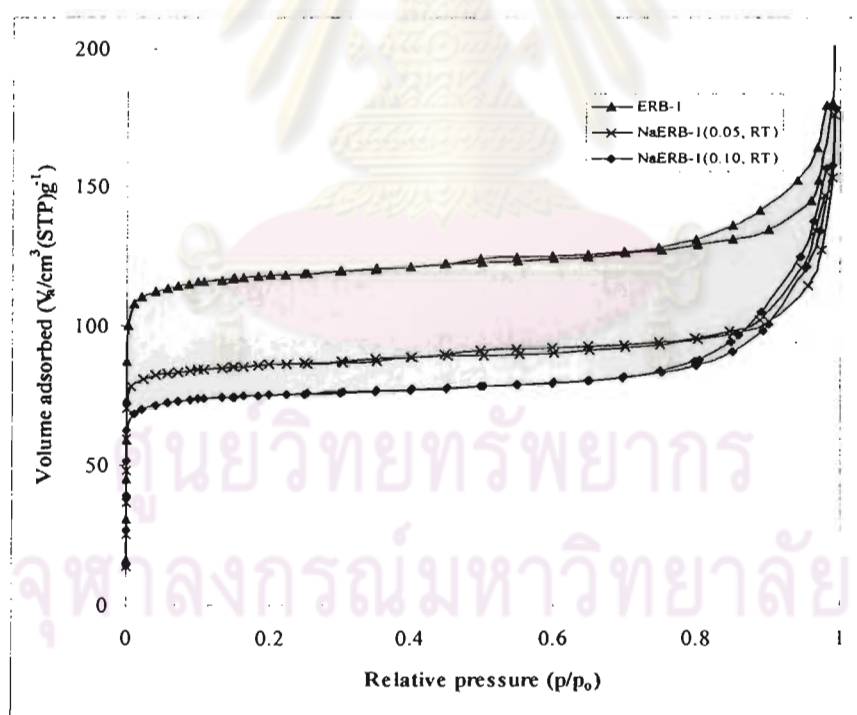


Figure A-2 N_2 adsorption-desorption isotherms of NaERB-1 catalysts prepared by refluxing at RT.

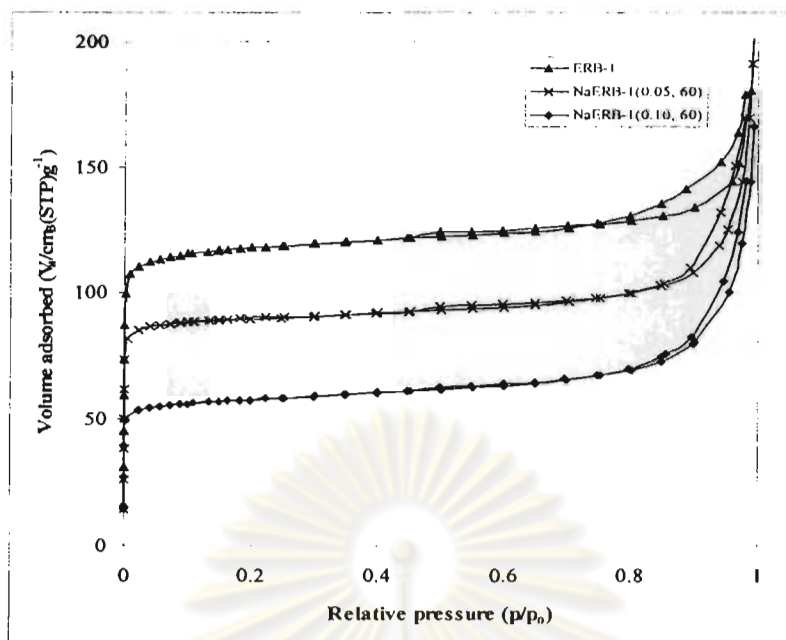


Figure A-3 N₂ adsorption-desorption isotherms of NaERB-1 catalysts prepared by refluxing at 60°C.

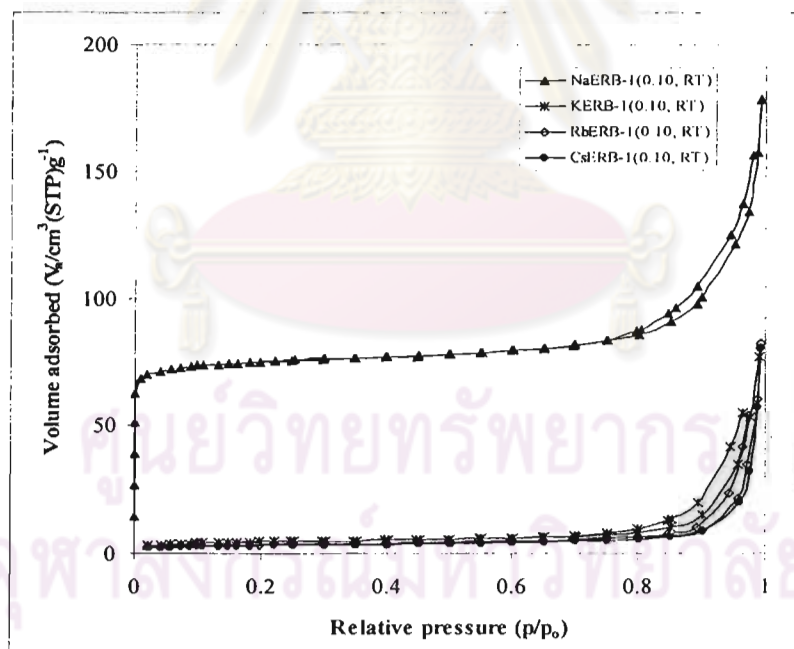


Figure A-4 N₂ adsorption-desorption isotherms of XERB-1 catalysts prepared by refluxing at RT.

1. Molecular weight calculation of triglycerides

Table A-1 Calculation mol % from fatty acid composition of Commercial Oleen palm oil

Fatty acid	wt %	MW	Mol % (wt % x MW)
Oleic acid (C18:1)	45.22	282.46	127.73
Palmitic acid (C16:0)	37.94	256.43	97.29
Linoleic acid (C18:2)	10.89	284.48	30.98
Stearic acid (C18:0)	3.84	284.48	10.92
Myristic acid (C14:0)	1.19	228.38	2.72
Lauric acid (C12:0)	0.67	200.30	1.34
Linolenic acid (C18:3)	0.27	278.44	0.75
		total	271.73

From structure of FA to TG

$$\begin{aligned}
 \text{TG} &= 3\text{FA} - 3\text{H} + (3\text{C} + 5\text{H}) \\
 &= 3\text{FA} + 3\text{C} + 2\text{H} \\
 &= 3(271.73) + 3(12) + 2(1) \\
 &= 853.20
 \end{aligned}$$

ศูนย์วิทยทรัพยากร
จุฬาลงกรณ์มหาวิทยาลัย

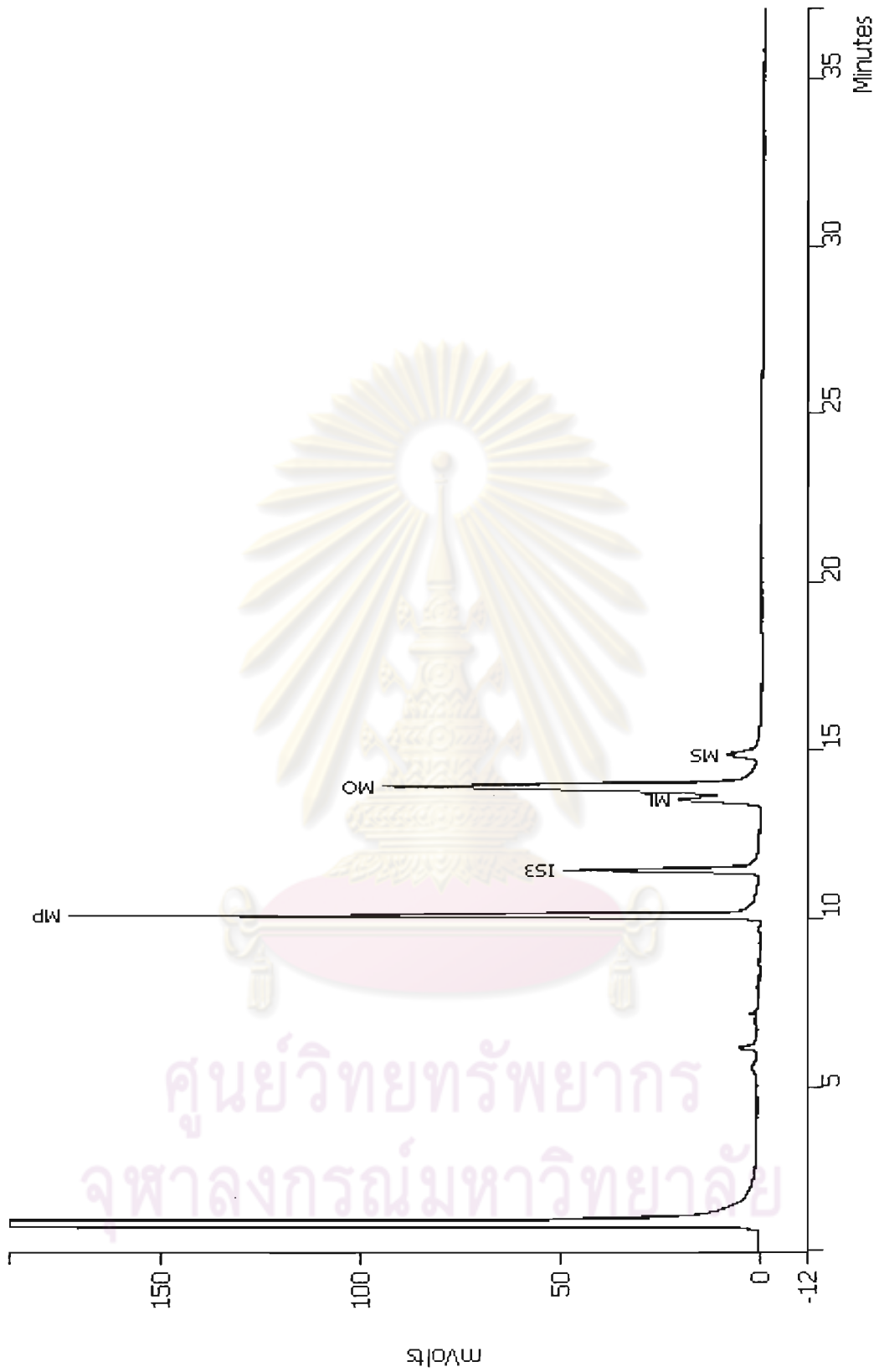


Figure A-5 Gas chromatogram of methyl esters.

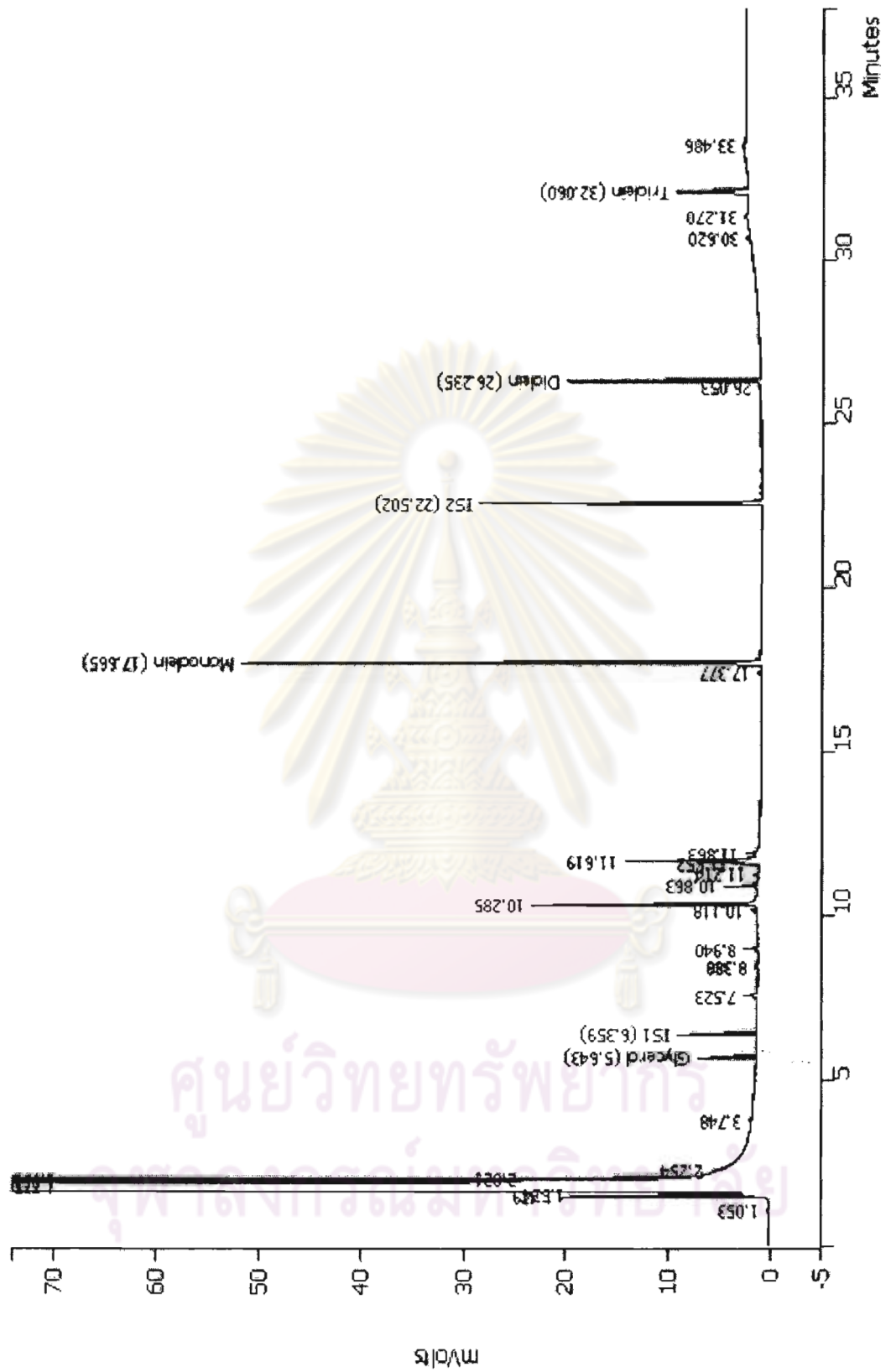


Figure A-6 Gas chromatogram of glycerol, mono-, di- and triolein.

2. Determination of methyl ester contents

2.1 Methyl esters calibration function

The calibration function was given by the following expression, obtained from the experimental data using the linear regression method.

Linear regression equation: $Y = aX + b$

$$M_{(MO+ML)}/M_{is3} = a_{(MO+ML)}(A_{(MO+ML)}/A_{is3}) + b_{(MO+ML)}$$

$$M_{MP}/M_{is3} = a_{MP}(A_{MP}/A_{is3}) + b_{MP}$$

$$M_{MS}/M_{is3} = a_{MS}(A_{MS}/A_{is3}) + b_{MS}$$

$M_{(MO+ML)}$, M_{MP} , M_{MS} = respectively the mass of methyl oleate and methyl linoleate combination, methyl palmitate and methyl stearate (mg)

M_{is3} = the mass of internal standard No.3 (mg)

$A_{(MO+ML)}$, A_{MP} , A_{MS} = the peak areas, respectively, methyl oleate and methyl linoleate combination, methyl palmitate and methyl stearate

A_{is3} = the peak area of internal standard No.3

$a_{(MO+ML)}$ and $b_{(MO+ML)}$ = constants coming from linear regression equation for methyl oleate and methyl linoleate combination

a_{MP} and b_{MP} = constants coming from linear regression equation for methyl palmitate

a_{MS} and b_{MS} = constants coming from linear regression equation for methyl stearate

In regression function X was represented by the term $A_{(MO+ML)}/A_{is3}$, A_{MP}/A_{is3} and A_{MS}/A_{is3} while Y was $M_{(MO+ML)}/M_{is3}$, M_{MP}/M_{is3} and M_{MS}/M_{is3} .

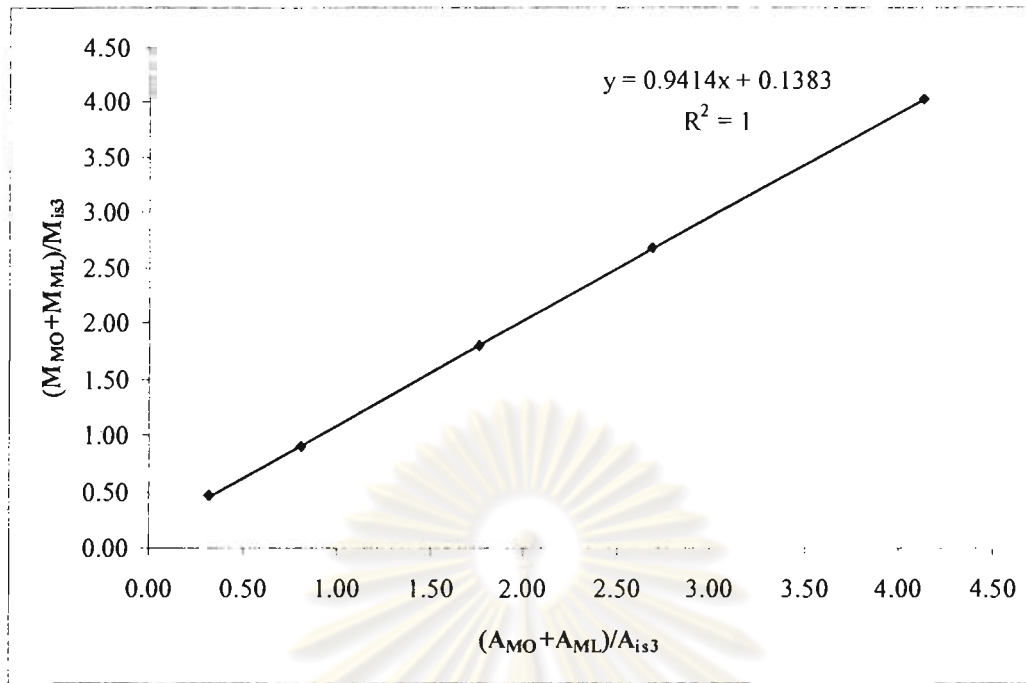


Figure A-8 Calibration curve of methyl oleate and methyl linoleate combination.

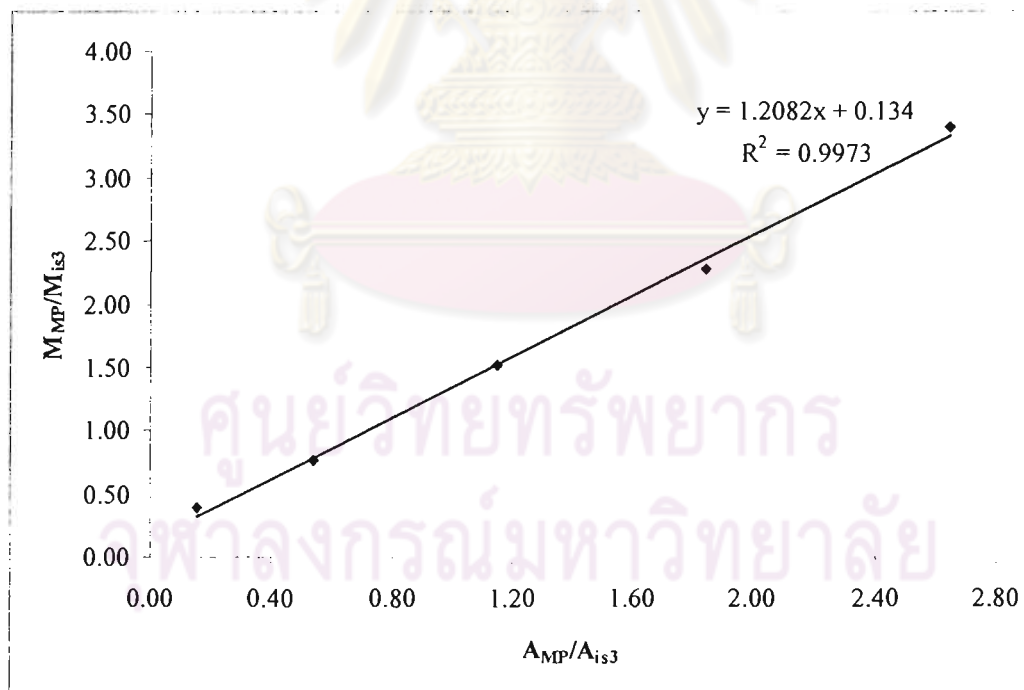


Figure A-9 Calibration curve of methyl palmitate.

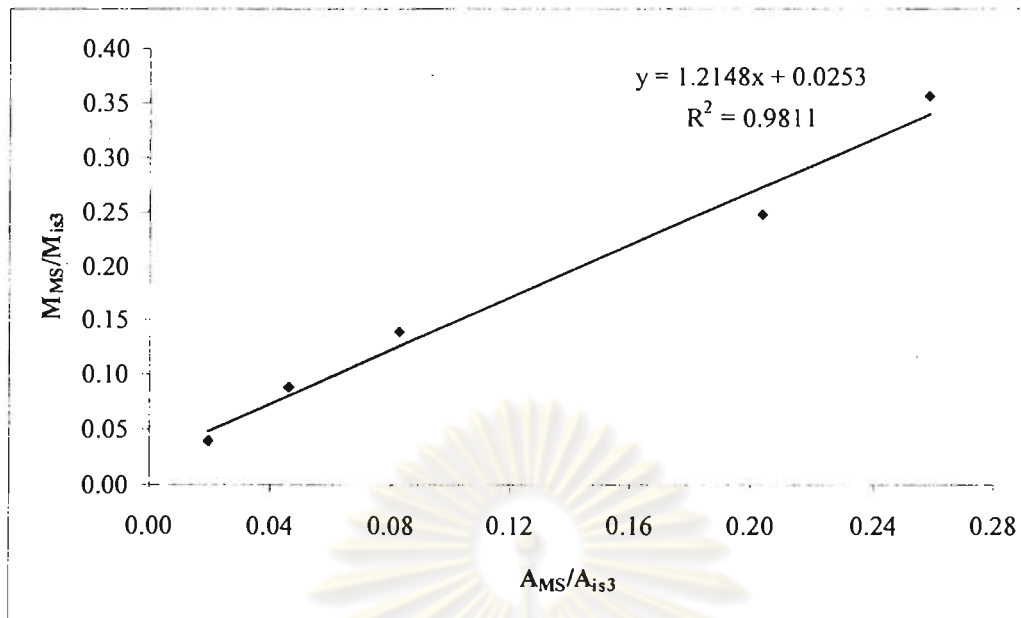


Figure A-10 Calibration of methyl stearate.

2.2 Calculation of the percentage of methyl esters

The percentage (m/m) of the methyl oleate and methyl linoleate combination, methyl palmitate and methyl stearate was calculated by using the expression:

$$MO+ML = [a_{(MO+ML)}(\Sigma A_{(MO+ML)}/A_{is3}) + b_{(MO+ML)}] \times (M_{is3}/m) \times 100$$

$$MP = [a_{MP}(\Sigma A_{MP}/A_{is3}) + b_{MP}] \times (M_{is3}/m) \times 100$$

$$MS = [a_{MS}(\Sigma A_{MS}/A_{is3}) + b_{MS}] \times (M_{is3}/m) \times 100$$

MO+ML, MP, MS = the methyl oleate and methyl linoleate combination, methyl palmitate and methyl stearate percentage (m/m) in the sample

M_{is3} = the mass of internal standard No.3 (mg)

$\Sigma A_{(MO+ML)}, \Sigma A_{MP}, \Sigma A_{MS}$ = the sum of the peak areas of the methyl oleate and methyl linoleate combination, methyl palmitate and methyl stearate

A_{is3} = the peak area of internal standard No.3

m = the mass of sample (mg)

$a_{(MO+ML)}$ and $b_{(MO+ML)}$	=	constants coming from regression method for methyl oleate and methyl linoleate combination
a_{MP} and b_{MP}	=	constants coming from regression method for methyl palmitate
a_{MS} and b_{MS}	=	constants coming from regression method for methyl stearate

3. Determination of free and total glycerol and mono-, di- and triglyceride content

3.1 Glycerol calibration function

The calibration function was given by the following expression, obtained from the experimental data using the linear regression method:

$$M_g/M_{is1} = a_g(A_g/A_{is1}) + b_g$$

M_g	=	the mass of glycerol (mg)
M_{is1}	=	the mass of internal standard No.1 (mg)
A_g	=	the peak area of glycerol
A_{is1}	=	the peak area of internal standard No.1
a_g and b_g	=	constants coming from regression method for glycerol

In regression function X was represented by the term A_g/A_{is1} while Y was M_g/M_{is1}

3.2 Glycerides calibration function

$$M_m/M_{is2} = a_m(A_m/A_{is2}) + b_m$$

$$M_d/M_{is2} = a_d(A_d/A_{is2}) + b_d$$

$$M_t/M_{is2} = a_t(A_t/A_{is2}) + b_t$$

M_m, M_d, M_t	=	respectively the mass of mono-, di- and triolein (mg)
M_{is2}	=	the mass of internal standard No.2 (mg)
A_m, A_d, A_t	=	the peak areas, respectively, mono-, di- and triolein

- A_{is2} = the peak area of internal standard No.2
 a_m and b_m = constants coming from regression method for monoglycerol
 a_d and b_d = constants coming from regression method for diglycerol
 a_t and b_t = constants coming from regression method for triglycerol

In regression function X was represented by the term A_m/A_{is2} , A_d/A_{is2} and A_t/A_{is2} while Y was M_m/M_{is2} , M_d/M_{is2} and M_t/M_{is2}

The calibration functions could be regarded as acceptable only if the correlation coefficient was equal or higher than 0.95.

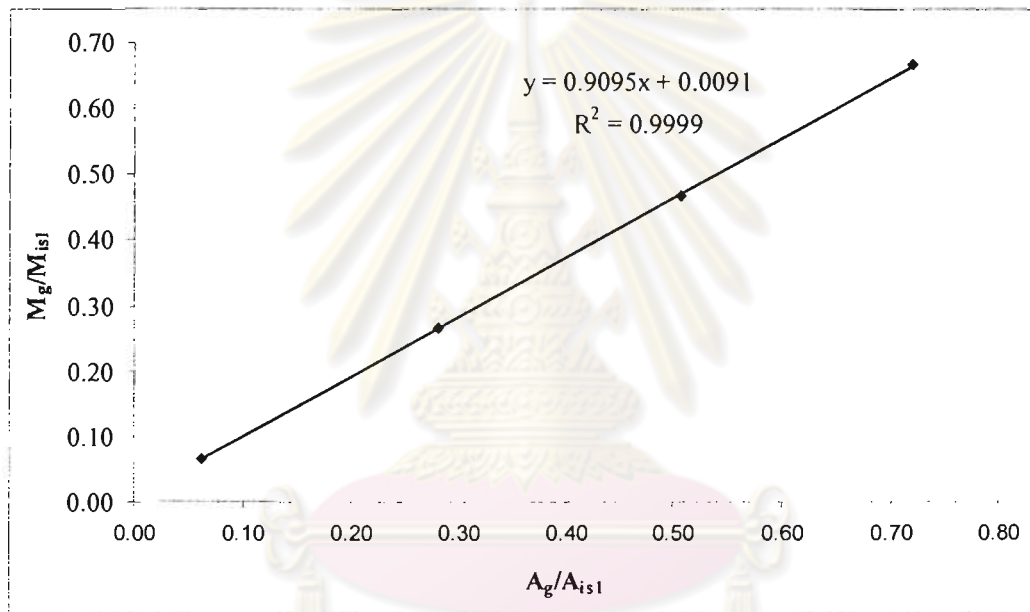


Figure A-11 Calibration of glycerol.

ศูนย์วิจัยทรัพยากร
จุฬาลงกรณ์มหาวิทยาลัย

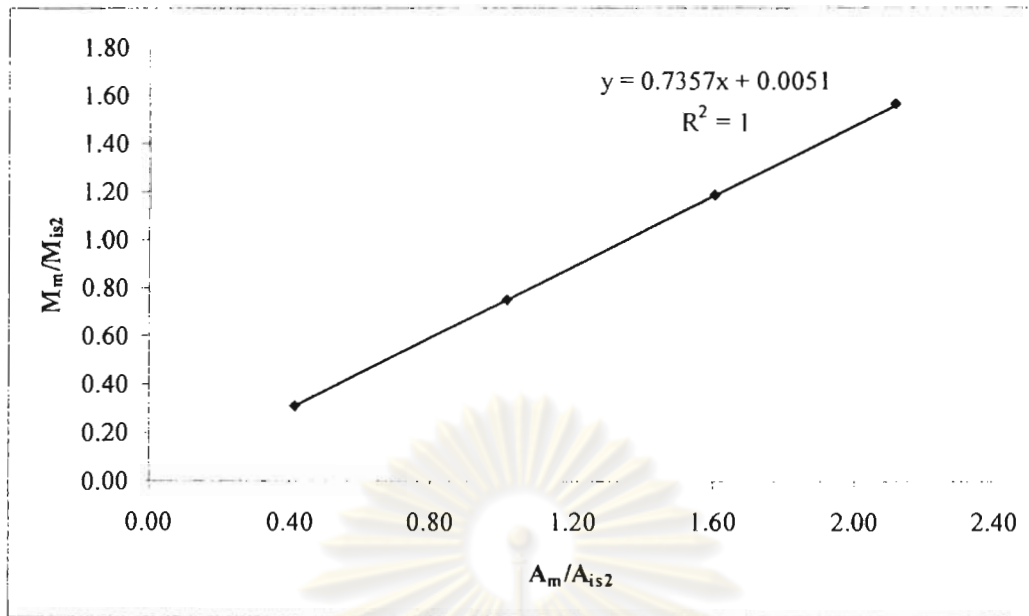


Figure A-12 Calibration of monoolein.

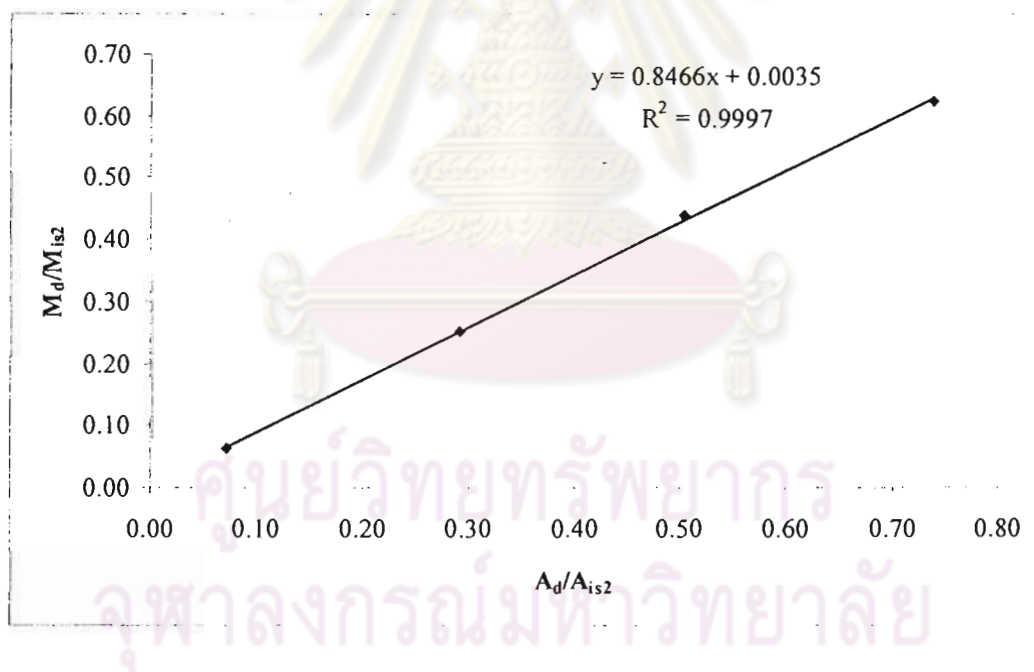


Figure A-13 Calibration of diolein.

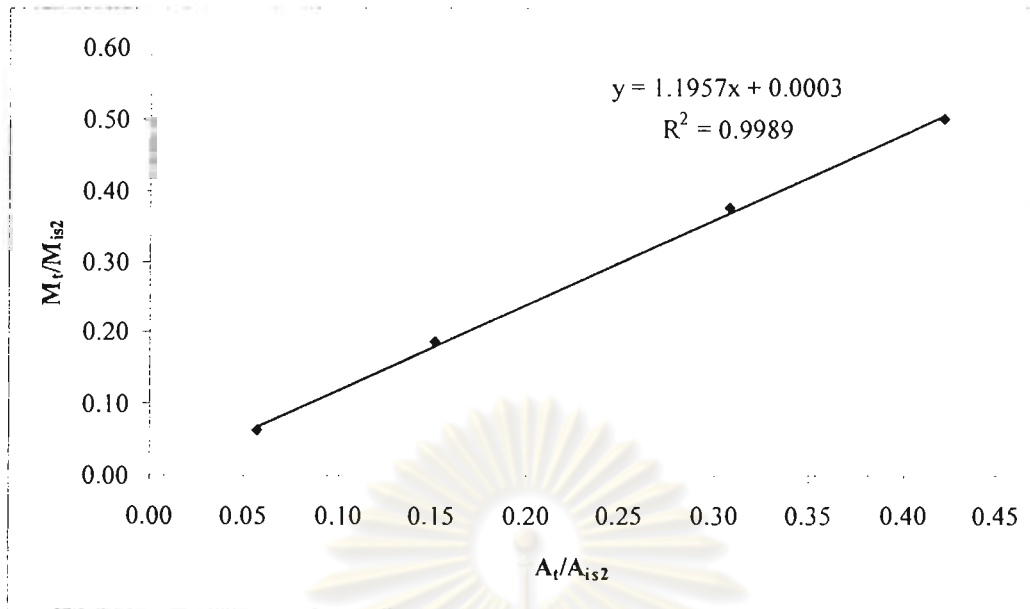


Figure A-14 Calibration of triolein.

3.3 Calculation of the percentage of free glycerol

The percentage (m/m) of free glycerol in the sample was calculated by using the expression:

$$G = [a_g(A_g/A_{is1}) + b_g] \times (M_{is1}/m) \times 100$$

- G = the percentage (m/m) of free glycerol in the sample
 A_g = the peak area of the glycerol
 A_{is1} = the peak area of internal standard No.1
 M_{is1} = the mass of internal standard No.1 (mg)
 m = the mass of sample (mg)
 a_g and b_g = constants coming from regression method for glycerol

3.4 Calculation of the percentage of glycerides

The percentage (m/m) of the mono-, di- and triglycerides was calculated by using the expression:

$$M = [\text{a}_m(\Sigma A_m/A_{is2}) + \text{b}_m] \times (M_{is2}/m) \times 100$$

$$D = [\text{a}_d(\Sigma A_d/A_{is2}) + \text{b}_d] \times (M_{is2}/m) \times 100$$

$$T = [\text{a}_t(\Sigma A_t/A_{is2}) + \text{b}_t] \times (M_{is2}/m) \times 100$$

M, D, T	=	the mono-, di- and triglyceride percentage (m/m) in the sample
$\Sigma A_m, \Sigma A_d, \Sigma A_t$	=	the sum of the peak areas of the mono-, di- and triglycerides
A_{is2}	=	the peak area of internal standard No.2
m	=	the mass of sample (mg)
a_m and b_m	=	constants coming from regression method for monoglycerol
a_d and b_d	=	constants coming from regression method for diglycerol
a_t and b_t	=	constants coming from regression method for triglycerol

3.5 Calculation of the percentage of total glycerol

The percentage (m/m) of total glycerol in the sample was calculated by using the expression:

$$G_T = G + 0.255 M + 0.146 D + 0.103 T$$

G_T	=	the percentage (m/m) of total glycerol (free and bound) in the sample
G	=	the percentage (m/m) of free glycerol in the sample
M	=	the percentage (m/m) of monoglycerides in the sample
D	=	the percentage (m/m) of diglycerides in the sample
T	=	the percentage (m/m) of triglycerides in the sample
0.255, 0.146, 0.103	=	Conversion factor of mono-, di- and triglycerides, respectively.

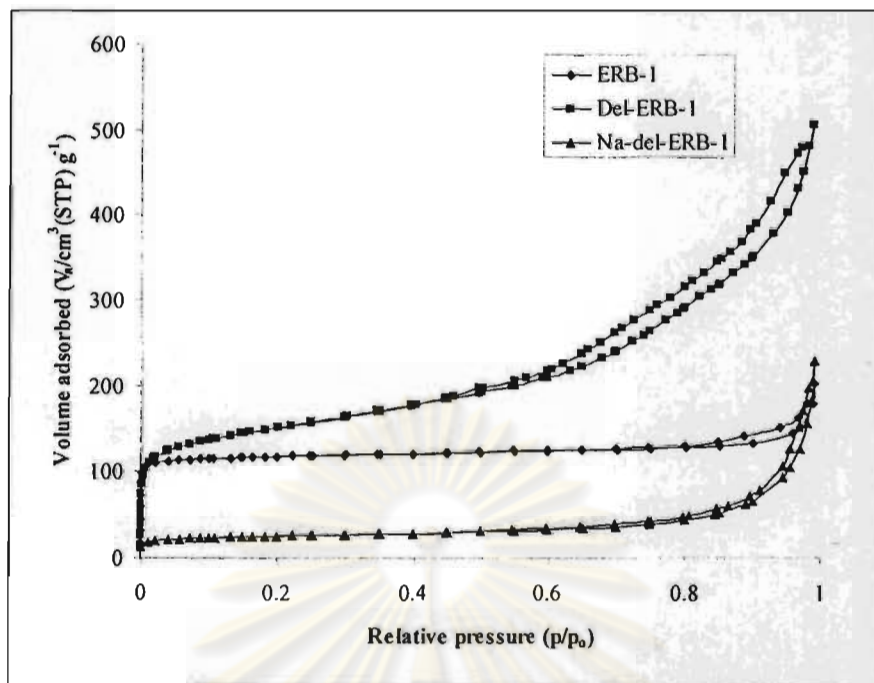


Figure A-15 N_2 adsorption-desorption isotherms of ERB-1, del-ERB-1 and Na-del-ERB-1.

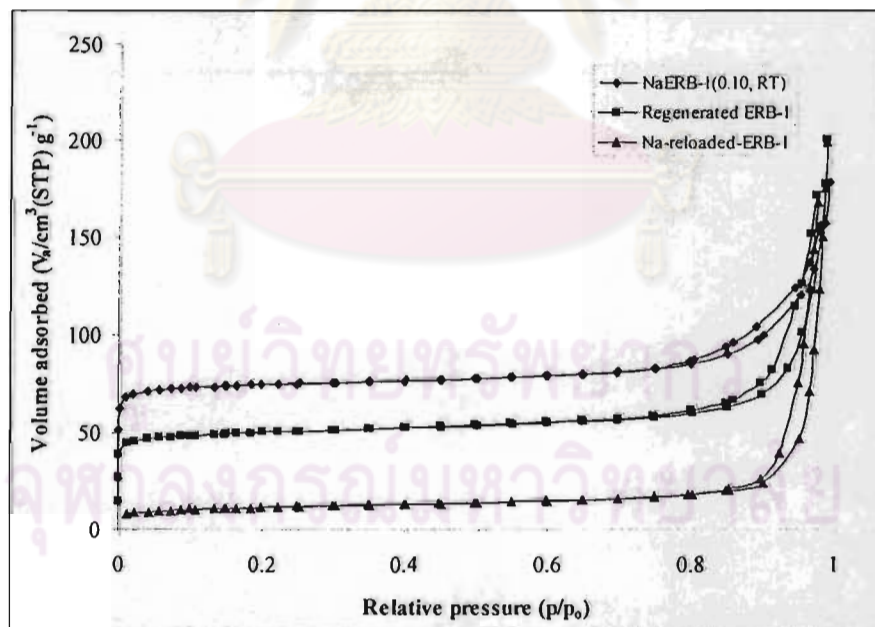
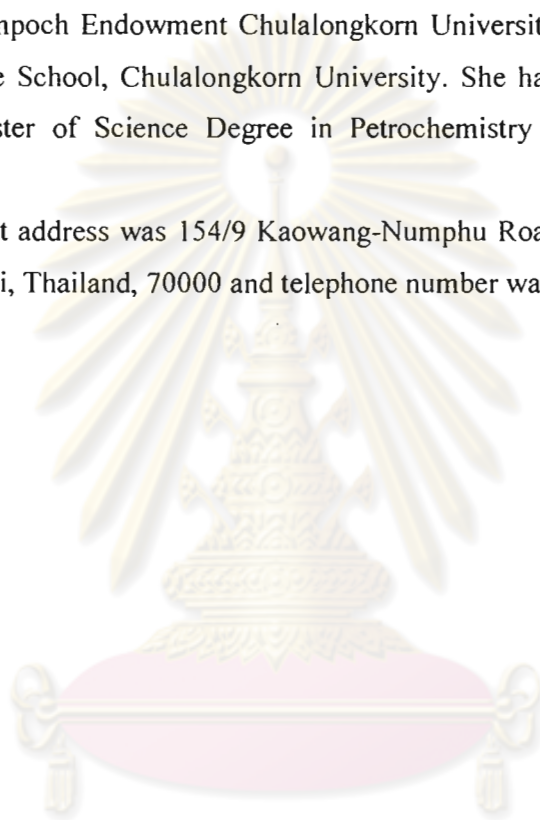


Figure A-15 N_2 adsorption-desorption isotherms of NaERB-1(0.10, RT), regenerated ERB-1 and Na-reloaded ERB-1.

VITAE

Miss Nanchana Srikongyoo was born on October 3, 1982 in Ratchaburi, Thailand. She graduated with Bachelor's Degree in Chemistry from Faculty of Science, Mahidol University in 2005. She continued her study in Petrochemistry and Polymer Science Program, Faculty of Science, Chulalongkorn University in 2005. During her graduate study, she also received a research assistantship from Rachadapisek Sompoch Endowment Chulalongkorn University and a research grant from the Graduate School, Chulalongkorn University. She has completed her study leading to a Master of Science Degree in Petrochemistry and Polymer Science Program in 2007.

Her present address was 154/9 Kaowang-Numphu Road, Moo. 12, Jedeehuk, Maung, Ratchaburi, Thailand, 70000 and telephone number was 081-7957871.



ศูนย์วิทยทรัพยากร
จุฬาลงกรณ์มหาวิทยาลัย